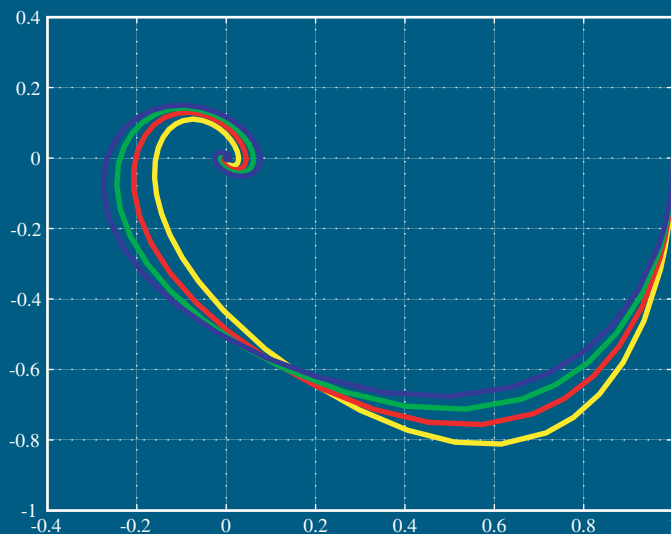


NONLINEAR CONTROL OF UNCERTAIN SYSTEMS

Some application-oriented issues



Francesc Pozo Montero



Doctoral Thesis

Barcelona, November 2004

UNIVERSITAT POLITÈCNICA DE CATALUNYA
PROGRAMA DE DOCTORAT DE MATEMÀTICA APLICADA



Departament de Matemàtica
Aplicada III

UNIVERSITAT POLITÈCNICA DE CATALUNYA



Tesi Doctoral

Memòria presentada per Francesc Pozo Montero per optar
al grau de Doctor en Matemàtiques per la Universitat
Politécnica de Catalunya.

**NONLINEAR CONTROL OF
UNCERTAIN SYSTEMS**

SOME APPLICATION-ORIENTED ISSUES

by **Francesc Pozo Montero**

Advisors: José Rodellar Benedé
Fayçal Ikhouane

Barcelona, November 2004

Al meu pare.
A la meva mare.
A la meva família.
A la Núria.

*Un cor de llauna dolça
batega sense sang;
i els ulls de vidre
dels semàfors
qui sap si veuen
aquells qui els miren.*

Pere Quart
Vacances pagades

Acknowledgements

Arribats a aquest punt, quan la tesi ja és una realitat, són moltes les persones a les que he d'agrair el seu suport i la seva confiança.

Primer de tot, res d'això no hauria estat possible sense la confiança inicial del Juanjo Villanueva, director del Centre de Visió per Computador (CVC), que va confiar en mi fins i tot abans d'haver acabat la llicenciatura de matemàtiques i que em va permetre iniciar la meva carrera acadèmica i de recerca a la Universitat. També envio un record als companys del CVC Joan Serrat i Enric Gòdia.

A l'Antonio Huerta, director del Departament de Matemàtica Aplicada III quan vaig entrar a formar part de la UPC, pel suport en moments difícils; i a l'Eusebi Jarauta, delegat de la secció d'Urgell, en aquells moments, director del Departament, ara, i company ideològic i amic, sempre.

Al José Rodellar, director de la meva tesi, pel seu talent, per la seva sensibilitat, per la seva orientació i perquè sempre ha estat al meu costat. Al Fayçal Ikhouane per les idees, i per les enriquidores discussions respecte als aspectes computacionals del control i el control teòric.

Al Jaume Peraire, per haver-me acollit tan bé al Massachusetts Institut of Technology.

A la Gisela Pujol, amiga i inestimable companya de recerca; al Pablo Buenestado, pel suport mutu.

A la Yolanda Vidal, pel que és i pel que ha de ser.

Al Francisco Pérez, per ser company de viatge i per les reflexions de la revetlla de reis de fa uns anys.

Als matemàtics, i molt en especial a l'Ester Bascuas, que va compartir amb mi tants anys de Facultat; a la Míriam Cabero, per ser com és; i al Sergio Gracia, per les aventures al sud de França i molt més...

Al Jesús Martínez, tot i que no he pogut canviar el títol de la tesi...

A l'Herminio Martínez, per les orientacions respecte els aspectes

més electrònics del control.

A la meva família: el meu pare ni s'ho imagina, però estaria molt orgullós; a la meva mare, mai li he dedicat res però sempre s'ho ha merescut; i a la Isabel i al Carlos, que me'ls estimo com no s'imaginem...

I per últim, a la Núria. Pels ànims en els moments baixos. Per la companyia en els moments de soledat. Per les idees en els viatges pel desert. Per les passejades infinites. Per les paraules a la porta de l'escola. Perquè no és el mateix...

*Doncs, està vist:
fer miracles no és pas cosa de sants
ara com ara.*

Contents

Objectives of the thesis	1	
I	ADAPTIVE CONTROL DESIGN	7
1	Introduction	9
1.1	A historical perspective of automatic control	10
1.2	Emergence of adaptive control	12
1.2.1	A structural obstacle	14
1.3	Adaptive backstepping and tuning functions	16
1.3.1	A first Lyapunov-based example	16
1.3.2	Backstepping preview with a generic third order system	17
2	Tuning functions design for linear systems	19
2.1	State estimation filters	20
2.2	Tuning functions design	24
2.2.1	Design procedure	24
2.2.2	Stability analysis	34
2.2.3	Transient performance with tuning functions	37
2.3	Recent developments	43
2.3.1	Stability and asymptotic performance	44
2.3.2	Robustness	45
2.3.3	Transient performance	48
2.4	Conclusions	48
3	Unknown linear systems in the presence of bounded disturbances	51

3.1	Problem statement	51
3.2	Controller design and robustness analysis	52
3.2.1	Controller design	52
3.2.2	Robustness analysis	54
3.3	Transient bounds	57
3.4	Conclusions	58
4	Adapt. backstepping control of hysteretic base-isolated struct.	59
4.1	Introduction	59
4.2	Structural models	60
4.3	Control strategies	62
4.4	Controller design	63
4.4.1	Model description	63
4.4.2	Adaptive backstepping control	66
4.4.3	Robustness analysis	67
4.4.4	Transient bounds	69
4.5	Numerical simulations	69
4.5.1	Results	71
4.5.2	Discussion of the results	73
4.6	Conclusions	84
5	Sensitivity analysis of the backstepping control design	95
5.1	Introduction	95
5.2	Plant and controller design	96
5.2.1	Plant	97
5.2.2	Design procedure	97
5.3	Sensitivity analysis	99
5.3.1	Elements of the analysis	101
5.3.2	First consideration	102
5.3.3	Second consideration	103
5.4	Conclusions	106
II	CONTROL SYNTHESIS BY SOS OPT.	107
6	Control synthesis of polynomial and rational systems	109
6.1	Introduction	109
6.2	Control synthesis of linear systems via LMI	110
6.2.1	Linear matrix inequalities	111

6.2.2	Synthesis of linear systems via LMI . . .	111
6.3	Control synthesis of polynomial systems	116
6.3.1	Hilbert's 17th problem	116
6.3.2	First relaxation: the sum of squares approach	117
6.3.3	Second relaxation: the dual theorem of Lyapunov	118
6.3.4	Convexity in nonlinear stabilization . . .	125
6.3.5	Polynomial systems	126
6.3.6	Extension to the rational case	132
6.4	Conclusions	133
7	Control synthesis of systems with uncertain parameters	135
7.1	Putinar's theorem	136
7.2	Synthesis procedure	137
7.3	A simple example	139
7.4	Conclusions	141
	Conclusions and future work	143
	Conclusions	143
	Future work	146
	Structural control	146
	Backstepping complexity	147
	Sum of squares applications	147
	Analysis, identification and control of systems with friction	148
	Bibliography	149

List of Tables

2.1	Kreisselmeier filters (K-filters)	22
2.2	The asymptotic performance of the adaptive backstepping tuning functions control design in the last few years.	44
2.3	The robustness of the adaptive backstepping tuning functions control design in the last few years.	46
2.4	The transient performance of the adaptive backstepping tuning functions control design in the last few years.	49
4.1	Model coefficients of the single-degree-of-freedom system.	70
4.2	Parameters of the hysteresis model.	70
4.3	List of figures.	72
4.4	Peak values of the base and structure relative displacements and the interstory drift for the cases in Figure 4.7.	75
4.5	Peak values of the base and structure absolute displacements and the interstory drift for the cases in Figure 4.8.	75
4.6	Root-mean-square norms of the base and structure relative displacements and the interstory drift for the cases in Figure 4.9.	75
4.7	Root-mean-square norms of the base and structure absolute displacements and the interstory drift for the cases in Figure 4.10.	84
4.8	Control effort.	84
5.1	Maximum values of the sensitivity functions $Dx(t)$, for $\varepsilon(t) = 10^{-7}$ and $a_1 = 5, a_2 = b_0 = 1$ (stable system). . .	104
5.2	Maximum values of the sensitivity functions $Dx(t)$, for $\varepsilon(t) = 10^{-7}$ and $a_1 = -1, a_2 = b_0 = 1$ (unstable). . . .	104

List of Figures

1.1	Traditional adaptive schemes and adaptive backstepping designs.	15
2.1	Virtual estimate \hat{x} generated with input filter λ and output filter η	24
2.2	Different authors interested in adaptive backstepping for linear systems. Each line corresponds to a published paper.	43
2.3	Main topics covered in adaptive backstepping for linear systems.	45
3.1	Tuning functions design	55
4.1	Building structure with hybrid control system.	61
4.2	Block diagram representation.	63
4.3	The control law and the parameter update laws are designed in $\rho = 2$ steps.	68
4.4	1952 Taft earthquake, ground acceleration (up), velocity (middle) and displacement (down).	76
4.5	1952 Taft earthquake. Model based in relative coordinates. From left to right and top to bottom: control signal acceleration, $u(t)/m_1$ (m/s ²); closed loop interstory drift (black) and open loop interstory drift (red) (m); closed loop base displacement (solid) and open loop base displacement (dashed) (m); closed loop structure displacement (solid) and open loop structure displacement (dashed) (m); closed loop base velocity (solid) and open loop base velocity (dashed) (m); closed loop structure velocity (solid) and open loop structure velocity (dashed) (m).	77

4.6	1952 Taft earthquake. Model based in absolute coordinates. From left to right and top to bottom: control signal acceleration, $u(t)/m_1$ (m/s ²); closed loop interstory drift (black) and open loop interstory drift (red) (m); closed loop base displacement (solid) and open loop base displacement (dashed) (m); closed loop structure displacement (solid) and open loop structure displacement (dashed) (m); closed loop base velocity (solid) and open loop base velocity (dashed) (m); closed loop structure velocity (solid) and open loop structure velocity (dashed) (m).	78
4.7	Taft earthquake. Index μ_∞ for some design parameters for the case of relative coordinates.	79
4.8	Taft earthquake. Index μ_∞ for some design parameters for the case of absolute coordinates.	80
4.9	Taft earthquake. Index μ_{RMS} for some design parameters for the case of relative coordinates.	81
4.10	Taft earthquake. Index μ_{RMS} for some design parameters for the case of absolute coordinates.	82
4.11	Taft earthquake. Infinity norm (up) and root-mean-square norm (down) of the control signal acceleration in both the relative and the absolute coordinates cases.	83
4.12	1989 Loma Prieta earthquake, ground acceleration (up), velocity (middle) and displacement (down).	86
4.13	1989 Loma Prieta earthquake. Model based in relative coordinates. From left to right and top to bottom: control signal acceleration, $u(t)/m_1$ (m/s ²); closed loop interstory drift (black) and open loop interstory drift (red) (m); closed loop base displacement (solid) and open loop base displacement (dashed) (m); closed loop structure displacement (solid) and open loop structure displacement (dashed) (m); closed loop base velocity (solid) and open loop base velocity (dashed) (m); closed loop structure velocity (solid) and open loop structure velocity (dashed) (m).	87

4.14	1989 Loma Prieta earthquake. Model based in absolute coordinates. From left to right and top to bottom: control signal acceleration, $u(t)/m_1$ (m/s ²); closed loop interstory drift (black) and open loop interstory drift (red) (m); closed loop base displacement (solid) and open loop base displacement (dashed) (m); closed loop structure displacement (solid) and open loop structure displacement (dashed) (m); closed loop base velocity (solid) and open loop base velocity (dashed) (m); closed loop structure velocity (solid) and open loop structure velocity (dashed) (m).	88
4.15	Loma Prieta earthquake. Index μ_∞ for some design parameters for the case of relative coordinates.	89
4.16	Loma Prieta earthquake. Index μ_∞ for some design parameters for the case of absolute coordinates.	90
4.17	Loma Prieta earthquake. Index μ_{RMS} for some design parameters for the case of relative coordinates.	91
4.18	Loma Prieta earthquake. Index μ_{RMS} for some design parameters for the case of absolute coordinates.	92
4.19	Loma Prieta Earthquake. Infinity norm (up) and root-mean-square norm (down) of the control signal acceleration in both the relative and the absolute coordinates cases.	93
5.1	The propagated errors are not significant for $c_i = d_i = \kappa = 0.5$, $i = 1, 2, 3$, in u (up), but the control signal is clearly corrupted for $c_i = d_i = \kappa = 2$, $i = 1, 2, 3$ (down).	100
5.2	Time history representation of $D\eta_1, D\eta_2, D\eta_3, D\lambda_1, D\lambda_2, D\lambda_3, D\hat{\theta}_1, D\hat{\theta}_2, D\hat{\theta}_3, D\hat{\rho}$ and D_y in a semi-logarithmic scale, with $\varepsilon(t) = 10^{-7}$, $t \in [0, 4]$ and $c_i = d_i = \gamma = 2$, $i = 1, 2, 3$	103
5.3	Time history of the coefficient $\nu_{1,12}$	105
6.1	Inverted pendulum.	112
6.2	Simulation of the linearized inverted pendulum with initial conditions $(x, \dot{x}, \theta, \dot{\theta}) = (0.1, -2, 0.2, -0.4)$	115
6.3	Phase plane plot for Example 6.2.	125
6.4	Phase plane plot for Example 6.3.	126

6.5	Phase plot of the closed-loop system in Example 6.4. The solid curve is the trajectory with initial conditions $(5, -5)$	128
6.6	Trajectory of the controlled rigid body with initial conditions $(\omega, \psi) = (-1, 1, 0, -1, 2, -3)$ (first and second row) and control law $u(t) = (u_1(t), u_2(t), u_3(t))$ (third row).	131
7.1	Phase plot of the closed-loop system in Section 7.3. Solid curves are trajectories with initial conditions $(x_1, x_2) = (1, 0)$ and for four different values for the parameter p , 0.7, 0.9, 1.1 and 1.3.	141

Objectives of the thesis

Analysis and control of uncertain systems are among the most challenging problems in systems and control theory. The last two decades have seen an increasing growth of the literature dedicated to analytically solve control problems where uncertainty is present either in the system representation or the measurements. However, this profusion of scientific production in the field of control with a marked *theoretical* orientation has not been paralleled with a similar production of *application-oriented issues* works. The present thesis is intended to contribute in the understanding of some practical implementation issues of some specific control algorithms. More precisely, we deal with the popular backstepping design and a recently developed computational technique for control synthesis.

For nonlinear systems, the 1990s started with a breakthrough: backstepping, a recursive design for systems with nonlinearities not constrained by linear bounds. Although the idea of integrator backstepping may be implicit in some earlier works, its use as a design tool was initiated by [Tsi89, BI89, SS89, KS89, SKS90]. However, the true potential of backstepping was discovered only when this approach was developed for nonlinear systems with structured uncertainty [KKK95]. The ease with which backstepping incorporated uncertainties and unknown parameters contributed to its instant popularity and rapid acceptance, mainly within the theoretically oriented control community. Applications of this technique have been recently reported ranging from robotics [LSLT01] to industry [FG98] or aerospace [KK03]. This thesis is concerned, at one hand, with applying the backstepping design in the field of Civil Engineering and, at the other hand, studying a practical implementation issue of this technique, namely its numerical sensitivity.

In our Civil Engineering application, a hybrid seismic control system for building structures is considered, which combines a class of

passive nonlinear base isolator with an active control system. The objective of the active control component applied to the structural base is to keep the base displacement relative to the ground and the inter-story drift within a reasonable range according to the design of the base isolator. The base isolator device exhibits a hysteretic nonlinear behavior which is described analytically by the Bouc-Wen model [Wen76]. The control problem is formulated representing the system dynamics in two alternative coordinates: absolute (with respect to an inertial frame) and relative to the ground. A comparison between both strategies is presented by means of numerical simulations, and it is shown that, in our case, the backstepping-based adaptive tuning functions design ensures reasonably good stability and performance properties of the closed loop.

There is a continuing and growing need in the systems and control community for good algorithms and robust numerical software for increasingly challenging applications [Var04, Doo04, HKMP04]. This way, in order to contribute to the accurate and efficient numerical solution of problems in control systems analysis and design we have focus on some sensitivity and accuracy issues. This way, another complementary line of research pursued in this thesis is the study of the numerical sensitivity of the backstepping-based adaptive tuning functions design. Indeed, the complexity of the controller makes inevitable the use of digital computers to perform the calculation of the control signal. Our work addresses for the first time the issue of the numerical sensitivity of the adaptive tuning functions design. It is shown that, while the increase of the design parameters may be desirable to achieve a good transient performance, it harms the control signal as this increase introduces large high-frequency components due to the numerical errors.

A third related line of research treated in this work is the use of computer-based solutions of control problems when analytical techniques as backstepping fail or are cumbersome. Indeed, a theoretical limitation of the backstepping technique is the necessity for the controlled system to be under a triangular form. Also, a practical limitation of this technique may lie in its numerical sensitivity or the great complexity of the controller. As an alternative to analytical solutions for control problems, a new computational approach has been introduced in [Par00]. This technique is based on a recent convergence criterion that can be viewed as a dual to Lyapunov's second theorem and recent numerical methods for verification of positivity of multivariate

polynomials based on sum of squares decompositions. Our contributions in this area consist in (1) extending this technique to rational systems and (2) include parametric uncertainty in the formulation of the controller synthesis.

Layout of the thesis

The thesis is organized in the following chapters:

► PART I. ADAPTIVE CONTROL DESIGN

- ▷ **Chapter 1** presents a historical perspective of automatic control and an introduction to adaptive control. A backstepping preview with a generic third order system is also considered.
- ▷ **Chapter 2** presents the adaptive backstepping tuning functions design for linear systems in a particular case, when both the relative degree and the plant order are known ($\rho = n = 3$) but with unknown plant parameters. It is also shown that all the signals in the closed-loop adaptive system are globally uniformly stable and asymptotic tracking is achieved. Computable bounds on both \mathcal{L}_2 and \mathcal{L}_∞ norm of the error variables are presented. Finally, it is showed that, with a correct choice of the design parameters, the transient performance can be improved.

Recent developments of the adaptive backstepping tuning functions design for linear systems are also presented in this chapter. The contributions are organized according to this scheme: robustness issues with respect to unmodelled dynamics and/or external disturbances; improvement of the transient performance; stability and asymptotic performance of modified versions (parameter variation, digital implementation, schemes that do not assume the knowledge of the high-frequency gain and multivariable versions). This section also presents the relationships among the different research groups dealing with tuning functions designs for linear systems.

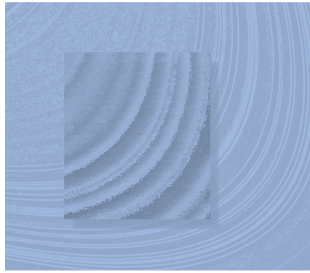
- ▷ **Chapter 3** deals with the problem of controlling unknown linear systems in the presence of bounded disturbances. In this chapter, the transient issue is addressed for backstepping adaptive controllers. A \mathcal{L}_∞ bound on the tracking error is explicitly given as a function of the design parameters. This

shows that the error can be made arbitrarily small by sufficiently increasing the design gains.

- ▷ In **Chapter 4** an application in the field of structural control is presented where a hybrid seismic control system for building structures is considered. The hybrid control system combines a class of passive nonlinear base isolator with an active control system. The analytical model of the system is represented in two different coordinates: absolute (with respect to an inertial frame) and relative to the ground. We also consider that the parameters of the models are uncertain. For that reason, we use adaptive control to stabilize the control loop. To have computable bounds on the transient behaviour, we use the backstepping approach. A comparison between the strategies is presented by means of numerical simulations.
 - ▷ In **Chapter 5** the numerical sensitivity of the adaptive tuning functions is analyzed. It is shown that while the increase of the design parameters may be desirable to achieve a good transient performance, it harms the control signal as this increase introduces large high-frequency components due to the numerical errors.
- ▶ **PART II. CONTROL SYNTHESIS BY SUM OF SQUARES OPTIMIZATION**
- ▷ In **Chapter 6** we show how the synthesis of linear systems is a problem completely solved via the computational methods using semidefinite programming or linear matrix inequalities (LMI). We introduce the basic notation for the LMI methods. The problem of the joint search of a controller and a Lyapunov function for a linear system is solved using this methodology. We also introduce in this Chapter a new computational approach to nonlinear control synthesis. The basis is a recent convergence criterion with a remarkable convexity property – that can be viewed as a dual to Lyapunov’s second theorem –, which is used for controller synthesis of polynomial and rational vector fields via convex optimization. Recent numerical methods for verification of positivity of multivariate polynomials based on sum of squares decompositions are used.
 - ▷ Using the theory of semialgebraic sets the computational tools presented in the previous chapter are extended in **Chapter 7**

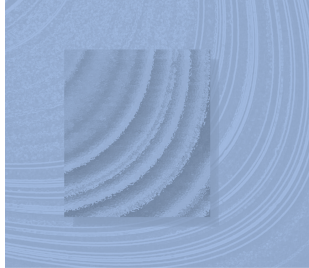
for the case of polynomial or rational systems with uncertainty parameters.

- ▶ **CONCLUSIONS AND FUTURE WORK.** We present the conclusions of the thesis and finally, the foreseen future developments are discussed.



Part I

ADAPTIVE CONTROL DE- SIGN



Chapter 1

Introduction

Engineering is concerned with understanding and controlling the materials and forces of nature for the benefit of humankind. Control system engineers are concerned with understanding and controlling segments of their environments –systems– to provide useful products for society. The two goals of understanding and control are complementary because effective systems control requires that the systems be understood and modelled. Perhaps, the most characteristic quality of control engineering is the opportunity to control machines and industrial and economic processes for the benefit of society.

Control engineering is based on the foundations of feedback theory and linear system analysis. Therefore its applicabilities are not restricted to any engineering area but it can be equally used in aeronautical, mechanical, environmental, civil, electrical engineering, etc.

Due to the increasing complexity of the systems under control and the interest in achieving optimum performance, the importance of control system engineering has grown in the past decades. Furthermore, as the systems become more and more complex, the interrelationship of the controlled variables must be considered in the control scheme.

One of the reasons for the emergence of adaptive control is its capability to build systems capable of controlling unknown plants or adapting to unpredictable changes in the environment.

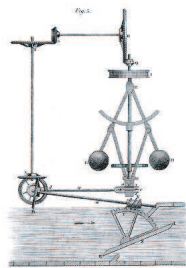
It is widely known that the cost of computers has dropped dramatically. This fact has given rise to their integration as a part of the control systems. Therefore, the research into adaptive control algorithms has increased and the applications of the modern control theory are not strictly related to the engineering, even with applications in different sciences such as biology, biomedicine and economy.

1.1 A historical perspective of automatic control

The use of feedback to control a system has had a fascinating history. The progress of feedback control, as an engineering discipline, is closely tied to the practical problems that needed to be solved during any phase of human history. The key developments in the history of mankind that affected the progress of feedback control were:

- ▷ **The preoccupation of the Greeks and Arabs with keeping accurate track of time.** The first applications of feedback control appeared in the development of float regulator mechanisms in Greece in the period 300 to 1 BC. The water clock of Ktesibios used a float regulator. An oil lamp devised by Philon in approximately 250 BC used also a float regulator in an oil lamp for maintaining a constant level of fuel oil. Heron of Alexandria, who lived in the first century AD, published a book which outlined several forms of water-level mechanisms using float regulators.

- ▷ **The Industrial Revolution in Europe.** The first feedback system to be invented in Modern Europe was the temperature regulator of Cornelis Drebbel (1572-1633) of Holland. Dennis Papin invented the first pressure regulator for steam boilers in 1681.



The first automatic feedback controller used in an industrial process is generally agreed to be James Watt's flyball governor, developed in 1769 for controlling the speed of a steam engine.

It is extremely important to realize that the Industrial Revolution did not start until the invention of improved engines and automatic control systems to regulate them.

The period preceding 1868 was characterized by the development of automatic control systems through intuition and invention. Efforts to increase the accuracy of the control system led to a slower attenuation of the transient oscillations and even to unstable systems. It then became imperative to develop a theory of automatic control. J.C. Maxwell analyzed the stability of Watt's flyball governor. His technique was to linearize the differential equations of motion to find the characteristic equation of the system (1868). He studied the effect of the system parameters on stability and showed that the system is stable if the roots of the characteristic equation have negative real parts. With the work of Maxwell we can say that the theory of control systems was firmly established.

During the same period, I.A. Vyshnegradskii formulated a mathematical theory of regulators.

The work of A.M. Lyapunov was seminal in control theory. He studied the stability of nonlinear differential equations using a generalized notion of energy in 1892. Unfortunately, though his work was applied and continued in Russia, the time was not ripe in the West for his elegant theory, and it remained unknown there until approximately 1960, when its importance was finally realized.

- ▷ **The beginning of mass communication and the First and Second World Wars.** Prior to World War II, control theory and practice developed in the United States and Western Europe in a different manner than in Russia and Eastern Europe. A main impetus for the use of feedback in the United States was the development of the telephone system and electronic feedback amplifiers by Bode, Nyquist and Black at Bell Telephone Laboratories. In contrast, the eminent mathematicians and applied mechanics in the former Soviet Union inspired and dominated the field of control theory.

A large impetus to the theory and practice of automatic control occurred during World War II when it became necessary to design and construct automatic airplane pilots, gun-positioning systems, radar antenna control systems and other military systems based on the feedback control approach.

Prior to 1940, for most cases, the design of control systems was an art involving a trial-and-error approach. During the 1940s, mathematical and analytical methods increased in number and in utility, and control engineering became an engineering discipline in its own right.

Frequency-domain techniques continued to dominate the field of control following World War II with the increased use of Laplace transform and the complex frequency plane. During the 1950s, the emphasis in control engineering theory was on the development and use of the s -plane methods.

- ▷ **The beginning of the space/computer age.** During the 1980s, the utilization of digital computers for control components became routine. The technology of these new control elements to perform accurate and rapid calculations was formerly unavailable to control engineers. These computers are employed especially for process control systems in which many variables are measured and controlled simultaneously by the computer.

With the advent of Sputnik –launched in 1957– and the space age, another new impetus was imparted to control engineering. It became necessary to design complex, highly accurate control systems for missile and space probes.

1.2 Emergence of adaptive control

Adaptive controllers were developed in the early 1950s with the aim of designing autopilots for high-performance aircraft when difficulties were encountered applying PID controllers to this task.

A sophisticated controller, such as an adaptive controller, that could learn and accommodate changes in the aircraft dynamics was needed.

But, when is a controller adaptive? A possible answer was offered by G. Zames during a presentation made at the 35th Conference on Decision and Control, Kobe, Dec. 1996:

“a non-adaptive controller is based solely on a-priori information whereas an adaptive controller is based also on a posteriori information”

The ability of adaptive control to adapt –“to adjust oneself to particular conditions; to bring oneself in harmony with a particular environment; to bring one’s acts, behaviour in harmony with a particular environment”, according to the Webster’s dictionary– to variations in flight characteristics caused by such factors as air speed, altitude and aircraft load, and the ability to incorporate all these factors into a single mathematical control strategy, made adaptive control the ideal candidate for this task.

Anyhow, to incorporate these factors requires the development of a mathematical model that can be used to represent the responses of the aircraft. From an academic perspective, adaptive control theory essentially deals with finding parameter adjustment algorithms that offer global stability and convergence guarantees. The mathematical development, along with the requirement of a fast computer to execute the algorithm, are the major reasons that the potential of adaptive control has taken so long to be realized in conventional industrial applications. Adaptive control has been limited primarily to specialized applications in aerospace and naval auto-pilots.

Model reference adaptive control was suggested by Whitaker *et al.* to solve the autopilot control problem. Although the original algorithm proved unstable, it led to the development during the 1970s and 1980s of algorithms with guaranteed stability, convergence and robustness properties.

The 1960s became one of the most important periods for the development of adaptive control. State space techniques and stability theory based on Lyapunov were introduced. Developments in dynamics programming (Bellman, 1957) and dual control (Feldbaum, 1960) played a crucial role in the reformulation and redesign of adaptive control.

In the 1970s, the simultaneous development and progress in computer and electronics that made the implementation of complex controllers, such as the adaptive ones, feasible contributed to an increased interest in applications of adaptive control. By the early 1980s, several types of adaptive schemes were proven to provide stable operation and asymptotic tracking and at the same time more and more examples of instabilities were published demonstrating lack of robustness in the presence of unmodelled dynamics or bounded disturbances.

We refer to the results of this period as *adaptive linear control* or *traditional adaptive control*. All the traditional schemes involve parameter identification with *parameter estimators* –in which the vital part is the parameter adaptation algorithm or *parameter update law*– and are classified as

- ▷ **direct**, when the updated parameters are those of the controller, and
- ▷ **indirect**, when the updated parameters are those of the plant,

and as

- ▷ **Lyapunov-based**
- ▷ **estimation-based**

The distinction between Lyapunov-based and estimation based is dictated in part by the type of parameter update law and the corresponding proof of stability and convergence.

An important feature of traditional adaptive control is its reliance on *certainty equivalence* controllers. Those schemes ignore the uncertainty on the estimates by treating them as true values. The resulting controller is either estimated (direct) or designed for the estimated plant (indirect).

1.2.1 A structural obstacle

Traditional estimation-based designs cannot be applied to nonlinear systems whereas Lyapunov-based can. However, in the linear case the Lyapunov-based design has been restricted to plants with transfer functions of relative degree one and two. In the nonlinear case, this structural restriction is translated into a *level of uncertainty* –number of integrators between the control input and the unknown parameter– zero or one. When the level of uncertainty is zero, the uncertainty and the control are *matched*, because they appear in the same equation. When the level of uncertainty is one it corresponds to the *extended-matching* case.

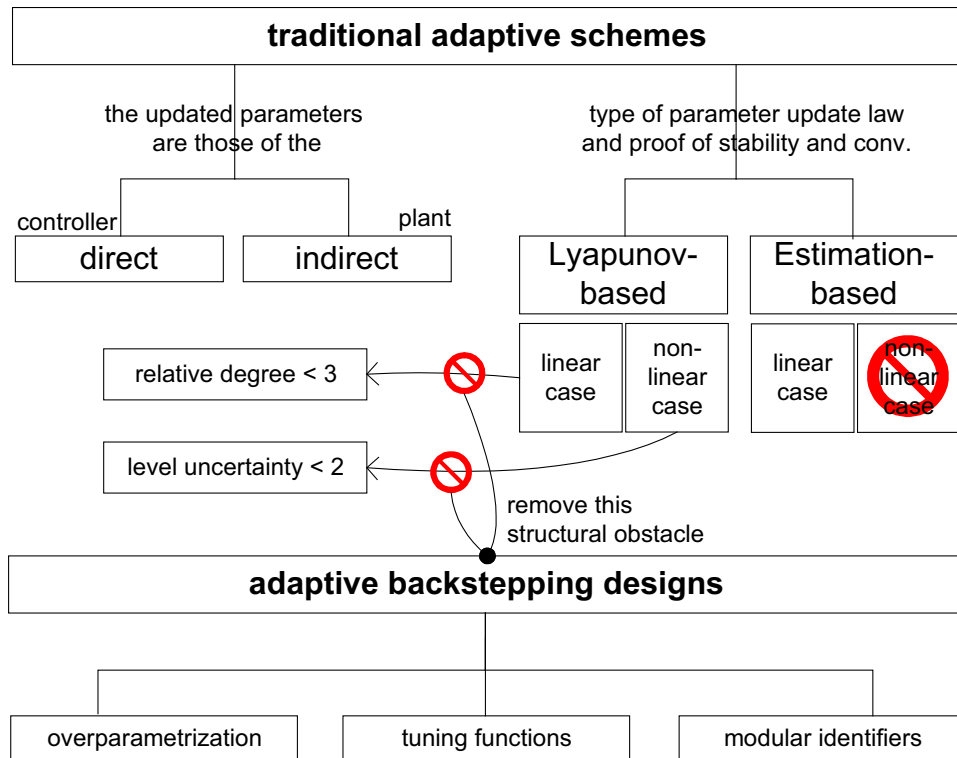


Figure 1.1. *Traditional adaptive schemes and adaptive backstepping designs.*

The extended matching barrier was finally broken with a new recursive design procedure called *adaptive backstepping*. The adaptive backstepping –emerged as a confluence of the adaptive estimation idea and nonlinear control ideas– removes this structural obstacle and allows the Lyapunov-based designs to be applied to wide classes of uncertain systems. Adaptive backstepping also stimulated efforts to reduce its overparametrization. Finally, with the invention of *tuning functions* was introduced a new design which completely removed the overparametrization.

We can summarize the three types of adaptive backstepping techniques –which differ in construction of adaptation law– as follows:

- ▷ **adaptive backstepping with overparametrization**, when at each step a new vector of adjustable parameters and the corresponding adaptation law are introduced;

- ▷ **adaptive backstepping with tuning functions**, when at each step a virtual adaptation law called *tuning function* is introduced, while the actual adaptation algorithm is defined at the final step in terms of all the previous tuning functions, as we will see in next sections;
- ▷ **adaptive backstepping with modular identifiers**, when a slight modification of the adaptive controller allows one to independently construct estimation-based identifiers of unknown parameters.

1.3 Adaptive backstepping and tuning functions

1.3.1 A first Lyapunov-based example

Let us start this section applying the Lyapunov-based approach to the adaptive control problem for the nonlinear plant

$$\dot{x} = u + \theta x^2, \quad (1.1)$$

where u is the control and θ is an unknown constant. In this procedure we seek a parameter update law for the estimate $\hat{\theta}(t)$,

$$\dot{\hat{\theta}} = \tau(x, \hat{\theta}), \quad (1.2)$$

which, along with a control law $u = \alpha(x, \hat{\theta})$, will make the Lyapunov function

$$V(x, \hat{\theta}) = \frac{1}{2}x^2 + \frac{1}{2}(\hat{\theta} - \theta)^2 \quad (1.3)$$

a nonincreasing function of time.

To this end, we express \dot{V} as a function of u and seek $\alpha(x, \hat{\theta})$ and $\tau(x, \hat{\theta})$ to guarantee that $\dot{V} \leq -px^2$ with $p > 0$, namely

$$\dot{V} = x\dot{x} + (\hat{\theta} - \theta)\dot{\hat{\theta}} \quad (1.4)$$

$$= x(u + \theta x^2) + (\hat{\theta} - \theta)\dot{\hat{\theta}} \quad (1.5)$$

$$= xu + \hat{\theta}\dot{\hat{\theta}} + \theta(x^3 - \dot{\hat{\theta}}). \quad (1.6)$$

The requirement $\dot{V} \leq -px^2$ imposes the following condition of the choice of an update law for $\hat{\theta}$ and a control law for u :

$$xu + \hat{\theta}\dot{\hat{\theta}} + \theta(x^3 - \dot{\hat{\theta}}) \leq -px^2. \quad (1.7)$$

To eliminate the unknown θ , a possible choice for the update law is $\tau(x, \hat{\theta}) = x^3$, that is

$$\dot{\hat{\theta}} = x^3, \quad (1.8)$$

so that (1.7) reduces to

$$xu + x^3\hat{\theta} \leq -px^2. \quad (1.9)$$

This condition allows us to select $\alpha(x, \hat{\theta})$ in various ways. One of them are, for example,

$$u = -px - \hat{\theta}x^2. \quad (1.10)$$

1.3.2 Backstepping preview with a generic third order system

Consider now, for example, the class of pure-feedback systems

$$\begin{aligned} \dot{x}_1 &= x_2 + \varphi_1^T(x_1, x_2)\theta \\ \dot{x}_2 &= x_3 + \varphi_2^T(x_1, x_2, x_3)\theta \\ \dot{x}_3 &= u + \varphi_3^T(x_1, x_2, x_3)\theta, \end{aligned} \quad (1.11)$$

where θ is constant and unknown.

The idea of backstepping is to design a controller for (1.11) recursively by considering some of the states variables as *virtual controls* and designing for them intermediate control laws. In (1.11) the first virtual control is x_2 . It is used to stabilize the first equation as a separate system. Since θ is unknown, this task is solved with an adaptive controller consisting of the control law $\alpha_1(x_1)$ and the update law $\dot{\hat{\theta}} = \tau(x_1)$, as in the previous example.

In the next step the state x_3 is the *virtual control* which is used to stabilize the subsystem consisting of the first two equations of (1.11). This is again an adaptive control task, and a new update law is to be designed.

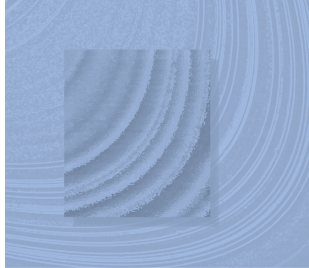
However, an update law $\dot{\hat{\theta}} = \tau(x_1)$ has already been designed in the first step and this does not seem to allow any freedom to proceed further. We can treat this in two different ways:

- ▷ **adaptive backstepping with overparametrization.** In this case the parameter θ in the second equation of (1.11) is treated as a new parameter and assigns to it a new estimate with a new update law. As a result, there are several estimates for the same parameter (*overparametrization*).

▷ **adaptive backstepping with tuning functions.** The over-parametrization is avoided by considering that in the first step $\dot{\hat{\theta}} = \tau(x_1)$ is not an update law but only a function $\tau(x_1)$. This *tuning function* is used in subsequent recursive steps and the discrepancy $\dot{\hat{\theta}} - \tau(x_1)$ is compensated with additional terms in the controller. Whenever the second derivative $\ddot{\hat{\theta}}$ would appear, it is replaced by the analytic expression for the first derivative of $\tau(x_1)$.

Both designs achieve the goals of stabilization and tracking. The proof of these properties is a direct consequence of the recursive procedure during which a Lyapunov function is constructed for the entire system, including the parameter estimates.

The tuning functions approach is an advanced form of adaptive backstepping. It has the advantage that the dynamic order of the adaptive controller is minimal. The dimension of the set to which the states and parameter estimates converge is also minimal.



Chapter 2

Tuning functions design for linear systems

We now present a more detailed approach to adaptive control of linear systems via a backstepping tuning function control design. This design removes several obstacles from adaptive linear control. Since the design is based on a single Lyapunov function incorporating both the state of the error system and the update law, the proof of global uniform stability is direct and simple. Moreover, all the error states except for the parameter error converge to zero.

However, the main advantage of the tuning functions design over traditional certainty equivalence adaptive designs is in the transient performance. The nonlinear control law which incorporates the parameter update law keeps the parameter estimation transients from causing bad tracking transients. The performance bounds obtained for the tuning functions scheme are computable and can be used for systematic improvement of transient performance.

As a prototype, we consider a linear single-input single-output system

$$y(s) = \frac{b}{s(s^2 + a_2s + a_1)}u(s), \quad (2.1)$$

where the coefficients $a_1, a_2, b \in \mathbb{R}$ are constant but unknown.

The control objective is to asymptotically track a given reference signal $y_r(t)$ with the output $y(t)$.

We assume the following for the plant:

Assumption 1 The sign of the high-frequency gain ($\text{sgn}(b)$) is known.

Assumption 2 The relative degree ($\rho = 3$) and the plant order ($n = 3$) are known.

The class of reference signal we employ, $y_r(t)$, and its first $\rho = 3$ derivatives are known and bounded, and, in addition, $y_r^{(3)}$ is piecewise continuous. In particular, we consider $y_r(t)$ as the output of a stable filter of order $\rho + 1$.

2.1 State estimation filters

We start by representing the plant (2.1) in the observer canonical form

$$\dot{x}_1 = x_2 - a_2 y \quad (2.2a)$$

$$\dot{x}_2 = x_3 - a_1 y \quad (2.2b)$$

$$\dot{x}_3 = bu \quad (2.2c)$$

$$y = x_1 \quad (2.2d)$$

or, in a more compact way, as

$$\dot{x} = Ax - y \begin{bmatrix} a \\ 0 \end{bmatrix} + \begin{bmatrix} \mathbf{0}_{2 \times 1} \\ b \end{bmatrix} u \quad (2.3)$$

$$y = e_1^T x, \quad (2.4)$$

where

$$A = \begin{bmatrix} 0 & 1 & 0 \\ 0 & 0 & 1 \\ 0 & 0 & 0 \end{bmatrix}, \quad a = \begin{bmatrix} a_2 \\ a_1 \end{bmatrix}. \quad (2.5)$$

In this situation, we are able to express (2.3)-(2.4) as

$$\dot{x} = Ax + F(y, u)^T \theta \quad (2.6)$$

$$y = e_1^T x, \quad (2.7)$$

where

$$F(y, u)^T = \left[\begin{array}{c|cc} 0 & -y & 0 \\ 0 & 0 & -y \\ \hline u & 0 & 0 \end{array} \right] \quad (2.8)$$

and the parameter vector θ is defined by

$$\theta^T = [b \quad a^T]. \quad (2.9)$$

For state estimation we employ the filters

$$\dot{\xi} = A_0\xi + ky \quad (2.10)$$

$$\dot{\Omega}^T = A_0\Omega^T + F(y, u)^T, \quad (2.11)$$

where the vector $k = [k_1, k_2, k_3]^T$ is chosen so that the matrix

$$A_0 = A - ke_1^T = \begin{bmatrix} -k_1 & 1 & 0 \\ -k_2 & 0 & 1 \\ -k_3 & 0 & 0 \end{bmatrix} \quad (2.12)$$

is Hurwitz, and hence P exists such that

$$PA_0 + A_0^T P = -I, \quad P = P^T > 0. \quad (2.13)$$

With the help of those filters our state estimate is

$$\hat{x} = \xi + \Omega^T\theta, \quad (2.14)$$

and the state estimation error

$$\varepsilon = x - \hat{x} \quad (2.15)$$

vanishes exponentially because it satisfies

$$\dot{\varepsilon} = A_0\varepsilon. \quad (2.16)$$

A further practical step is to lower the dynamic order of the Ω -filter by exploiting the structure of $F(y, u)$ in (2.8). We denote the first column of Ω^T by v_0 and the remaining 2 columns by Ξ ,

$$\Omega^T = [v_0, \Xi], \quad (2.17)$$

and show that due to the special dependence of $F(y, u)$ of u , the equation for the first column of Ω^T is governed by

$$\dot{v}_0 = A_0v_0 + e_3u. \quad (2.18)$$

This means that the vector v_0 can be obtained from only the input filter

$$\dot{\lambda} = A_0\lambda + e_3u \quad (2.19)$$

considering $v_0 = \lambda$.

In a similar manner, Ξ is governed by

$$\dot{\Xi} = A_0\Xi - \begin{bmatrix} I_2 \\ \mathbf{0}_{1 \times 2} \end{bmatrix} y, \quad (2.20)$$

or equivalently, if $\Xi = [\Xi_1, \Xi_2]$,

$$\dot{\Xi}_1 = A_0 \Xi_1 - e_1 y \quad (2.21)$$

$$\dot{\Xi}_2 = A_0 \Xi_2 - e_2 y \quad (2.22)$$

and thanks to the special structure of A_0 ,

$$A_0^j e_3 = e_{3-j}, \quad j = 0, 1, 2 \quad (2.23)$$

Ξ can be obtained from only one input filter

$$\dot{\eta} = A_0 \eta + e_3 y, \quad (2.24)$$

through the algebraic expression

$$\Xi = -[A_0^2 \eta, A_0 \eta]. \quad (2.25)$$

Finally, with the identity

$$A_0^3 e_3 = -k, \quad (2.26)$$

the vector ξ in (2.10) can be obtained from the filter (2.24) through the algebraic expression

$$\xi = -A_0^3 \eta. \quad (2.27)$$

What has been achieved thus far is a static relationship between the state x and the unknown parameter θ :

$$x = \xi + \Omega^T \theta + \varepsilon. \quad (2.28)$$

In conclusion, the table of the K -filters is:

$\dot{\eta}$	$= A_0 \eta + e_3 y$
$\dot{\lambda}$	$= A_0 \lambda + e_3 u$
Ξ	$= -[A_0^2 \eta, A_0 \eta]$
ξ	$= -A_0^3 \eta$
v_0	$= \lambda$
Ω^T	$= [v_0, \Xi]$

Table 2.1. *Kreisselmeier filters (K-filters)*

Remark 1 From (2.28) and the expressions in Table 2.1 an equivalent expression for the virtual estimate \hat{x} is

$$\begin{aligned}\hat{x} &= -A_0^3\eta - \sum_{i=1}^2 a_i A_0^i \eta + b_0 \lambda \\ &= B(A_0)\lambda - A(A_0)\eta,\end{aligned}\tag{2.29}$$

where $A(\cdot)$ and $B(\cdot)$ are matrix-valued polynomial functions. With (2.29) we get an explicit relationship among λ , η , and ε and x :

$$x = B(A_0)\lambda - A(A_0)\eta + \varepsilon.\tag{2.30}$$

The backstepping design for the plant (2.1) starts with its output y , which will be the only plant state allowed to appear in the control law. For this reason, (2.2) is rewritten as:

$$\dot{y} = x_2 - a_2 y = x_2 - y e_1^T a.\tag{2.31}$$

From the algebraic expressions (2.28) we have

$$\begin{aligned}x_2 &= \xi_2 + \Omega_{(2)}^T \theta + \varepsilon_2 \\ &= \xi_2 + [v_{0,2}, \Xi_{(2)}] \theta + \varepsilon_2\end{aligned}\tag{2.32}$$

$$= b v_{0,2} + \xi_2 + [0, \Xi_{(2)}] \theta + \varepsilon_2\tag{2.33}$$

Substituting both (2.32) and (2.33) into (2.31), we obtain the following two important expressions for \dot{y} :

$$\dot{y} = \xi_2 + \omega^T \theta + \varepsilon_2\tag{2.34}$$

$$= b v_{0,2} + \xi_2 + \bar{\omega}^T \theta + \varepsilon_2,\tag{2.35}$$

where the ‘regressor’ ω and the ‘truncated regressor’ $\bar{\omega}$ are defined as

$$\omega = [v_{0,2}, \Xi_{(2)} - y e_1^T]^T\tag{2.36}$$

$$\bar{\omega} = [0, \Xi_{(2)} - y e_1^T]^T\tag{2.37}$$

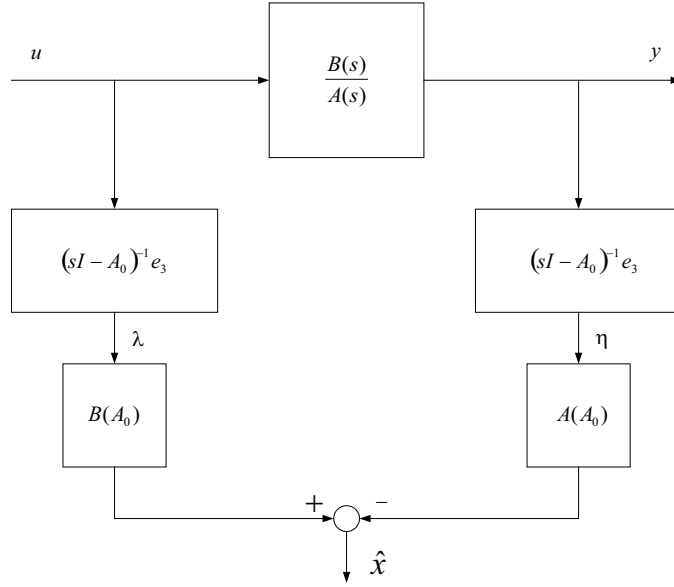


Figure 2.1. Virtual estimate \hat{x} generated with input filter λ and output filter η .

2.2 Tuning functions design

2.2.1 Design procedure

Thanks to the minimum phase of the plant the design is restricted to the $\rho = 3$ equations in (2.2):

$$\begin{aligned}\dot{x}_1 &= x_2 - a_2 y \\ \dot{x}_2 &= x_3 - a_1 y \\ \dot{x}_3 &= bu\end{aligned}\tag{2.38}$$

In the backstepping approach we view the state variable x_{i+1} as a control input to the subsystem consisting of the states x_1, \dots, x_i , and we design a *stabilizing function* α_i which would achieve the control objective if x_{i+1} were available as a control input. The control law for the actual control input u is obtained at the ρ th step of the recursive design.

Because only the system output $y = x_1$ is measured, we replace (2.39) with a new system whose states are available.

We start with (2.35), with is just an alternative form of the first equation in (2.39). Equation (2.35) suggests that $v_{0,2}$ is chosen instead of the unmeasured x_2 to be the ‘virtual control’ input for backstepping. The reason for this choice is that both x_2 and $v_{0,2}$ are separated by only $\rho - 1 = 2$ integrators from the actual control u , which is clear from (2.18).

A closer examination of the filters in Table 2.1 reveals that more integrators stand in the way of any other variable. Therefore, the design system chosen to replace (2.39) is

$$\begin{aligned}\dot{y} &= bv_{0,2} + \xi_2 + \bar{\omega}^T \theta + \varepsilon_2 \\ \dot{v}_{0,2} &= v_{0,3} - k_2 v_{0,1} \\ \dot{v}_{0,3} &= -k_3 v_{0,1} + u.\end{aligned}\tag{2.39}$$

or equivalently

$$\begin{aligned}\dot{y} &= b\lambda_2 + \xi_2 + \bar{\omega}^T \theta + \varepsilon_2 \\ \dot{\lambda}_2 &= -k_2 \lambda_1 + \lambda_3 \\ \dot{\lambda}_3 &= -k_3 \lambda_1 + u.\end{aligned}\tag{2.40}$$

All of these states are available for feedback. Our design task is to force the output y to asymptotically track the reference output y_r while keeping all the closed-loop signals bounded.

We employ the change of coordinates

$$z_1 = y - y_r\tag{2.41}$$

$$z_2 = \lambda_2 - \hat{\varrho} \dot{y}_r - \alpha_1\tag{2.42}$$

$$z_3 = \lambda_3 - \hat{\varrho} \ddot{y}_r - \alpha_2,\tag{2.43}$$

where $\hat{\varrho}$ is an estimate of $\varrho = 1/b$. Our goal is to regulate $z = [z_1, z_2, z_3]^T$ to zero because by regulating z to zero we will achieve asymptotic tracking of $y_r(t)$ by $y(t)$.

Step 1. We start with the equation for the tracking error z_1 obtained from (2.41) and (2.40):

$$\begin{aligned}\dot{z}_1 &= \dot{y} - \dot{y}_r \\ &= b\lambda_2 + \xi_2 + \bar{\omega}^T \theta + \varepsilon_2 - \dot{y}_r.\end{aligned}\tag{2.44}$$

By substituting $\lambda_2 = z_2 + \hat{\rho}\dot{y}_r + \alpha_1$ from (2.42) into (2.44), we get

$$\begin{aligned}\dot{z}_1 &= bz_2 + b\alpha_1 + b\hat{\rho}\dot{y}_r + \xi_2 + \bar{\omega}^T\theta + \varepsilon_2 - \dot{y}_r \\ &= b\alpha_1 + \xi_2 + \bar{\omega}^T\theta + \varepsilon_2 - b\tilde{\rho}\dot{y}_r + bz_2.\end{aligned}\quad (2.45)$$

Scaling the first stabilizing function α_1 as

$$\alpha_1 = \hat{\rho}\bar{\alpha}_1, \quad (2.46)$$

we obtain

$$\dot{z}_1 = \bar{\alpha}_1 + \xi_2 + \bar{\omega}^T\theta + \varepsilon_2 - b(\dot{y}_r + \bar{\alpha}_1)\tilde{\rho} + bz_2. \quad (2.47)$$

Then the choice

$$\bar{\alpha}_1 = -c_1z_1 - d_1z_1 - \xi_2 - \bar{\omega}^T\hat{\theta} \quad (2.48)$$

results in the system

$$\dot{z}_1 = -c_1z_1 - d_1z_1 + \varepsilon_2 + \bar{\omega}^T\tilde{\theta} - b(\dot{y}_r + \bar{\alpha}_1)\tilde{\rho} + bz_2. \quad (2.49)$$

We stress that (2.49) along with (2.16) would be globally asymptotically stable if $\tilde{\theta}$, $\tilde{\rho}$ and z_2 were zero. With (2.42), (2.46), and (2.36), we have

$$\begin{aligned}\bar{\omega}^T\tilde{\theta} + bz_2 &= \bar{\omega}^T\tilde{\theta} + \tilde{b}z_2 + \hat{b}z_2 \\ &= \bar{\omega}^T\tilde{\theta} + \underbrace{(\lambda_2 - \hat{\rho}\dot{y}_r - \alpha_1)}_{z_2} \underbrace{e_1^T\tilde{\theta}}_{\tilde{b}} + \hat{b}z_2 \\ &= \underbrace{\bar{\omega}^T\tilde{\theta}}_{\omega^T\tilde{\theta}} + \lambda_2 e_1^T\tilde{\theta} - \hat{\rho}(\dot{y}_r + \bar{\alpha}_1)e_1^T\tilde{\theta} + \hat{b}z_2 \\ &= (\omega - \hat{\rho}(\dot{y}_r + \bar{\alpha}_1)e_1)^T\tilde{\theta} + \hat{b}z_2.\end{aligned}\quad (2.50)$$

Substituting (2.50) into (2.49) we get

$$\dot{z}_1 = -c_1z_1 - d_1z_1 + \varepsilon_2 + (\omega - \hat{\rho}(\dot{y}_r + \bar{\alpha}_1)e_1)^T\tilde{\theta} - b(\dot{y}_r + \bar{\alpha}_1)\tilde{\rho} + \hat{b}z_2. \quad (2.51)$$

This system along with (2.16) is to be stabilized by selecting update laws for the parameter estimates $\hat{\theta}$ and $\hat{\rho}$. These update laws will be chosen to achieve stability with respect to the Lyapunov function

$$V_1 = \frac{1}{2}z_1^2 + \frac{1}{2}\tilde{\theta}^T\Gamma^{-1}\tilde{\theta} + \frac{|b|}{2\gamma}\tilde{\rho}^2 + \frac{1}{4d_1}\varepsilon^T P\varepsilon \quad (2.52)$$

We examine the derivative of V_1 :

$$\begin{aligned}
\dot{V}_1 &= z_1 \left[-c_1 z_1 - d_1 z_1 + \varepsilon_2 + (\omega - \hat{\varrho}(\dot{y}_r + \bar{\alpha}_1)e_1^T)\tilde{\theta} - b(\dot{y}_r + \bar{\alpha}_1)\tilde{\varrho} + \hat{b}z_2 \right] \\
&\quad - \tilde{\theta}^T \Gamma^{-1} \dot{\hat{\theta}} - \frac{|b|}{\gamma} \tilde{\varrho} \dot{\hat{\varrho}} - \frac{1}{4d_1} \varepsilon^T \varepsilon \\
&= -c_1 z_1^2 + \hat{b}z_1 z_2 - |b| \frac{1}{\gamma} \left[\gamma \operatorname{sgn}(b)(\dot{y}_r + \bar{\alpha}_1)z_1 + \dot{\hat{\varrho}} \right] \\
&\quad + \tilde{\theta}^T \Gamma^{-1} \left[\Gamma(\omega - \hat{\varrho}(\dot{y}_r + \bar{\alpha}_1)e_1)z_1 - \dot{\hat{\theta}} \right] - d_1 z_1^2 + z_1 \varepsilon_2 - \frac{1}{4d_1} \varepsilon^T \varepsilon.
\end{aligned} \tag{2.53}$$

To eliminate the unknown indefinite $\tilde{\theta}$, $\tilde{\varrho}$ -terms in (2.53) we choose

$$\dot{\hat{\varrho}} = -\gamma \operatorname{sgn}(b)(\dot{y}_r + \bar{\alpha}_1)z_1, \quad \gamma > 0 \tag{2.54}$$

and $\dot{\hat{\theta}} = \Gamma \tau_1$, where

$$\tau_1 = (\omega - \hat{\varrho}(\dot{y}_r + \bar{\alpha}_1)e_1)z_1. \tag{2.55}$$

We do not use $\dot{\hat{\theta}} = \Gamma \tau_1$ as the update law for $\hat{\theta}$, because θ will reappear in subsequent steps. However, ϱ will not reappear, so we do use (2.54) as the actual **update law** for $\hat{\varrho}$. We retain (2.55) as our first **tuning function** for $\hat{\theta}$. Substituting (2.54) and (2.55) into (2.53), we obtain

$$\dot{V}_1 \leq -c_1 z_1^2 + \hat{b}z_1 z_2 + \tilde{\theta}^T \left(\tau_1 - \Gamma^{-1} \dot{\hat{\theta}} \right). \tag{2.56}$$

We pause to determine the arguments of the function α_1 . By examining (2.48) along with (2.37), we see that α_1 is a function of $y, \eta, \hat{\theta}, \hat{\varrho}$, and y_r .

Step 2. Differentiating (2.42) with the help of the second equation in (2.40) we obtain

$$\begin{aligned}
\dot{z}_2 &= \dot{\lambda}_2 - \hat{\rho}\ddot{y}_r - \dot{\hat{\rho}}\dot{y}_r - \dot{\alpha}_1(y, \eta, \hat{\theta}, \hat{\rho}, y_r) \\
&= \lambda_3 - k_2\lambda_1 - \hat{\rho}\ddot{y}_r - \dot{\hat{\rho}}\dot{y}_r - \frac{\partial\alpha_1}{\partial y} \underbrace{(\xi_2 + \omega^T\theta + \varepsilon_2)}_y \\
&\quad - \frac{\partial\alpha_1}{\partial\eta} \underbrace{(A_0\eta + e_3y)}_{\dot{\eta}} - \frac{\partial\alpha_1}{\partial y_r}\dot{y}_r - \frac{\partial\alpha_1}{\partial\hat{\theta}}\dot{\hat{\theta}} - \frac{\partial\alpha_1}{\partial\hat{\rho}}\dot{\hat{\rho}} \\
&\triangleq \lambda_3 - \beta_2 - \hat{\rho}\ddot{y}_r - \frac{\partial\alpha_1}{\partial y} (\omega^T\tilde{\theta} + \varepsilon_2) - \frac{\partial\alpha_1}{\partial\hat{\theta}}\dot{\hat{\theta}}, \tag{2.57}
\end{aligned}$$

where β_2 is a function of available signals:

$$\begin{aligned}
\beta_2 &= k_2\lambda_1 + \frac{\partial\alpha_1}{\partial y} (\xi_2 + \omega^T\hat{\theta}) + \frac{\partial\alpha_1}{\partial\eta} (A_0\eta + e_ny) \\
&\quad + \frac{\partial\alpha_1}{\partial y_r}\dot{y}_r + \left(\dot{y}_r + \frac{\partial\alpha_1}{\partial\hat{\rho}}\right)\dot{\hat{\rho}}. \tag{2.58}
\end{aligned}$$

Noting from (2.43) that $\lambda_3 - \hat{\rho}\ddot{y}_r = z_3 + \alpha_2$, we get

$$\dot{z}_2 = \alpha_2 - \beta_2 - \frac{\partial\alpha_1}{\partial y} (\omega^T\tilde{\theta} + \varepsilon_2) - \frac{\partial\alpha_1}{\partial\hat{\theta}}\dot{\hat{\theta}} + z_3. \tag{2.59}$$

Since our system is augmented by the new state z_2 , we augment the Lyapunov function (2.52) as

$$V_2 = V_1 + \frac{1}{2}z_2^2 + \frac{1}{4d_2}\varepsilon^T P\varepsilon, \tag{2.60}$$

where another ε -term was included to account for the presence of ε_2 in (2.59). In view of (2.56), (2.59), and (2.16), the derivative of V_2 satisfies

$$\begin{aligned}
\dot{V}_2 &\leq -c_1 z_1^2 + b z_1 z_2 + \tilde{\theta}^T \left(\tau_1 - \Gamma^{-1} \dot{\hat{\theta}} \right) \\
&\quad + z_2 \left[\alpha_2 - \beta_2 - \frac{\partial \alpha_1}{\partial y} \left(\omega^T \tilde{\theta} + \varepsilon_2 \right) - \frac{\partial \alpha_1}{\partial \hat{\theta}} \dot{\hat{\theta}} + z_3 \right] - \frac{1}{4d_2} \varepsilon^T \varepsilon \\
&\leq -c_1 z_1^2 + z_2 z_3 + \tilde{\theta}^T \left(\tau_1 - \frac{\partial \alpha_1}{\partial y} \omega z_2 - \Gamma^{-1} \dot{\hat{\theta}} \right) \\
&\quad + z_2 \left[\alpha_2 + \hat{b} z_1 - \beta_2 - \frac{\partial \alpha_1}{\partial \hat{\theta}} \dot{\hat{\theta}} \right] - z_2 \frac{\partial \alpha_1}{\partial y} \varepsilon_2 - \frac{1}{4d_2} \varepsilon_2^2 \\
&= -c_1 z_1^2 + z_2 z_3 + \tilde{\theta}^T \left(\tau_1 - \frac{\partial \alpha_1}{\partial y} \omega z_2 - \Gamma^{-1} \dot{\hat{\theta}} \right) \\
&\quad + z_2 \left[\alpha_2 + \hat{b} z_1 - \beta_2 - \frac{\partial \alpha_1}{\partial \hat{\theta}} \dot{\hat{\theta}} \right] \\
&\quad + d_2 \left(\frac{\partial \alpha_1}{\partial y} \right)^2 z_2^2 - d_2 \left(z_2 \frac{\partial \alpha_1}{\partial y} + \frac{1}{2d_2} \varepsilon_2 \right)^2. \tag{2.61}
\end{aligned}$$

The elimination of the unknown indefinite $\tilde{\theta}$ -term from (2.61) can be achieved with the update law $\dot{\hat{\theta}} = \Gamma \tau_2$, where

$$\tau_2 = \tau_1 - \frac{\partial \alpha_1}{\partial y} \omega z_2. \tag{2.62}$$

Then, if z_3 were zero, the stabilization function

$$\alpha_2 = -c_2 z_2 - d_2 \left(\frac{\partial \alpha_1}{\partial y} \right)^2 z_2^2 - \hat{b} z_1 + \beta_2 + \frac{\partial \alpha_1}{\partial \hat{\theta}} \Gamma \tau_2 \tag{2.63}$$

would yield

$$\dot{V}_2 \leq -c_1 z_1^2 - c_2 z_2^2 - d_2 \left(z_2 \frac{\partial \alpha_1}{\partial y} + \frac{1}{2d_2} \varepsilon_2 \right)^2 \leq -c_1 z_1^2 - c_1 z_2^2. \tag{2.64}$$

However, since $z_3 \neq 0$, we do not use $\dot{\hat{\theta}} = \Gamma \tau_2$ as an update law. Instead, we retain τ_2 as our second tuning function and α_2 as our second stabilizing function. Upon the substitution into (2.61), we obtain

$$\dot{V}_2 \leq -c_1 z_1^2 - c_2 z_2^2 + z_2 z_3 + \tilde{\theta}^T \left(\tau_2 - \Gamma^{-1} \dot{\hat{\theta}} \right) + z_2 \frac{\partial \alpha_1}{\partial \hat{\theta}} \left(\Gamma \tau_2 - \dot{\hat{\theta}} \right). \tag{2.65}$$

Step 3. By differentiating (2.43) with the help of the third equation in (2.40), we have

$$\begin{aligned}
\dot{z}_3 &= \dot{\lambda}_3 - \hat{\rho}y_r^{(3)} - \dot{\hat{\rho}}\ddot{y}_r - \dot{\alpha}_2(y, \eta, \hat{\theta}, \hat{\rho}, \lambda_1, \lambda_2, y_r, \dot{y}_r) \\
&= u - k_3\lambda_1 - \hat{\rho}y_r^{(3)} - \dot{\hat{\rho}}\ddot{y}_r - \frac{\partial\alpha_2}{\partial y}\dot{y} - \frac{\partial\alpha_2}{\partial\eta}\dot{\eta} - \frac{\partial\alpha_2}{\partial\hat{\theta}}\dot{\hat{\theta}} \\
&\quad - \frac{\partial\alpha_2}{\partial\hat{\rho}}\dot{\hat{\rho}} - \frac{\partial\alpha_2}{\partial\lambda_1}\dot{\lambda}_1 - \frac{\partial\alpha_2}{\partial\lambda_2}\dot{\lambda}_2 - \frac{\partial\alpha_2}{\partial y_r}\dot{y}_r - \frac{\partial\alpha_2}{\partial\dot{y}_r}\dot{\ddot{y}}_r \\
&= u - k_3\lambda_1 - \hat{\rho}y_r^{(3)} - \dot{\hat{\rho}}\ddot{y}_r - \frac{\partial\alpha_2}{\partial y} \left(\xi_2 + \omega^T(\tilde{\theta} + \hat{\theta}) + \varepsilon_2 \right) \\
&\quad - \frac{\partial\alpha_2}{\partial\eta} (A_0\eta + e_3y) - \frac{\partial\alpha_2}{\partial\hat{\theta}}\dot{\hat{\theta}} - \frac{\partial\alpha_2}{\partial\hat{\rho}}\dot{\hat{\rho}} - \frac{\partial\alpha_2}{\partial\lambda_1}(-k_1\lambda_1 + \lambda_2) \\
&\quad - \frac{\partial\alpha_2}{\partial\lambda_2}(-k_2\lambda_1 + \lambda_3) - \frac{\partial\alpha_2}{\partial y_r}\dot{y}_r - \frac{\partial\alpha_2}{\partial\dot{y}_r}\dot{\ddot{y}}_r \\
&= u - \hat{\rho}y_r^{(3)} - \beta_3 - \frac{\partial\alpha_2}{\partial y} \left(\omega^T\tilde{\theta} + \varepsilon_2 \right) - \frac{\partial\alpha_2}{\partial\hat{\theta}}\dot{\hat{\theta}}, \tag{2.66}
\end{aligned}$$

where

$$\begin{aligned}
\beta_3 &= k_3\lambda_1 + \frac{\partial\alpha_2}{\partial y}(\xi_2 + \omega^T\hat{\theta}) + \frac{\partial\alpha_2}{\partial\eta}(A_0\eta + e_3y) + \frac{\partial\alpha_2}{\partial y_r}\dot{y}_r + \frac{\partial\alpha_2}{\partial\dot{y}_r}\dot{\ddot{y}}_r \\
&\quad + \frac{\partial\alpha_2}{\partial\lambda_1}(-k_1\lambda_1 + \lambda_2) + \frac{\partial\alpha_2}{\partial\lambda_2}(-k_2\lambda_1 + \lambda_3) + \left(\dot{y}_r + \frac{\partial\alpha_2}{\partial\hat{\rho}} \right) \dot{\hat{\rho}}. \tag{2.67}
\end{aligned}$$

If we define

$$\alpha_3 = u - \hat{\rho}y_r^{(3)}, \tag{2.68}$$

we can write

$$\dot{z}_3 = \alpha_3 - \beta_3 - \frac{\partial\alpha_2}{\partial y} \left(\omega^T\tilde{\theta} + \varepsilon_2 \right) - \frac{\partial\alpha_2}{\partial\hat{\theta}}\dot{\hat{\theta}}. \tag{2.69}$$

Since our system is augmented by the new state z_3 , we also augment the Lyapunov function (2.60):

$$V_3 = V_2 + \frac{1}{2}z_3^2 + \frac{1}{4d_3}\varepsilon^T P \varepsilon. \tag{2.70}$$

In view of (2.65), (2.69), and (2.16), the derivative of V_3 is

$$\begin{aligned} \dot{V}_3 &\leq -c_1 z_1^2 - c_2 z_2^2 \\ &\quad + \tilde{\theta}^T \left(\tau_2 - \frac{\partial \alpha_2}{\partial y} \omega z_3 - \Gamma^{-1} \dot{\hat{\theta}} \right) + z_2 \frac{\partial \alpha_1}{\partial \hat{\theta}} \left(\Gamma \tau_2 - \dot{\hat{\theta}} \right) \\ &\quad + z_3 \left(\alpha_3 + z_2 - \beta_3 - \frac{\partial \alpha_2}{\partial \hat{\theta}} \dot{\hat{\theta}} \right) - z_3 \frac{\partial \alpha_2}{\partial y} \varepsilon_2 - \frac{1}{4d_3} \varepsilon_2^2. \end{aligned} \quad (2.71)$$

As in the previous steps, for the elimination of the unknown indefinite $\dot{\hat{\theta}}$ -term from (2.71), we can choose the update law

$$\dot{\hat{\theta}} = \Gamma \tau_3, \quad (2.72)$$

where

$$\tau_3 = \tau_2 - \frac{\partial \alpha_2}{\partial y} \omega z_3. \quad (2.73)$$

Noting that

$$\Gamma \tau_2 - \dot{\hat{\theta}} = \Gamma \tau_2 - \Gamma \tau_3 + \Gamma \tau_3 - \dot{\hat{\theta}} = \Gamma \frac{\partial \alpha_2}{\partial y} \omega z_3 + \left(\Gamma \tau_3 - \dot{\hat{\theta}} \right), \quad (2.74)$$

(2.71) becomes

$$\begin{aligned} \dot{V}_3 &\leq -c_1 z_1^2 - c_2 z_2^2 \\ &\quad + \tilde{\theta}^T \left(\tau_3 - \Gamma^{-1} \dot{\hat{\theta}} \right) + z_2 \frac{\partial \alpha_1}{\partial \hat{\theta}} \left(\Gamma \tau_3 - \dot{\hat{\theta}} \right) + z_2 \frac{\partial \alpha_1}{\partial \hat{\theta}} \Gamma \frac{\partial \alpha_2}{\partial y} \omega z_3 \\ &\quad + z_3 \left(\alpha_3 + z_2 - \beta_3 - \frac{\partial \alpha_2}{\partial \hat{\theta}} \dot{\hat{\theta}} \right) \\ &\quad + d_3 \left(\frac{\partial \alpha_2}{\partial y} \right)^2 z_3^2 - d_3 \left(z_3 \frac{\partial \alpha_2}{\partial y} + \frac{1}{2d_3} \varepsilon_2 \right)^2 \\ &\leq -c_1 z_1^2 - c_2 z_2^2 + \tilde{\theta}^T \left(\tau_3 - \Gamma^{-1} \dot{\hat{\theta}} \right) + z_2 \frac{\partial \alpha_1}{\partial \hat{\theta}} \left(\Gamma \tau_3 - \dot{\hat{\theta}} \right) \\ &\quad + z_3 \left(\alpha_3 + z_2 - \beta_3 - \frac{\partial \alpha_2}{\partial \hat{\theta}} \dot{\hat{\theta}} + z_2 \frac{\partial \alpha_1}{\partial \hat{\theta}} \Gamma \frac{\partial \alpha_2}{\partial y} \omega \right) \\ &\quad + d_3 \left(\frac{\partial \alpha_2}{\partial y} \right)^2 z_3^2. \end{aligned} \quad (2.75)$$

Remembering that our actual update law for $\hat{\theta}$ is $\dot{\hat{\theta}} = \Gamma\tau_3$ and the choice of the stabilization function as

$$\alpha_3 = -c_3 z_3 - d_3 \left(\frac{\partial \alpha_2}{\partial y} \right)^2 z_3 - z_2 + \beta_3 + \frac{\partial \alpha_2}{\partial \hat{\theta}} \Gamma \tau_3 - z_2 \frac{\partial \alpha_1}{\partial \hat{\theta}} \Gamma \frac{\partial \alpha_2}{\partial y} \omega \quad (2.76)$$

makes \dot{V}_3 negative semidefinite:

$$\dot{V}_3 \leq -c_1 z_1^2 - c_2 z_2^2 - c_3 z_3^2. \quad (2.77)$$

The control law (2.68) which has helped us to achieve (2.77) is our actual control law:

$$u = \alpha_3 + \hat{\rho} y_r^{(3)}. \quad (2.78)$$

The resulting error system is

$$\begin{aligned} \dot{z}_1 &= -c_1 z_1 - d_1 z_1 + \hat{b} z_2 + \varepsilon_2 + (\omega - \hat{\rho}(\dot{y}_r + \bar{\alpha}_1) e_1)^T \tilde{\theta} \\ &\quad - b(\dot{y}_r + \bar{\alpha}_1) \tilde{\rho} \end{aligned} \quad (2.79)$$

$$\begin{aligned} \dot{z}_2 &= -c_2 z_2 - d_2 \left(\frac{\partial \alpha_1}{\partial y} \right)^2 z_2 - \hat{b} z_1 + z_3 - \frac{\partial \alpha_1}{\partial \hat{\theta}} (\dot{\hat{\theta}} - \Gamma \tau_2) \\ &\quad - \frac{\partial \alpha_1}{\partial y} \varepsilon_2 - \frac{\partial \alpha_1}{\partial y} \omega^T \tilde{\theta} \end{aligned} \quad (2.80)$$

$$\begin{aligned} \dot{z}_3 &= -c_3 z_3 - d_3 \left(\frac{\partial \alpha_2}{\partial y} \right)^2 z_3 - z_2 - \frac{\partial \alpha_1}{\partial \hat{\theta}} \Gamma \frac{\partial \alpha_2}{\partial y} z_2 \\ &\quad - \frac{\partial \alpha_2}{\partial \hat{\theta}} (\dot{\hat{\theta}} - \Gamma \tau_3) - \frac{\partial \alpha_2}{\partial y} \varepsilon_2 - \frac{\partial \alpha_2}{\partial y} \omega^T \tilde{\theta}. \end{aligned} \quad (2.81)$$

In view of (2.62) and (2.73) we have

$$\dot{\hat{\theta}} - \Gamma \tau_2 = \Gamma \tau_3 - \Gamma \tau_2 = \Gamma(\tau_3 - \tau_2) = -\Gamma \frac{\partial \alpha_2}{\partial y} \omega z_3 \quad (2.82)$$

$$\begin{aligned} \dot{\hat{\theta}} - \Gamma \tau_1 &= \Gamma \tau_3 - \Gamma \tau_1 = (\Gamma \tau_3 - \Gamma \tau_2) + (\Gamma \tau_2 - \Gamma \tau_1) \\ &\quad - \Gamma \frac{\partial \alpha_2}{\partial y} \omega z_3 - \Gamma \frac{\partial \alpha_1}{\partial y} \omega z_2. \end{aligned} \quad (2.83)$$

Defining

$$\sigma_{ij} \triangleq \frac{\partial \alpha_{i-1}}{\partial \hat{\theta}} \Gamma \frac{\partial \alpha_{j-1}}{\partial y} \omega, \quad (2.84)$$

(2.82)-(2.83) yields

$$-\frac{\partial \alpha_1}{\partial \hat{\theta}} \left(\dot{\hat{\theta}} - \Gamma \tau_2 \right) = \sigma_{23} z_3. \quad (2.85)$$

By substituting (2.85), we bring the error system (2.79)-(2.81) into the compact form

$$\dot{z} = A_z(z, t)z + W_\varepsilon(z, t)\varepsilon_2 + W_\theta(z, t)^\top \tilde{\theta} - b(\dot{y}_r + \bar{\alpha}_1)e_1 \tilde{\varrho}, \quad (2.86)$$

where the system matrix $A_z(z, t)$ is given by

$$A_z(z, t) = \begin{bmatrix} -c_1 - d_1 & \hat{b} & 0 \\ -\hat{b} & -c_2 - d_2 \left(\frac{\partial \alpha_1}{\partial y} \right)^2 & 1 + \sigma_{23} \\ 0 & -1 - \sigma_{23} & -c_3 - d_3 \left(\frac{\partial \alpha_2}{\partial y} \right)^2 \end{bmatrix} \quad (2.87)$$

and $W_\varepsilon(z, t)$ and $W_\theta(z, t)$ are

$$W_\varepsilon(z, t) = \begin{bmatrix} 1 \\ -\frac{\partial \alpha_1}{\partial y} \\ -\frac{\partial \alpha_2}{\partial y} \end{bmatrix} \quad (2.88)$$

$$W_\theta(z, t)^\top = W_\varepsilon(z, t)\omega^\top - \hat{\varrho}(\dot{y}_r + \bar{\alpha}_1)e_1 e_1^\top. \quad (2.89)$$

In a generic case, i.e., when we consider linear single-input single-output systems

$$y(s) = \frac{b_m s^m + \dots + b_1 s + b_0}{s^n + a_{n-1} s^{n-1} + \dots + a_1 s + a_0}, \quad (2.90)$$

the design of the control law is analogous to the preceding description, but an extra assumption is needed:

Assumption 3 The plant is minimum-phase, i.e., the polynomial $B(s) = b_m s^m + \dots + b_1 s + b_0$ is Hurwitz.

We can summarize the tuning functions design for linear systems in the generic case as follows:

Error variables

$\begin{aligned} z_1 &= y - y_r \\ z_i &= v_{m,i} - \hat{\varrho} y_r^{(i-1)} - \alpha_{i-1}, \quad i = 2, \dots, \rho \end{aligned}$

Stabilizing functions

$$\begin{aligned}
\alpha_1 &= \hat{\rho}\bar{\alpha}_1 \\
\bar{\alpha}_1 &= -(c_1 + d_1)z_1 - \xi_2 - \bar{\omega}^T\hat{\theta} \\
\alpha_2 &= -\hat{b}_m z_1 - \left[c_2 + d_2 \left(\frac{\partial \alpha_1}{\partial y} \right)^2 \right] z_2 + \beta_2 + \frac{\partial \alpha_1}{\partial \hat{\theta}} \Gamma \tau_2 \\
\alpha_i &= -z_{i-1} - \left[c_i + d_i \left(\frac{\partial \alpha_{i-1}}{\partial y} \right)^2 \right] z_i + \beta_i + \frac{\partial \alpha_{i-1}}{\partial \hat{\theta}} \Gamma \tau_i \\
&\quad - \sum_{j=2}^{i-1} \frac{\partial \alpha_{j-1}}{\partial \hat{\theta}} \Gamma \frac{\partial \alpha_{i-1}}{\partial y} z_j \omega, \quad i = 3, \dots, \rho \\
\beta_i &= \frac{\partial \alpha_{i-1}}{\partial y} (\xi_2 + \omega^T \hat{\theta}) + \frac{\partial \alpha_{i-1}}{\partial \eta} (A_0 \eta + e_n y) + \sum_{j=1}^{i-1} \frac{\partial \alpha_{i-1}}{\partial y_r^{(j-1)}} y_r^{(j)} + k_i v_{m,1} \\
&\quad + \sum_{j=1}^{m+i-1} \frac{\partial \alpha_{i-1}}{\partial \lambda_j} (-k_j \lambda_1 + \lambda_{j+1}) + \left(y_r^{(i-1)} + \frac{\partial \alpha_{i-1}}{\partial \hat{\rho}} \right) \hat{\rho}
\end{aligned}$$

Tuning functions

$$\begin{aligned}
\tau_1 &= (\omega - \hat{\rho}(\dot{y}_r + \bar{\alpha}_1)e_1)z_1 \\
\tau_i &= \tau_{i-1} - \frac{\partial \alpha_{i-1}}{\partial y} \omega z_i, \quad i = 2, \dots, \rho
\end{aligned}$$

Parameter update laws

$$\begin{aligned}
\dot{\hat{\theta}} &= \Gamma \tau_\rho \\
\dot{\hat{\rho}} &= -\gamma \text{sgn}(b_m)(\dot{y}_r + \bar{\alpha}_1)z_1
\end{aligned}$$

Adaptive control law

$$u = \alpha_\rho - v_{m,\rho+1} + \hat{\rho} y_r^{(\rho)}$$

2.2.2 Stability analysis

For the adaptive scheme developed in the previous subsection, we establish the following result. In a generic case, both the result and its proof are done in a similar way.

Theorem 1 (Tuning Functions) [KKK95, Chapter 10] All the signals in the closed-loop adaptive system consisting of the plant (2.1), the control (2.78) and update laws (2.54)-(2.72) and filters in Table 2.1 are **globally uniformly bounded**, and asymptotic tracking is achieved:

$$\lim_{t \rightarrow \infty} [y(t) - y_r(t)] = 0 \quad (2.91)$$

Proof. Due to the piecewise continuity of $y_r(t), \dot{y}_r(t), \ddot{y}_r(t)$ and $y_r^{(3)}(t)$ (Assumption 2) and the smoothness of the control law (see eq. (2.78)), the update law and the filters, the solution of the closed-loop adaptive system exists and is unique. Let its maximum interval of existence be $[0, t_f)$. Let us consider the Lyapunov function

$$V_3 = \frac{1}{2} z^T z + \frac{1}{2} \sum_{k=1}^3 \frac{1}{4d_k} \varepsilon^T P \varepsilon + \frac{1}{2} \tilde{\theta}^T \Gamma^{-1} \tilde{\theta} + \frac{|b_m|}{2\gamma} \tilde{\varrho}^2. \quad (2.92)$$

In (2.77) we established that $V_3(t)$ is nonincreasing $\left(\dot{V}_3 \leq - \sum_{k=1}^3 c_k z_k^2 \right)$.

Hence, $z, \hat{\theta}, \hat{\varrho}$, and ε are bounded on $[0, t_f)$. Since z_1 and y_r are bounded, y is also bounded ($z_1 = y - y_r$). Then, from (2.24) ($\dot{\eta} = A_0 \eta + e_3 y$) we conclude that η is bounded. Our main concern is λ because the boundedness of x will be immediate from the boundedness of ε, η and λ . From (2.19) $\left(\dot{\lambda} = A_0 \lambda + e_3 u \right)$ it follows that

$$\lambda_i(s) = \frac{s^{i-1} + k_1 s^{i-2} + \dots + k_{i-1}}{K(s)} u(s), \quad i = 1, 2, 3, \quad (2.93)$$

where $K(s) = s^3 + k_1 s^2 + k_2 s + k_3$. By substituting (2.1) we get

$$\lambda_i(s) = \frac{(s^{i-1} + k_1 s^{i-2} + \dots + k_{i-1}) A(s)}{K(s) B(s)} y(s), \quad i = 1, 2, 3. \quad (2.94)$$

In view of the boundedness of y and the plant is minimum phase, the last expression proves that λ_1 is bounded. We now return to the coordinate change (2.41)-(2.43) which gives

$$\lambda_2 = z_2 + \hat{\varrho} \dot{y}_r + \alpha_1(y, \eta, \hat{\theta}, \hat{\varrho}, y_r) \quad (2.95)$$

$$\lambda_3 = z_3 + \hat{\varrho} \ddot{y}_r + \alpha_2(y, \eta, \hat{\theta}, \hat{\varrho}, \lambda_1, \lambda_2, y_r, \dot{y}_r). \quad (2.96)$$

The boundedness of z_2 and $y, \eta, \hat{\theta}, \hat{\varrho}, y_r$ and \dot{y}_r proves that λ_2 is bounded. The boundedness of $\lambda_1, \lambda_2, z_3, y, \eta, \hat{\theta}, \hat{\varrho}, y_r$ and \dot{y}_r proves that λ_3 is also bounded. Finally, in view of (2.30) and the boundedness of η, λ , and ε , we conclude that x is bounded.

We have thus shown that all the signals of the closed-loop adaptive system are bounded on $[0, t_f)$ by constants depending only on the initial conditions, design gains, and the external signals $y_r(t), \dots, y_r^{(n)}(t)$, but not on t_f . The independence of the bound of t_f proves that $t_f = \infty$. Hence, all signals are globally uniformly bounded on $[0, \infty)$.

By applying the LaSalle-Yoshizawa theorem to (2.77), it further follows that $z(t) \rightarrow 0$ as $t \rightarrow \infty$, which implies that

$$\lim_{t \rightarrow \infty} [y(t) - y_r(t)] = 0,$$

as we wanted. \square

Theorem 1 establishes global uniform boundedness of all signals but not global uniform stability of individual trajectories.

- We now determine an error system which translates the investigated system to the origin.
- Then we prove that the equilibrium at the origin is globally uniformly stable, and all the error states except the parameter error are regulated to zero.

We start with the subsystem $(z, \varepsilon, \tilde{\theta}, \tilde{\varrho})$ whose 10 states are encompassed by the Lyapunov function (2.92), and construct additional equations to form a complete error system. We first introduce the equation for the reference signal η^r

$$\dot{\eta}^r = A_0 \eta^r + e_3 y_r, \quad (2.97)$$

so that the error state $\tilde{\eta} = \eta - \eta^r$ is governed by

$$\dot{\tilde{\eta}} = A_0 \tilde{\eta} + e_3 z_1. \quad (2.98)$$

The system $(z, \varepsilon, \tilde{\eta}, \tilde{\theta}, \tilde{\varrho})$ has 13 states as the original $(x, \eta, \lambda, \hat{\theta}, \hat{\varrho})$ system.

We have now characterized the error system

$$\dot{z} = A_z(z, t)z + W_\varepsilon(z, t)\varepsilon_2 + W_\theta(z, t)^T \tilde{\theta} - b(\dot{y}_r + \bar{\alpha}_1)e_1 \tilde{\varrho} \quad (2.99)$$

$$\dot{\varepsilon} = A_0 \varepsilon \quad (2.100)$$

$$\dot{\tilde{\eta}} = A_0 \tilde{\eta} + e_3 z_1 \quad (2.101)$$

$$\dot{\tilde{\theta}} = -\Gamma W_\theta(z, t)z \quad (2.102)$$

$$\dot{\tilde{\varrho}} = \gamma \operatorname{sgn}(b)(\dot{y}_r + \bar{\alpha}_1)e_1^T z \quad (2.103)$$

which possesses the desired stability and regulation properties.

Corollary 1 The error system (2.99)-(2.103) has a globally uniformly stable equilibrium at the origin. Moreover, its 13-dimensional state converges to the 9-dimensional manifold

$$M = \{z = 0, \varepsilon = 0, \tilde{\eta} = 0\}. \quad (2.104)$$

Corollary 1 has not dealt with a correspondence between the original system $(x, \lambda, \eta, \hat{\theta}, \hat{\varrho})$ and the error system $(z, \varepsilon, \tilde{\eta}, \tilde{\theta}, \tilde{\varrho})$, which can be done by analyzing the coordinate change

$$(x, \lambda, \eta, \hat{\theta}, \hat{\varrho}) \mapsto (z, \varepsilon, \tilde{\eta}, \tilde{\theta}, \tilde{\varrho}). \quad (2.105)$$

Whenever $B(s)$ and $K(s)$ are coprime, this coordinate change is a global \mathcal{C}^∞ -diffeomorphism for each $t \geq 0$. Although the coprimeness condition cannot be guaranteed by design because the coefficients of $B(s)$ are unknown, it is satisfied with probability one.

2.2.3 Transient performance with tuning functions

In the absence of disturbances and unmodeled dynamics, the tracking error of most adaptive control schemes converges to zero, that is, they try to achieve the stated asymptotic performance objective. In applications, however, the system's transient performance is also important.

Transient performance of the adaptive system

We derive computable bounds on both \mathcal{L}_2 and \mathcal{L}_∞ norms of the states z and $\tilde{\eta}$ of the adaptive system, and we show how they can be made arbitrarily small by a choice of the design parameters $c_1, c_2, c_3, d_1, d_2, d_3$ and Γ .

Theorem 2 (\mathcal{L}_2 performance) [KKK95, Chapter 10] The \mathcal{L}_2 norms of the states z and $\tilde{\eta}$ of the adaptive system (2.99)-(2.102), are bounded by

$$\|z\|_2 \leq \frac{1}{\sqrt{c_0}} \sqrt{V_\rho(0)} \quad (2.106)$$

$$\|\tilde{\eta}\|_2 \leq \frac{1}{\sqrt{c_0}} \sqrt{V_\rho(0)} \|W_{\tilde{\eta}}\|_\infty \quad (2.107)$$

where $\|W_{\tilde{\eta}}\|_\infty$ is independent of c_0, d_0 and Γ .

Proof. As shown in (2.77) $\left(\dot{V}_3 \leq -c_1 z_1^2 - c_2 z_2^2 - c_3 z_3^2\right)$, the derivative of V_3 along the solutions of (2.99)-(2.100) is

$$\dot{V}_3 \leq -c_0 |z|^2. \quad (2.108)$$

Since V_3 is nonincreasing, we have

$$\|z\|_2^2 = \int_0^\infty |z(\tau)|^2 d\tau \leq \frac{1}{c_0}(V_3(0) - V_3(\infty)) \leq \frac{1}{c_0}V_3(0), \quad (2.109)$$

which implies (2.106). From (2.100) and if we define $W_{\tilde{\eta}}(s) \triangleq (sI - A_0)^{-1}e_3$ we get

$$\|\tilde{\eta}\|_2^2 \leq \|W_{\tilde{\eta}}\|_\infty \|z_1\|_2 \leq \frac{1}{\sqrt{c_0}} \sqrt{V_\rho(0)} \|W_{\tilde{\eta}}\|_\infty. \quad (2.110)$$

□

The initial value of the Lyapunov function is

$$V_\rho(0) = \frac{1}{2}|z(0)|^2 + \frac{1}{4d_0}|\varepsilon|_P^2 + \frac{1}{2}|\tilde{\theta}(0)|_{\Gamma^{-1}}^2. \quad (2.111)$$

From (2.106) and (2.111) it may appear that by increasing c_0 we reduce the bound on $\|z\|_2$. This would be so only if $\varepsilon(0)$, $\tilde{\theta}(0)$, and $z(0)$ were independent on c_0 . While $\varepsilon(0)$, $\tilde{\theta}(0)$, and $z_1(0) = y(0) - y_r(0)$ are clearly independent of c_i , d_i , and Γ , the initial values $z_2(0)$, $z_3(0)$ depend on c_i , d_i , and Γ . Fortunately, we can set $z(0)$ to zero by appropriately *initializing the reference trajectory*. Following (2.41)-(2.43), $z(0)$ is set to zero by selecting

$$y_r(0) = y(0) \quad (2.112)$$

$$\dot{y}_r(0) = \frac{1}{\hat{\rho}(0)} \left[\lambda_2(0) - \alpha_1 \left(y(0), \eta(0), \hat{\theta}(0), \hat{\rho}(0), y_r(0) \right) \right] \quad (2.113)$$

$$\ddot{y}_r(0) = \frac{1}{\hat{\rho}(0)} \left[\lambda_3(0) - \alpha_2 \left(y(0), \eta(0), \hat{\theta}(0), \hat{\rho}(0), \lambda_1(0), \lambda_2(0), y_r(0), \dot{y}_r(0) \right) \right] \quad (2.114)$$

Since $b \neq 0$ it is reasonable to choose $\hat{b}(0) \neq 0$. Then the choice $\hat{\rho}(0) = 1/\hat{b}(0)$ makes (2.113)-(2.114) well-defined. Thus, by setting $z(0) = 0$, we make

$$V_3(0) = \frac{1}{4d_0}|\varepsilon|_P^2 + \frac{1}{2}|\tilde{\theta}(0)|_{\Gamma^{-1}}^2 \quad (2.115)$$

a decreasing function of d_0 and Γ , independent of c_0 . This means that the bounds resulting from (2.106) and (2.107) for $\Gamma = \gamma I$,

$$\|z\|_2 \leq \frac{1}{\sqrt{2c_0}} \left(\frac{1}{\gamma} |\tilde{\theta}(0)|^2 + \frac{1}{4d_0} |\varepsilon(0)|_P^2 \right)^{1/2} \quad (2.116)$$

$$\|\tilde{\eta}\|_2 \leq \frac{1}{\sqrt{2c_0}} \left(\frac{1}{\gamma} |\tilde{\theta}(0)|^2 + \frac{1}{4d_0} |\varepsilon(0)|_P^2 \right)^{1/2} \|W_{\tilde{\eta}}\|_\infty \quad (2.117)$$

$$(2.118)$$

can be systematically reduced either by increasing c_0 or by simultaneously increasing d_0 and γ . The possibility to improve performance with the adaptation gain γ is particularly clear in the case $\varepsilon(0) = 0$, when the \mathcal{L}_2 bounds of Theorem 2 become

$$\|z\|_2 \leq \frac{1}{\sqrt{2c_0\gamma}} |\tilde{\theta}(0)| \quad (2.119)$$

$$\|\tilde{\eta}\|_2 \leq \frac{1}{\sqrt{2c_0\gamma}} |\tilde{\theta}(0)| \|W_{\tilde{\eta}}\|_\infty. \quad (2.120)$$

For a further characterization of the achieved performance, we proceed to derive \mathcal{L}_∞ norm bound for the states of the adaptive system (2.99)-(2.102). These bounds are also useful for a comparison with nonadaptive systems.

We first give simple bounds on $\|z\|_\infty$ and $\|\tilde{\theta}\|_\infty$:

$$\|z\|_\infty \leq \sqrt{2V_3(0)} \quad (2.121)$$

$$\|\tilde{\theta}\|_\infty \leq \sqrt{\bar{\lambda}(\Gamma)} \sqrt{2V_3(0)}. \quad (2.122)$$

Since $\dot{V}_3 \leq 0$, the bound (2.121) follows immediately from

$$2V_3(t) = |z(t)|^2 + \frac{1}{2d_0} |\varepsilon(t)|_P^2 + |\tilde{\theta}(t)|_{\Gamma^{-1}}^2 \leq 2V_3(0), \quad (2.123)$$

and the bound (2.122) is obtained by noting that

$$\frac{1}{\bar{\lambda}(\Gamma)} |\tilde{\theta}|^2 \leq |\tilde{\theta}|_{\Gamma^{-1}}^2 \leq 2V_3(0). \quad (2.124)$$

For $\Gamma = \gamma I$, it further follows from (2.122)-(2.123) that

$$\|\tilde{\theta}\|_\infty \leq \sqrt{\gamma} |z(0)| + \sqrt{\frac{\gamma}{2d_0}} |\varepsilon(0)|_P + |\tilde{\theta}(0)|. \quad (2.125)$$

In this way, $\|\tilde{\theta}\|_\infty$ is explicitly related to initial conditions and design parameters.

Theorem 3 (\mathcal{L}_∞ Performance) [KKK95, Chapter 10] The states z and $\tilde{\eta}$ of the adaptive system (2.99)-(2.102) are bounded by

$$|z(t)| \leq \frac{1}{\sqrt{c_0 d_0}} M + |z(0)| e^{-c_0 t} \quad (2.126)$$

$$|\tilde{\eta}(t)| \leq \left(\frac{1}{\sqrt{c_0 d_0}} M + |z(0)| \right) \|w_{\tilde{\eta}}\|_1, \quad (2.127)$$

where

$$M \triangleq \frac{1}{2} \left\{ \sqrt{\lambda(\Gamma)} \sqrt{2V_3(0)} \left[\|h_\omega\|_1 \left(\sqrt{2V_3(0)} + \|y_r\|_\infty \right) + \kappa_\omega \right] + \frac{1}{\underline{\lambda}(P)} |\varepsilon(0)|_P \right\}, \quad (2.128)$$

and $\|w_{\tilde{\eta}}\|_1$, $\|w_{\tilde{\zeta}}\|_1$, $\|h_\omega\|_1$, and κ_ω are independent of c_0 , d_0 , and Γ .

Proof. Differentiating $\frac{1}{2}|z|^2$ along the solutions of (2.99), we get

$$\begin{aligned} \frac{d}{dt} \left(\frac{1}{2}|z|^2 \right) &= - \sum_{k=1}^3 c_k z_k^2 - \sum_{k=1}^3 d_k z_k^2 \left(\frac{\partial \alpha_{k-1}}{\partial y} \right)^2 \\ &\quad - \sum_{k=1}^3 z_k \frac{\partial \alpha_{k-1}}{\partial y} \left(\tilde{\theta}^T \omega + \varepsilon_2 \right) \\ &\leq -c_0 |z|^2 + \frac{1}{4d_0} \left(\tilde{\theta}^T \omega + \varepsilon_2 \right)^2. \end{aligned} \quad (2.129)$$

Lemma 1 Let v and ρ be real-valued functions defined on \mathbb{R}_+ , and let b and c be positive constants. If they satisfy the differential inequality

$$\dot{v} \leq -cv + b\rho(t)^2, \quad v(0) \geq 0,$$

then the following holds:

(i) If $\rho \in \mathcal{L}_\infty$, then $v \in \mathcal{L}_\infty$ and

$$v(t) \leq v(0)e^{-ct} + \frac{b}{c} \|\rho\|_\infty^2.$$

By applying Lemma 1, we obtain

$$|z(t)|^2 \leq |z(0)|^2 e^{-2c_0 t} + \frac{1}{4c_0 d_0} \|\tilde{\theta}^T \omega + \varepsilon_2\|_\infty^2. \quad (2.130)$$

From (2.16) ($\dot{\varepsilon} = A_0 \varepsilon$) and (2.13) ($PA_0 + A_0^T P = -I$, $P = P^T > 0$) we have $\frac{d}{dt} |\varepsilon|_P^2 \leq -|\varepsilon|^2$, which gives

$$\|\varepsilon_2\|_\infty^2 \leq \frac{1}{\underline{\lambda}(P)} |\varepsilon(0)|_P^2. \quad (2.131)$$

With (2.130) and (2.131) we obtain

$$|z(t)| \leq \frac{1}{2\sqrt{c_0 d_0}} \left(\|\tilde{\theta}\|_\infty \|\omega\|_\infty + \frac{1}{\sqrt{\underline{\lambda}(P)}} |\varepsilon(0)|_P \right) + |z(0)| e^{-c_0 t}. \quad (2.132)$$

We can express the regressor ω as

$$\omega = H_\omega(s)^1 y + \omega_0(t), \quad (2.133)$$

where

$$H_\omega(s) = \frac{s + k_1}{K(s)} \left[\frac{A(s)}{B(s)}, [s^2, s] \right]^T \quad (2.134)$$

and $|\omega_0(t)| \leq \kappa_\omega e^{-\sigma t}$ is the response due to the initial conditions of $\eta(0)$ and $\lambda(0)$, and κ_ω and σ depend only on the plant and filter parameters and not on c_0 , d_0 , and Γ . Now, using $y = z_1 + y_r$ and (2.121), we get

$$\begin{aligned} \|\omega\|_\infty &\leq \|h_\omega\|_1 (\|z_1\|_\infty + \|y_r\|_\infty) + \kappa_\omega e^{-\sigma t} \\ &\leq \|h_\omega\|_1 \left(\sqrt{2V_3(0)} + \|y_r\|_\infty \right) + \kappa_\omega, \end{aligned} \quad (2.135)$$

where $h_\omega(t)$ denotes the inverse Laplace transform of $H_\omega(s)$.

Substituting (2.135) into (2.132) and using (2.122) we obtain

$$\begin{aligned} |z(t)| &\leq \frac{1}{\sqrt{c_0 d_0}} \frac{1}{2} \left\{ \sqrt{\underline{\lambda}(\Gamma)} \sqrt{2V_3(0)} \left[\|h_\omega\|_1 \left(\sqrt{2V_3(0)} + \|y_r\|_\infty \right) + \kappa_\omega \right] \right. \\ &\quad \left. + \frac{1}{\sqrt{\underline{\lambda}(P)}} |\varepsilon(0)|_P \right\} + |z(0)| e^{-c_0 t} \\ &= \frac{1}{\sqrt{c_0 d_0}} M + |z(0)| e^{-c_0 t} \end{aligned} \quad (2.136)$$

¹ $H_\omega(s)$ is proper and stable, and its coefficients depend only on the plant parameters θ and the filter coefficients k_1, k_2, k_3 .

From (2.101)

$$\dot{\tilde{\eta}} = A_0 \tilde{\eta} + e_3 z_1 \quad (2.137)$$

$$W_{\tilde{\eta}}(s) \triangleq (sI - A_0)^{-1} e_3, \quad (2.138)$$

we get

$$|\tilde{\eta}(t)| \leq \|w_{\tilde{\eta}}\|_1 \|z_1\|_\infty \leq \left(\frac{1}{\sqrt{c_0 d_0}} M + |z(0)| \right) \|w_{\tilde{\eta}}\|_1. \quad (2.139)$$

□

A special form of the above \mathcal{L}_∞ bounds is more revealing.

Corollary 2 In the case $z(0) = 0, \varepsilon(0) = \eta(0) = \lambda(0) = 0$, and $\Gamma = \gamma I$, the \mathcal{L}_∞ bounds of Theorem 3 become

$$\|z\|_\infty \leq \frac{|\tilde{\theta}(0)| \|h_\omega\|_1}{2\sqrt{c_0 d_0}} \left(\|y_r\|_\infty + \frac{1}{\sqrt{\gamma}} |\tilde{\theta}(0)| \right) \quad (2.140)$$

$$\|\tilde{\eta}\|_\infty \leq \frac{|\tilde{\theta}(0)| \|h_\omega\|_1}{2\sqrt{c_0 d_0}} \left(\|y_r\|_\infty + \frac{1}{\sqrt{\gamma}} |\tilde{\theta}(0)| \right) \|w_{\tilde{\eta}}\|_1. \quad (2.141)$$

The assumption $z(0) = 0, \varepsilon(0) = \eta(0) = \lambda(0) = 0$ is satisfied in the particular case where $x(0) = \eta(0) = \lambda(0) = 0$ and the trajectory initialization is performed. In this case the system is driven only by the reference trajectory. The form in bounds in Corollary 2 clarifies the dependence of the \mathcal{L}_∞ performance on the parameter uncertainty $|\tilde{\theta}(0)|$ and the design parameters c_0, d_0 , and γ . Any increase on those parameters results in an improvement of the \mathcal{L}_∞ performance. It is of interest to observe that d_0 , present in the \mathcal{L}_∞ bounds (2.140)-(2.141), is absent from the \mathcal{L}_2 bounds (2.119)-(2.120).

2.3 Recent developments

An increasing interest in the backstepping based designs has been witnessed during the last few years, especially the adaptive version presented in Sections 2.1-2.2. In the following sections, we present the latest results with respect to the adaptive backstepping tuning functions design for linear systems. The research on this field can be organized in three categories: (1) stability and asymptotic performance (2) robustness and (3) transient performance.

For the sake of obtaining a global vision of the state-of-the-art in this field, we have depicted in Figure 2.2 a simple scheme with the different authors interested in adaptive backstepping for linear systems. We have also included in Figure 2.2 the papers as they are referenced in this work. The main topics of research covered in adaptive backstepping for linear systems can be found in Figure 2.3.

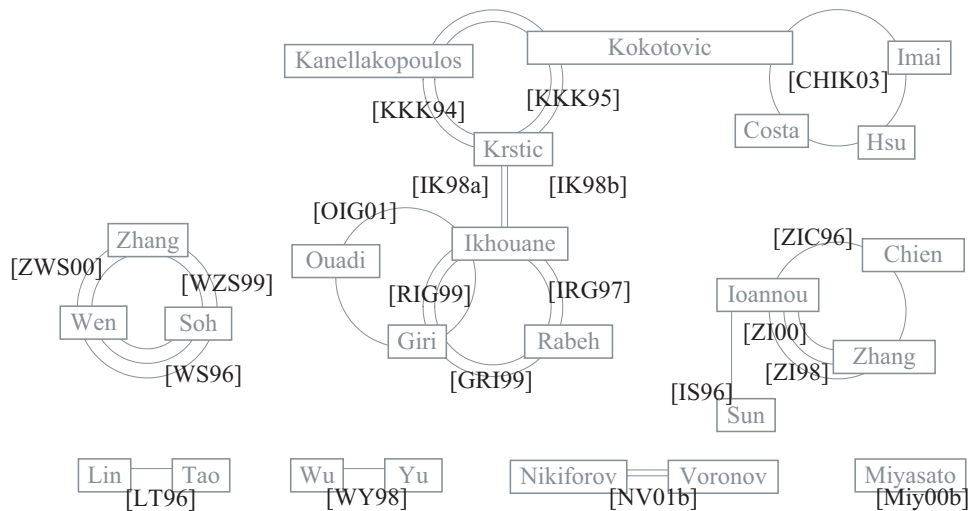


Figure 2.2. Different authors interested in adaptive backstepping for linear systems. Each line corresponds to a published paper.

STABILITY AND ASYMPTOTIC PERFORMANCE		
Paper		modifications
[GRI99]	plant parameters unknown and time varying	σ -modification in the parameter update law
[RIG99]	digital implementation of continuous control	δ -operator σ -modification
[Miy00b]	unknown high-frequency gain partially unknown rel. degree	Nussbaum Gain
[ZWS00]	unknown high-frequency gain	Nussbaum Gain augmented error
[LT96]	MIMO plant	
[WY98]	MIMO plant	
[CHIK03]	MIMO plant	

Table 2.2. *The asymptotic performance of the adaptive backstepping tuning functions control design in the last few years.*

2.3.1 Stability and asymptotic performance

The parameter variation has been treated in [GRI99] by using a σ -modification in the parameter update law. In this case, the slower the plant variation, the larger the region of attraction and the best the asymptotic performance. The digital implementation of the continuous backstepping adaptive counterpart has been considered in [RIG99], given a discrete-time representation in the δ -operator and a σ -modification in the parameter update law. The knowledge of the high-frequency gain is supposed in all the previous works. [Miy00b, ZWS00] present schemes that do not assume the knowledge of the high-frequency gain. In both works a Nussbaum gain is introduced in the backstepping algorithm. In [Miy00b] the relative degree is partially unknown and in [ZWS00] an augmented error is used in the design.

Multivariable versions of the tuning functions design were proposed in [LT96, WY98, CHIK03]. A nonlinear backstepping design for adaptive control of linear plants with multiple inputs and multiple outputs is developed in a similar way that the original backstepping in [LT96], and in a different approach in [WY98]. In both cases, global stability of the closed-loop system is guaranteed and the tracking error tends to zero. On the contrary, [CHIK03] develops a multivariable analog of the Lyapunov-based model-reference design of minimum phase linear systems with relative degree one.

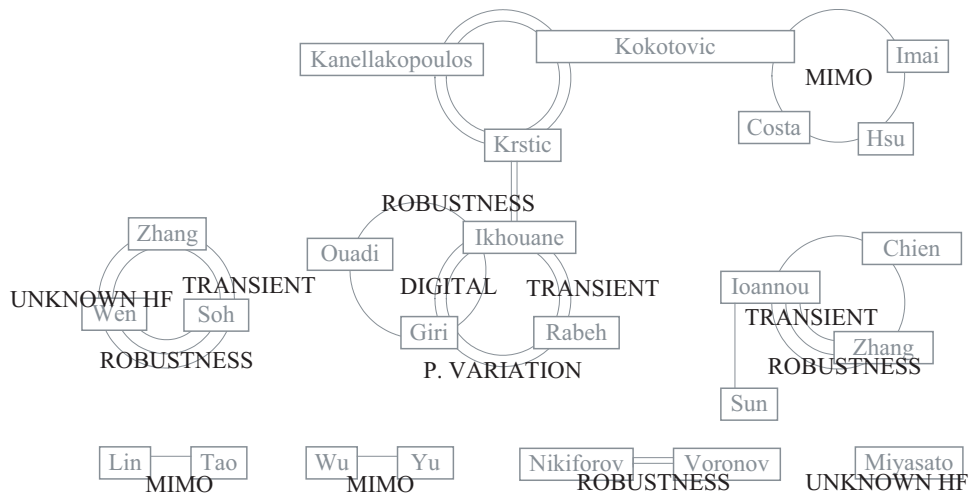


Figure 2.3. Main topics covered in adaptive backstepping for linear systems.

The recent developments with respect to the stability and asymptotic performance of the adaptive backstepping tuning functions control design are summarized in Table 2.2.

2.3.2 Robustness

Since the publication of adaptive tuning functions design applied to linear systems [KKK94], research on this field has focused mainly on robustness with respect to unmodelled dynamics and/or external disturbances [WS96, ZI98, IK98a, IK98b, WZS99, OIG01, NV01b].

In [WS96] a design approach of robust adaptive control using backstepping and parameter projection is presented. In this design, no a priori knowledge on the unmodelled dynamics is required. The class of systems considered

$$y(t) = \left\{ \frac{B(s)}{A(s)} [1 + \mu_1 \Delta_1(s)] + \mu_2 \Delta_2(s) \right\} u + d(t), \quad (2.142)$$

where the size of the uncertainties, μ_1 and μ_2 , are nonnegative constants, $\Delta_1(s)$ and $\Delta_2(s)$ are the multiplicative and additive stable and proper unstructured uncertainties and $d(t)$ denotes an output disturbance. Modifying the adaptive law by using the projection operation, global stability of the system is guaranteed and the output tracking error is bounded by a function of the sizes of the unmodelled dynamics and external disturbances.

ROBUSTNESS		
Paper	kind of uncertainties	modifications
[IK98a]	$y(t) = \frac{B(s)}{A(s)}(1 + \mu\Delta(s))u(t) + d(t)$	parameter projection
[IK98b]	$y(t) = \frac{B(s)}{A(s)}(1 + \mu\Delta(s))u(t) + d(t)$	σ -modification in tuning functions
[NV01b]	$y(t) = \frac{B(s)}{A(s)}[u(t) + f]$	
[OIG01]	$y(t) = \frac{B(s)}{A(s)} \frac{1}{1 + \mu\Delta(s)} u(t) + d(t)$	σ -modification
[WS96]	$y(t) = \left\{ \frac{B(s)}{A(s)} [1 + \mu_1\Delta_1(s)] + \mu_2\Delta_2(s) \right\} u + d(t)$	parameter projection
[WZS99]	$y(t) = \frac{B(s)}{A(s)}(1 + \mu_1\Delta_1(s))u(t) + \mu_2\Delta_2(s)y(t)$	
[ZI98]	$y(t) = \frac{B(s)}{A(s)}(1 + \Delta(s))(u(t) + d_u(t)) + d_y(t)$	dynamic norm. signal σ -modification

Table 2.3. *The robustness of the adaptive backstepping tuning functions control design in the last few years.*

[ZI98] considers not only multiplicative uncertainties but also input and output disturbances in the SISO model plant

$$y(t) = \frac{B(s)}{A(s)}(1 + \Delta(s))(u(t) + d_u(t)) + d_y(t), \quad (2.143)$$

where $\Delta(s)$ is stable and proper.

In order to improve the robustness of the original schemes with respect to this model plant, a $(\rho-1)$ -differentiable dynamic normalizing signal and a $(\rho-1)$ -differentiable switching σ -modification have been introduced. It is also important that choosing the design parameters in an appropriate way, performance can be improved without sacrificing robustness and stability bounds.

In [IK98a, IK98b] a multiplicative uncertainty and external disturbances has been introduced in the linear single-input single-output plant:

$$y(t) = \frac{B(s)}{A(s)}(1 + \mu\Delta(s))u(t) + d(t), \quad (2.144)$$

where $\Delta(s)$ is stable but possibly improper. In [IK98b] a switching σ -modification is added to the tuning functions and as a result, achievable robustness results are not global in the improper case but regional, with a region of attraction inversely proportional to the size of the unmodelled dynamics. The solution presented in [IK98a] can be summarized as *tuning functions with damping*. In this new design is proposed a controller modification which enables the use of projection. In fact, the projection operator is used in the choice of the update law for the parameter estimates.

[OIG01] considers the problem of controlling linear systems in presence of external disturbances and unmodelled dynamics represented by the inverse multiplicative form

$$y(t) = \frac{B(s)}{A(s)} \frac{1}{1 + \mu\Delta(s)} u(t) + d(t), \quad (2.145)$$

where $\Delta(s)$ is asymptotically stable. In order to make the involved parameter adaptive law robust, a switching σ -modification is introduced and so the closed-loop is locally stable with a region of attraction inversely proportional to the size of the unmodelled dynamics.

Even without any modification on the backstepping design, [WZS99] shows that the stabilization of the system can be achieved with respect to a class of unmodelled dynamics described by

$$y(t) = \frac{B(s)}{A(s)}(1 + \mu_1\Delta_1(s))u(t) + \mu_2\Delta_2(s)y(t), \quad (2.146)$$

where both $\Delta_1(s)$ and $\Delta_2(s)$ are stable and strictly proper.

In the presence of inaccessible constant input disturbances

$$y(t) = \frac{B(s)}{A(s)}[u(t) + f], \quad (2.147)$$

it is shown in [NV01b] that the standard backstepping design results in an adaptive controller with *integral action*, i.e., with a special parametrization the design procedure leads to a controller completely eliminating these constant input disturbances.

The recent developments with respect to the robustness of the adaptive backstepping tuning functions control design are summarized in Table 2.3.

2.3.3 Transient performance

A modified tuning functions scheme that borrows elements from the certainty-equivalence controllers have been proposed in [ZI00]. This new controller can achieve the same level of performance as promised by the tuning functions design, though the way they achieve such performance is different.

The transient performance of unknown linear systems in the presence of strictly proper unmodelled dynamics and bounded disturbances,

$$y(t) = \frac{B(s)}{A(s)}(1 + \mu\Delta(s))u(t) + d(t), \quad (2.148)$$

has been considered in [IRG97], where the unmodelled effects have been coped with using a σ -modification in the parameter update law. A \mathcal{L}_∞ bound on the tracking error is given and it can be made arbitrarily small by sufficiently increasing the design gains.

Besides the robustness of the adaptive controller designed using the backstepping technique proposed in [KKK95], the system transient performance in the presence of multiplicative unmodelled dynamics (2.146) is evaluated in [WZS99] by both \mathcal{L}_∞ and \mathcal{L}_2 bounds of the states. It is also proved that these bounds can be made arbitrary small by properly choosing the control design parameters.

The recent developments with respect to the transient performance of the adaptive backstepping tuning functions control design are summarized in Table 2.2.

2.4 Conclusions

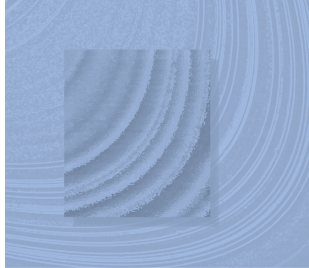
We have presented a class of adaptive design for linear systems. The tuning functions design removes several other obstacles from adaptive linear control. Since the design is based on a single Lyapunov function incorporating both the state of the error system and the update law, the proof of global uniform stability is direct and simple. Moreover, all the error states except for the parameter error converge to zero. This is the strongest convergence without persistency of excitation.

TRANSIENT PERFORMANCE		
Paper	plant	modifications
[IRG97]	$y(t) = \frac{B(s)}{A(s)}(1 + \mu\Delta(s))u(t) + d(t)$	σ -modification in the parameter update law
[WZS99]	$y(t) = \frac{B(s)}{A(s)}(1 + \mu_1\Delta_1(s))u(t) + \mu_2\Delta_2(s)y(t)$	no modification
[ZI00]	$y(t) = \frac{B(s)}{A(s)}u(t)$	normalized adaptive law

Table 2.4. *The transient performance of the adaptive backstepping tuning functions control design in the last few years.*

The main advantage of the tuning functions design over traditional certainty equivalence adaptive designs is in transient performance. The nonlinear control law which incorporates the parameter update law keeps the parameter estimation transients from causing bad tracking transients. The performance bounds obtained for the tuning functions scheme are computable and can be used for systematic improvement of transient performance.

We have also presented the latest developments with respect to the adaptive backstepping tuning functions design for linear systems.



Chapter 3

Unknown linear systems in the presence of bounded disturbances

This chapter deals with the problem of controlling unknown linear systems in the presence of bounded disturbances. Adaptive controllers that ensure the closed-loop global (uniform) stability and asymptotic performances can be designed following either the backstepping approach or the certainty-equivalence method. The main shortcoming of the involved controllers is that they do not allow quantification of the closed-loop transient behaviour. In this chapter, the transient issue is addressed for backstepping adaptive controllers as we have described in the previous chapter. A \mathcal{L}_∞ bound on the tracking error is explicitly given as a function of the design parameters. This shows that the error can be made arbitrarily small by sufficiently increasing the design gains.

3.1 Problem statement

We are interested in controlling plants that can be described by a model of the form

$$y(t) = \frac{B(s)}{A(s)}u(t) + p(t), \quad (3.1)$$

where $A(s)$ and $B(s)$ are polynomial operators of the form

$$A(s) = s^n + a_{n-1}s^{n-1} + \cdots + a_1s + a_0, \quad (3.2)$$

$$B(s) = b_ms^m + \cdots + b_1s + b_0. \quad (3.3)$$

The parameters a_i and b_i are constant but unknown. The following assumptions complete the plant description:

Assumption 4 The plant is minimum phase, i.e., the polynomial $B(s)$ is Hurwitz. The plant order (n), relative degree ($\rho = n - m$) and sign of the high frequency gain ($\text{sgn}(b_m)$) are known.

Assumption 5 The output disturbance $p(t)$ and its first derivative are uniformly bounded. $\dot{p}(t)$ is piecewise continuous.

Assumption 6 Upper bounds M_θ and M_ϱ of $\|\theta\|$ and $|\varrho| = |1/b_m|$, respectively, are known, where $\theta = (b_m, \dots, b_0, a_{n-1}, \dots, a_0)^\top$ is the unknown parameter vector.

Note that the above assumptions are very standard in the literature devoted to robust adaptive control [IS96].

Let $y_r(t)$ be any bounded reference signal such that $y_r(t)$ and its first ρ derivatives are known and bounded and, in addition, $y_r^{(\rho)}$ is piecewise continuous. For instance, $y_r(t)$ may be the output of a reference model of relative degree $\rho_r \geq \rho$ with piecewise continuous input $r(t)$. Our objective is to design an adaptive controller such that

- (i) all the closed-loop signals should be globally bounded;
- (ii) the output tracking error $y(t) - y_r(t)$ should be proportional, in the mean, to the size of the unmodelled effects. Furthermore, the transient behaviour of $y(t) - y_r(t)$ should be explicitly quantified;
- (iii) in the ideal case, i.e., $p(t) \equiv 0$, the error should converge to zero.

3.2 Controller design and robustness analysis

3.2.1 Controller design

In this section, we design a backstepping-based adaptive controller for the system (3.1). Following the tuning functions backstepping design in Chapter 2 [KKK95, Chapter 10], we first represent the plant (3.1) in the observer canonical form:

$$\dot{x} = A_0 x + (k - a)x_1 + bu, \quad y = x_1 + p,$$

where

$$A_0 = \begin{bmatrix} -k_1 & 1 & 0 & \cdots & 0 \\ -k_2 & 0 & 1 & \cdots & 0 \\ \vdots & \vdots & \vdots & \ddots & \vdots \\ -k_{n-1} & 0 & 0 & \cdots & 1 \\ -k_n & 0 & 0 & \cdots & 0 \end{bmatrix}, \quad k = [k_1 \ \cdots \ k_n]^T,$$

$$a = [a_{n-1} \ \cdots \ a_0]^T, \quad b = [0_{(\rho-1) \times 1} \ b_m \ \cdots \ b_0]^T,$$

where the parameters k_i are chosen so that the polynomial

$$K(s) = k_n + k_{n-1}s + \cdots + k_1s^{n-1} + s^n$$

is Hurwitz. By filtering u and y with two n -dimensional filters

$$\dot{\eta} = A_0\eta + e_n y, \quad \dot{\lambda} = A_0\lambda + e_n u, \quad (3.4)$$

the state estimate is formed as

$$\hat{x} = B(A_0)\lambda - A(A_0)\eta, \quad (3.5)$$

where $B(X)$ and $A(X)$ are described by (3.2) and (3.3). Then the estimation error $\varepsilon = x - \hat{x}$ satisfies

$$\dot{\varepsilon} = A_0\varepsilon + (a - k)p. \quad (3.6)$$

We define the vectors v_j, Ξ, ξ, ω and $\bar{\omega}$ as

$$v_j = A_0^j \lambda, \quad j = 0, \dots, m, \quad (3.7)$$

$$\Xi = -[A_0^{n-1}\eta, \dots, \eta], \quad (3.8)$$

$$\xi = -A_0^n \eta, \quad (3.9)$$

$$\omega = [v_{m,2}, \dots, v_{0,2}, \Xi_{(2)} - ye_1^T]^T, \quad (3.10)$$

$$\bar{\omega} = [0, v_{m-1,2}, \dots, v_{0,2}, \Xi_{(2)} - ye_1^T]^T. \quad (3.11)$$

The control law and the parameter update laws are designed in ρ steps (see Figure 3.1). To estimate the unknown plant parameters θ and ϱ , we propose the following switching σ -modification algorithm:

$$\dot{\hat{\theta}} = \Gamma\tau_\rho - \Gamma\sigma_\theta\hat{\theta}, \quad (3.12)$$

$$\dot{\hat{\varrho}} = -\gamma\text{sgn}(b_m)(\dot{y}_r + \bar{\alpha}_1)z_1, \quad (3.13)$$

where σ_θ and σ_ϱ are updated as follows:

$$\sigma_\theta = \begin{cases} 0, & \|\hat{\theta}\| \leq M_\theta \\ \sigma_{s\theta}, & \|\hat{\theta}\| \geq 2M_\theta \\ \text{smooth connecting function,} & \text{otherwise} \end{cases} \quad (3.14)$$

$$\sigma_\varrho = \begin{cases} 0, & |\hat{\varrho}| \leq M_\varrho \\ \sigma_{s\varrho}, & |\hat{\varrho}| \geq 2M_\varrho \\ \text{smooth connecting function,} & \text{otherwise} \end{cases} \quad (3.15)$$

for some positive constants $\sigma_{s\theta}$ and $\sigma_{s\varrho}$ and adaptation gains $\gamma > 0$ and $\Gamma = \Gamma^T > 0$. The switching σ -modification has proved to be useful to deal with the plant unmodelled dynamics and disturbances [IK98b]. Note that in the standard tuning functions design derived in the ideal case (i.e. in the absence of external disturbances) [KKK95, Section 10.2.1], the terms Υ_i , $i = 1, 2, \dots, \rho$ are zero. In a nonideal situation, we introduce the following modifications:

$$\Upsilon_1 = -g_0 \text{sgn}(b_m)(\dot{y}_r + \bar{\alpha}_1)^2 z_1, \quad (3.16)$$

$$\Upsilon_i = -\frac{\partial \alpha_{i-1}}{\partial \hat{\theta}} \Gamma \sigma_\theta \hat{\theta} - \left(y_r^{(i-1)} + \frac{\partial \alpha_{i-1}}{\partial \hat{\varrho}} \right) \gamma \sigma_\varrho \hat{\varrho}, \quad i = 2, 3, \dots, \rho \quad (3.17)$$

for some positive design constant g_0 . The modification (3.16) takes account of the perturbation terms introduced by the parameter estimates \hat{b}_m and $\hat{\varrho}$. If b_m is known, then we can take $g_0 = 0$. The term (3.17) is introduced so that the control law is compatible with the switching σ -modification present in the parameter update laws (3.12)-(3.13).

3.2.2 Robustness analysis

In this section we present the robustness and asymptotic performance result obtained using the design of the previous section. We also give the notations and definitions that will be used in the next section.

Theorem 4 Consider the plant (3.1) subject to Assumptions 4-6 and the adaptive controller composed of the control law of Figure 3.1 and the parameter update law 3.12-3.13. There exist positive constants c and g independent of p and \dot{p} such that we have

- (i) all the signals of the closed loop are globally bounded,
- (ii) the tracking error is proportional to the size of perturbations:

Error variables

$$z_1 = y - y_r, \quad z_i = v_{m,i} - \hat{\rho} y_r^{(i-1)} - \alpha_{i-1}, \quad i = 2, \dots, \rho$$

Stabilizing functions

$$\begin{aligned} \alpha_1 &= \hat{\rho} \bar{\alpha}_1 + \Upsilon_1 \\ \bar{\alpha}_1 &= -(c_1 + d_1)z_1 - \xi_2 - \bar{\omega}^T \hat{\theta} \\ \alpha_2 &= -\hat{b}_m z_1 - \left[c_2 + d_2 \left(\frac{\partial \alpha_1}{\partial y} \right)^2 \right] z_2 + \beta_2 + \frac{\partial \alpha_1}{\partial \hat{\theta}} \Gamma \tau_2 + \Upsilon_2 \\ \alpha_i &= -z_{i-1} - \left[c_i + d_i \left(\frac{\partial \alpha_{i-1}}{\partial y} \right)^2 \right] z_i + \beta_i + \frac{\partial \alpha_{i-1}}{\partial \hat{\theta}} \Gamma \tau_i \\ &\quad - \sum_{j=2}^{i-1} \frac{\partial \alpha_{j-1}}{\partial \hat{\theta}} \Gamma \frac{\partial \alpha_{i-1}}{\partial y} z_j + \Upsilon_i, \quad i = 3, \dots, \rho \\ \beta_i &= \frac{\partial \alpha_{i-1}}{\partial y} (\xi_2 + \omega^T \hat{\theta}) + \frac{\partial \alpha_{i-1}}{\partial \eta} (A_0 \eta + e_n y) + \sum_{j=1}^{i-1} \frac{\partial \alpha_{i-1}}{\partial y_r^{(j-1)}} y_r^{(j)} + k_i v_{m,1} \\ &\quad + \sum_{j=1}^{m+i-1} \frac{\partial \alpha_{i-1}}{\partial \lambda_j} (-k_j \lambda_1 + \lambda_{j+1}) \\ &\quad - \left(y_r^{(i-1)} + \frac{\partial \alpha_{i-1}}{\partial \hat{\rho}} \right) \gamma \operatorname{sgn}(b_m) (\dot{y}_r + \bar{\alpha}_1) z_1, \quad i = 2, \dots, \rho \\ \Upsilon_1 &= -g_0 \operatorname{sgn}(b_2) (\dot{y}_r + \bar{\alpha}_1)^2 z_1 \\ \Upsilon_i &= -\frac{\partial \alpha_{i-1}}{\partial \hat{\theta}} \Gamma \sigma_\theta \hat{\theta} - \left(y_r^{(i-1)} + \frac{\partial \alpha_{i-1}}{\partial \hat{\rho}} \right) \gamma \sigma_\rho \hat{\rho}, \quad i = 2, \dots, \rho \end{aligned}$$

Tuning functions

$$\tau_1 = (\omega - \hat{\rho} (\dot{y}_r + \bar{\alpha}_1) e_1) z_1, \quad \tau_i = \tau_{i-1} - \frac{\partial \alpha_{i-1}}{\partial y} \omega z_i, \quad i = 2, \dots, \rho$$

Parameter update laws

$$\dot{\hat{\theta}} = \Gamma \tau_\rho - \Gamma \sigma_\theta \hat{\theta}, \quad \dot{\hat{\rho}} = -\gamma \operatorname{sgn}(b_m) (\dot{y}_r + \bar{\alpha}_1) z_1 - \gamma \sigma_\rho \hat{\rho}$$

Adaptive control law

$$u = \alpha_2 - v_{2,3} + \hat{\rho} \ddot{y}_r$$

Figure 3.1. *Tuning functions design*

$$\int_t^{t+T} (y(\tau) - y_r(\tau))^2 d\tau \leq g + c \int_t^{t+T} (p(\tau)^2 + \dot{p}(\tau)^2) d\tau, \quad \forall t, T \geq 0. \quad (3.18)$$

Proof. The stability analysis is carried out by using a similarity transformation which yields

$$\begin{aligned} \dot{x}_1 &= x_2 - a_{n-1}x_1, \\ &\vdots \\ \dot{x}_\rho &= c_b^T \bar{x} - a_m x_1 + b_m u, \\ \dot{\zeta} &= A_b \zeta + b_b x_1, \\ y &= x_1 + p, \end{aligned} \quad (3.19)$$

where $\bar{x} = (x_1, \dots, x_\rho, \zeta^T)^T$, $c_b \in \mathbb{R}^n$, and $b_b \in \mathbb{R}^m$. The deviation $\tilde{\zeta} = \zeta - \zeta_r$ is governed by

$$\dot{\tilde{\zeta}} = A_b \tilde{\zeta} + b_b x_{1r}, \quad \tilde{\zeta}(0) = 0 \quad (3.20)$$

and x_{1r} is defined as

$$x_{1r} = x_1 - y_r. \quad (3.21)$$

For the η variables we have

$$\dot{\tilde{\eta}} = A_0 \tilde{\eta} + e_n z_1, \quad \tilde{\eta}(0) = 0.$$

A Lyapunov function V for the closed loop is

$$\begin{aligned} V &= \sum_{j=1}^{\rho} \left(\frac{1}{2} z_j^2 + \frac{1}{d_j} \varepsilon^T P_0 \varepsilon \right) + \frac{|b_m|}{2\gamma} (\varrho - \hat{\varrho})^2 + \frac{1}{2} (\theta - \hat{\theta})^T \Gamma^{-1} (\theta - \hat{\theta}) \\ &\quad + \frac{1}{k_n} \tilde{\eta}^T P_0 \tilde{\eta} + \frac{1}{k_\zeta} \tilde{\zeta}^T P_b \tilde{\zeta}. \end{aligned} \quad (3.22)$$

V can be given the form $V = \chi^T P_\chi \chi$ with

$$\chi = (z^T, \varepsilon^T, \tilde{\eta}^T, \tilde{\zeta}^T, \tilde{\theta}^T, \tilde{\varrho})^T. \quad (3.23)$$

Then, it can be shown that [IK98b]

$$\dot{V} \leq -\frac{\alpha}{2}V + 2\beta, \quad (3.24)$$

$$\dot{V} \leq -\frac{\alpha}{2}(y(t) - y_r(t))^2 + \beta_0 \quad (3.25)$$

where

$$\alpha = \min \left\{ \frac{c_1}{4}, 2c_2, \dots, 2c_\rho, \frac{\lambda_{\min}^{-1}(P_0)}{4}, \frac{\lambda_{\min}^{-1}(P_b)}{4}, \right. \\ \left. \frac{\lambda_{\min}^{-1}(P_1)}{8}, \frac{\lambda_{\min}^{-1}(P_2)}{8}, \frac{\gamma\sigma_{s\varrho}}{|b_m|}, \frac{\sigma_{s\theta}}{\lambda_{\min}(\Gamma^{-1})} \right\}, \quad (3.26)$$

$$\beta = c(\dot{p}^2 + p^2 + \sigma_{s\varrho} + \sigma_{s\theta}), \quad (3.27)$$

$$\beta_0 = c(\dot{p}^2 + p^2) \quad (3.28)$$

for some positive constant c independent of p and \dot{p} . This shows that $V(t)$ is globally bounded. The asymptotic performance result (3.18) is obtained by integrating both parts of (3.25). \square

3.3 Transient bounds

In this section, we give explicit \mathcal{L}_∞ bounds on the tracking error z_1 . This results will be summarized in Theorem 5.

Theorem 5 Consider the plant (3.1) subject to Assumptions 4-6 and the adaptive controller composed of the control law of Figure 3.1 and the parameter update law 3.12-3.13. There exist positive constants c and g independent of p and \dot{p} such that the \mathcal{L}_∞ norm of the tracking error can be made arbitrarily small by increasing sufficiently d_0 and g_0 :

$$\|y(t) - y_r(t)\|_\infty \leq \frac{1}{2\sqrt{c_0 d_0}} \left((\omega^T \tilde{\theta})_\infty + \varepsilon_{2\infty} + \|\dot{p}\|_\infty + |a_{n-1}| \|p\|_\infty \right) \\ + \frac{\tilde{\theta}_\infty(\tilde{\varrho} + |\varrho|) + |b_m| \tilde{\varrho}_\infty}{2\sqrt{c_0 g_0} |b_m|}, \quad (3.29)$$

where $(\omega^T \tilde{\theta})_\infty, \varepsilon_{2\infty}, \tilde{\theta}_\infty, \tilde{\varrho}_\infty \in \mathbb{R}$ such that

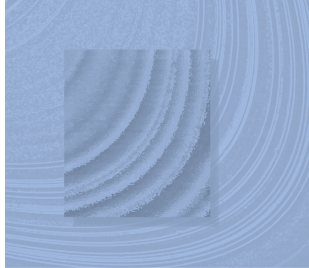
$$\begin{aligned}\|\omega^T \tilde{\theta}\|_\infty &\leq (\omega^T \tilde{\theta})_\infty \\ \|\varepsilon_2\| &\leq \varepsilon_{2\infty} \\ \|\tilde{\theta}\|_\infty &\leq \tilde{\theta}_\infty \\ \|\tilde{\varrho}\|_\infty &\leq \tilde{\varrho}_\infty.\end{aligned}$$

Remark 2 It is worth noticing that the above \mathcal{L}_∞ bounds depends only on $\tilde{\theta}(0), \varepsilon(0), \|p\|_\infty, \|\dot{p}\|_\infty$ and $\sigma_{s\theta}$.

Proof. See [IRG97] for details. □

3.4 Conclusions

In this chapter we have generalized the results of Chapter 2 to the non-ideal case, that is when the controlled plant is subject to bounded output disturbances. The above effects have been coped with using a σ -modification in the parameter adaptive law, and changing accordingly the adaptive control law. An explicit \mathcal{L}_∞ bound on the state error is derived and shown to be a decreasing function of the design parameters. More precisely, the state error can be made arbitrarily small by increasing sufficiently the involved design parameters. The control presented here is used in the next chapter to develop control schemes for a class of structural control problem.



Chapter 4

Adaptive backstepping control of hysteretic base-isolated structures

A hybrid seismic control system for building structures is considered, which combines a class of passive nonlinear base isolator with an active control system. The objective of the active control component applied to the structural base is to keep the base displacement relative to the ground and the interstory drift within a reasonable range according to the design of the base isolator. We use the techniques developed in Chapter 3 for the control design. The base isolator device exhibits a hysteretic nonlinear behavior which is described analytically by the Bouc-Wen model. The control problem is formulated representing the system dynamics in two alternative coordinates: absolute (with respect to an inertial frame) and relative to the ground. A comparison between both strategies is presented by means of numerical simulations.

4.1 Introduction

With the aim of keeping the seismic response of structures within safety, service and comfort limits, the idea of cooperatively combining both passive base isolators and feedback controllers (applying forces to the base) has been increasingly considered in the last years. Some works have proposed active feedback systems, like for instance [BRRM95], [ISK98] and [KLS87]. More recently, semiactive controllers have been proposed in the same setting trying to get advantages of their easier implementation (see for instance [LRVIS01] and [RJS02]).

The basic concept of base isolation is to ideally make the structure behave like a rigid body through a certain degree of decoupling from the ground motion. In this way it is possible to absorb part of the energy induced by the earthquake, by reducing simultaneously the relative displacements of the structure with respect to the base (damage source) and the absolute accelerations (endangering human comfort and safety of installations). The feasibility of adding a feedback control is based on the premise that only a control action is to be applied at the base with force magnitudes which are not excessive due to the high flexibility of the isolators. The benefits of the inclusion of the control lie mainly in that the “cooperation” of such a force can avoid large displacements of the base isolator, which could endanger the scheme integrity; and it may also introduce an additional resistant scheme not dependable of the interstory drifts, which are already small due to the effect of the isolator. This may be useful, particularly for structures having sensitive installations, like hospitals, public services, computer facilities, etc.

From a theoretical point of view, the development of a control law to calculate the active forces involves difficulties associated with the nonlinear behavior of the base isolators and with the uncertainties in the model describing the structure-base-isolator system and in the seismic excitation. An important issue in considering the model for the control formulation is the coordinates adopted to represent the motion. In the vein of the most common practice in the earthquake engineering design of base isolation systems, some authors have used models based on coordinates relative to the ground for the control design (see for example [ISK98] and [RJS02]). Other authors have approached the problem by using absolute coordinates with respect to an inertial frame of reference, like in [BRRM95], [KLS87] and [LRVIS01].

In this work, we design a control system for a simple prototype base isolated uncertain structure by using models in both coordinates trying to give some insight on their advantages and drawbacks.

4.2 Structural models

Consider a base isolated structure with an active controller as illustrated in Figure 4.1. The passive component consists of a hysteretic base isolator.

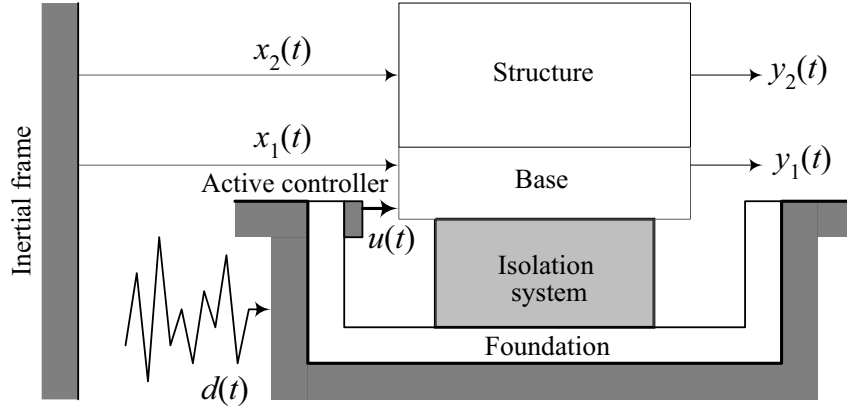


Figure 4.1. Building structure with hybrid control system.

The whole system can be described by a model composed of two coupled systems: Σ_s (the structure) and Σ_b (the base). It can be represented in two different coordinate systems: absolute (with respect to an inertial frame) and relative to the ground.

The relative equations Σ_b^r, Σ_s^r of motion are

$$\begin{aligned} \Sigma_b^r : m_1 \ddot{y}_1 + (\bar{c}_1 + \bar{c}_2) \dot{y}_1 + (\bar{k}_1 + \bar{k}_2) y_1 &= \\ &= \bar{k}_2 y_2 + \bar{c}_2 \dot{y}_2 - \Phi(y_1, t) - m_1 \ddot{d} + u \end{aligned} \quad (4.1)$$

$$\Sigma_s^r : m_2 \ddot{y}_2 + \bar{c}_2 \dot{y}_2 + \bar{k}_2 y_2 - \bar{c}_2 \dot{y}_1 - \bar{k}_2 y_1 = -m_2 \ddot{d} \quad (4.2)$$

The absolute equations of motion Σ_b^a, Σ_s^a are the following

$$\begin{aligned} \Sigma_b^a : m_1 \ddot{x}_1 + (\bar{c}_1 + \bar{c}_2) \dot{x}_1 + (\bar{k}_1 + \bar{k}_2) x_1 &= \\ &= \bar{k}_2 x_2 + \bar{c}_2 \dot{x}_2 - \Phi(x_1 - d, t) + \bar{c}_1 \dot{d} + \bar{k}_1 d + u \end{aligned} \quad (4.3)$$

$$\Sigma_s^a : m_2 \ddot{x}_2 + \bar{c}_2 \dot{x}_2 + \bar{k}_2 x_2 - \bar{c}_2 \dot{x}_1 - \bar{k}_2 x_1 = 0 \quad (4.4)$$

where m_1 and m_2 are the mass of the base and the structure, respectively; \bar{c}_1 and \bar{c}_2 are the damping coefficients; \bar{k}_1 and \bar{k}_2 are the stiffness coefficients; the absolute displacement of the base is x_1 and the absolute displacement of the structure is x_2 , which can be measured by using some recently developed technique [ISGS96];

the dynamic earthquake excitation is produced by a horizontal seismic ground motion characterized by an inertial displacement $d(t)$, velocity $\dot{d}(t)$ and acceleration $\ddot{d}(t)$; the base displacement relative to the ground is $y_1 = x_1 - d$ while $y_2 = x_2 - d$ is the relative structure displacement;

Φ is the restoring force characterizing the hysteretic behavior of the isolator material, which is usually made with inelastic rubber bearings; and u is the control force supplied by an appropriate actuator.

The hysteretic force Φ is described by the Bouc-Wen model [Wen76] in the following form:

$$\Phi(x) = \alpha k_0 x + (1 - \alpha) D k_0 z \quad (4.5)$$

$$\dot{z} = D^{-1} [\bar{A} \dot{x} - \beta |\dot{x}| |z|^{n-1} z - \bar{\gamma} \dot{x} |z|^n] \quad (4.6)$$

where $\Phi(x, t)$ can be considered as the superposition of an elastic component $\alpha k_0 x(t)$ and a hysteretic component $(1 - \alpha) D k_0 z(t)$, in which $D > 0$ is the yield constant displacement, $\alpha \in [0, 1]$ is the post to pre-yielding stiffness ratio. The hysteretic part involves a dimensionless auxiliary variable z which is the solution of the nonlinear first order differential equation (4.6). In this equation, \bar{A} , β and $\bar{\gamma}$ are dimensionless parameters which control the shape and the size of the hysteresis loop, while n is a scalar that governs the smoothness of the transition from elastic to plastic response.

4.3 Control strategies

Looking at (4.1), it is clear that a feedback control law can be designed to supply a force u able to control the relative displacement of the base against the earthquake excitation, which is the ground acceleration. However, this excitation enters also in (4.2), which has no control. This means that the relative motion of the structure is subjected to the seismic acceleration but no feedback control is directly exerted to mitigate the effect of this excitation. In fact, the use of relative coordinates arises from the desire to keep the motion (displacement and velocity) of each floor relative to the ground small (and hence, of a given floor relative to those below and above it). Roughly speaking, feedback control is employed to achieve that end attempting “to move the whole structure” so as to follow the motion of the ground [KLS87].

Looking at (4.3), it is clear that a feedback control law can be designed to supply a force u able to control the absolute displacement of the base against the earthquake excitation, which is now a linear combination of the ground displacement and velocity.

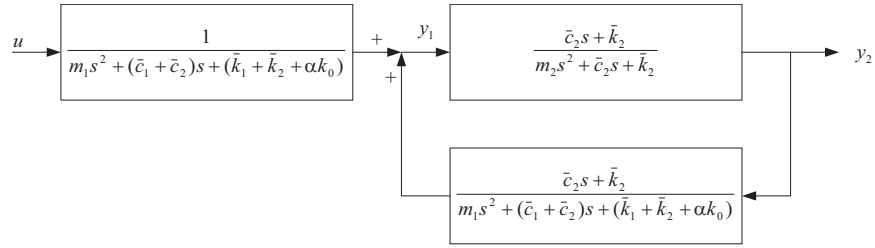


Figure 4.2. Block diagram representation.

We may observe that this excitation does not enter in (4.4). Then, the control of the base motion leads to the control of the structure's motion. Also, it is expectable that the effort to control the system (4.3)-(4.4) be smoother than in the case of controlling system (4.1)-(4.2) since the ground displacement and velocity are smoother than the ground acceleration. The origin of the use of absolute coordinates can be found in [KLS87] based on the idea of keeping the whole structure stationary relative to its initial configuration (i.e., relative to an inertial frame of reference) and, roughly speaking, “letting the ground move under it”.

In order to establish a comparison between both alternatives we consider two control strategies:

- (a) when using the relative coordinates: measure y_1 and regulate y_1 ;
- (b) when using the absolute coordinates: measure x_1 and regulate x_1 .

In Section 4.5, a comparison between the strategies is presented by means of numerical simulations.

4.4 Controller design

In order to use the techniques developed in Chapter 3 for the control design, we need to describe the models (4.1)-(4.2) and (4.3)-(4.4), respectively, along with equations (4.5)-(4.6), in the transfer function form.

4.4.1 Model description

Applying the Laplace transform to the equations (4.1)-(4.2) we obtain

$$\begin{aligned} [m_1 s^2 + (\bar{c}_1 + \bar{c}_2)s + (\bar{k}_1 + \bar{k}_2 + \alpha k_0)] y_1(s) - [\bar{c}_2 s + \bar{k}_2] y_2(s) = \\ = u(s) + (1 - \alpha) Dk_0 z(s) - m_1 s^2 d(s) \end{aligned} \quad (4.7)$$

$$[m_2 s^2 + \bar{c}_2 s + \bar{k}_2] y_2(s) - [\bar{c}_2 s + \bar{k}_2] y_1(s) = -m_2 s^2 d(s) \quad (4.8)$$

We consider $d(t)$ and $z(t)$ as external disturbances. In the particular case $d(t) = 0$ and $z(t) = 0$, we can write the equations (4.7)-(4.8) in a block diagram representation depicted in Figure 4.2.

In this case it can be shown, using the Nyquist stability criterion, that the system represented in Figure 4.2 is always stable, that is, the transfer function between the signals y_2 and u is stable. The explicit expression of this transfer function is

$$y_2(s) = \frac{\frac{c_2}{m_1 m_2} s + \frac{k_2}{m_1 m_2}}{A(s)} u(s) \quad (4.9)$$

where

$$\begin{aligned} A(s) = & s^4 + \frac{m_1 \bar{c}_2 + \bar{c}_2 m_2 + \bar{c}_1 m_2}{m_1 m_2} s^3 \\ & + \frac{m_1 \bar{k}_2 + \bar{k}_1 m_2 + \bar{k}_2 m_2 + \alpha k_0 m_2 + \bar{c}_1 \bar{c}_2}{m_1 m_2} s^2 \\ & + \frac{\bar{k}_1 \bar{c}_2 + \bar{c}_1 \bar{k}_2 + \alpha k_0 \bar{c}_2}{m_1 m_2} s + \frac{\alpha k_0 \bar{k}_2 + \bar{k}_1 \bar{k}_2}{m_1 m_2} \end{aligned} \quad (4.10)$$

The stability of the transfer function in equation (4.9) implies the stability of the denominator $A(s)$, that is, the roots of $A(s)$ have negative real parts. The stability of this polynomial expression will be used in the following lines.

In the general case ($d(t) \neq 0, z(t) \neq 0$), after some manipulations and eliminating the variables y_2 and x_2 , the models (4.1)-(4.2) and (4.3)-(4.4), respectively, along with equations (4.5)-(4.6), can be written as

$$\begin{aligned}
y_1(t) &= \frac{B(s)}{A(s)}u(t) + \overbrace{\frac{B_d^r(s)}{A(s)}d(t) + \frac{B_z^r(s)}{A(s)}z(t)}^{p_r(t)} \\
&= \frac{B(s)}{A(s)}u(t) + p_r(t)
\end{aligned} \tag{4.11}$$

$$\begin{aligned}
x_1(t) &= \frac{B(s)}{A(s)}u(t) + \underbrace{\frac{B_d^a(s)}{A(s)}d(t) + \frac{B_z^a(s)}{A(s)}z(t)}_{p_a(t)} \\
&= \frac{B(s)}{A(s)}u(t) + p_a(t)
\end{aligned} \tag{4.12}$$

where $A(s)$ coincides with the polynomial expression in equation (4.10) and

$$\begin{aligned}
B(s) &= \frac{1}{m_1}s^2 + \frac{\bar{c}_2}{m_1m_2}s + \frac{\bar{k}_2}{m_1m_2} \\
B_d^r(s) &= -s^4 - \frac{m_1\bar{c}_2 + m_2\bar{c}_2}{m_1m_2}s^3 - \frac{m_2\bar{k}_2 + m_1\bar{k}_2}{m_1m_2}s^2 \\
B_z^r(s) &= \frac{-(1-\alpha)Dk_0}{m_1}s^2 + \frac{-\bar{c}_2(1-\alpha)Dk_0}{m_1m_2}s + \frac{-\bar{k}_2(1-\alpha)Dk_0}{m_1m_2} \\
B_d^a(s) &= \frac{\bar{c}_1}{m_1}s^3 + \frac{\bar{k}_1m_2 + \alpha k_0m_2 + \bar{c}_1\bar{c}_2}{m_1m_2}s^2 + \frac{\bar{c}_2\alpha k_0 + \bar{k}_2\bar{c}_1 + \bar{c}_2\bar{k}_1}{m_1m_2}s \\
&\quad + \frac{\alpha k_0\bar{k}_2 + \bar{k}_1\bar{k}_2}{m_1m_2} \\
B_z^a(s) &= \frac{-(1-\alpha)Dk_0}{m_1}s^2 + \frac{-\bar{c}_2(1-\alpha)Dk_0}{m_1m_2}s + \frac{-\bar{k}_2(1-\alpha)Dk_0}{m_1m_2}
\end{aligned}$$

In models (4.11) and (4.12), we consider both the earthquake motion $d(t)$ and the hysteretic variable $z(t)$ as unknown disturbances. This is why we define the signals $p_r(t)$ and $p_a(t)$. The direct transfer function between the control force u and the controlled output is the same for both models:

$$\frac{B(s)}{A(s)} = \frac{b_2s^2 + b_1s + b_0}{s^4 + a_3s^3 + a_2s^2 + a_1s + a_0} \tag{4.13}$$

where the coefficients are

$$\begin{aligned}
 b_2 &= \frac{1}{m_1}, & b_1 &= \frac{\bar{c}_2}{m_1 m_2}, & b_0 &= \frac{\bar{k}_2}{m_1 m_2} \\
 a_3 &= \frac{m_1 \bar{c}_2 + \bar{c}_2 m_2 + \bar{c}_1 m_2}{m_1 m_2} \\
 a_2 &= \frac{\bar{k}_2 m_2 + \bar{c}_1 \bar{c}_2 + \alpha k_0 m_1 + \bar{k}_1 m_2 + m_1 \bar{k}_2}{m_1 m_2} \\
 a_1 &= \frac{\bar{k}_1 \bar{c}_2 + \alpha k_0 \bar{c}_2 + \bar{c}_1 \bar{k}_2}{m_1 m_2} \\
 a_0 &= \frac{\alpha k_0 \bar{k}_2 + \bar{k}_1 \bar{k}_2}{m_1 m_2}.
 \end{aligned}$$

In order to use the adaptive backstepping controller developed in Chapter 4, we need to show that the signals $p_a(t)$ and $p_r(t)$ are bounded disturbances.

On one hand, we assume that the earthquake motion $d(t)$ is bounded. On the other hand, it has been shown, in a previous work [IMR04], that the hysteretic component $z(t)$ is always bounded under a particular choice of the parameters \bar{A}, β and $\bar{\gamma}$ ($\bar{A} > 0, \beta + \bar{\gamma} > 0, \beta - \bar{\gamma} \geq 0$ or $\bar{A} > 0, \beta - \bar{\gamma} < 0, \beta \geq 0$).

The boundedness of the signals $d(t)$ and $z(t)$ and the stability of the polynomial expression $A(s)$ allows us to consider $p_r(t)$ and $p_a(t)$ as *bounded disturbances*.

4.4.2 Adaptive backstepping control

Since we consider that the parameters of the models are uncertain, we use adaptive control to stabilize the control loop. Denoting anyone of the parameters $m_i, \bar{k}_i, \bar{c}_i, (i = 1, 2), k_0$ and α by p , we assume that $p \in [p_{\min}, p_{\max}]$, p_{\min} and p_{\max} being known, i.e. we assume the knowledge of an interval for each parameter.

To have computable bounds on the transient behavior, we use the backstepping approach in the presence of bounded disturbances described in Chapter 3.

Our objective is to design an adaptive controller such that

- (i) all the closed-loop signals should be globally bounded;

- (ii) the output tracking error $y_1(t) - y_r(t)$ (resp. $x_1(t) - x_r(t)$) should be proportional, in the mean, to the size of the unmodelled effects. Furthermore, the transient behaviour of $y_1(t) - y_r(t)$ (resp. $x_1(t) - x_r(t)$) should be explicitly quantified;
- (iii) in the ideal case, i.e., $p_r(t) \equiv 0$ (resp. $p_a(t) \equiv 0$), the error should converge to zero.

In our implementation, the reference signals $y_r(t)$ and $x_r(t)$ are chosen as $y_r(t) = x_r(t) \equiv 0$.

The control law and the parameter update law are designed in $\rho = 2$ steps. Figure 4.3 summarizes these steps and serves as an algorithm for the control implementation. In this table, the quantities $c_1, c_2, d_1, d_2, g_0, \gamma, \sigma_{s\varrho}, \sigma_{s\theta}$ and Γ are positive design parameters and M_θ is defined as

$$M_\theta = \sqrt{\sum_{i=0}^3 a_i^2 + \sum_{i=0}^2 b_i^2}.$$

4.4.3 Robustness analysis

In this section we present the robustness and asymptotic performance result obtained using Theorem 4 in Chapter 3.

If we consider the system (4.11) (resp. 4.12) and the adaptive controller composed of the control law and the parameter update law described in Figure 4.3, then there exists positive constants c and g independent of p_r and \dot{p}_r (resp. p_a and \dot{p}_a) such that

- (i) all the signals of the closed loop are globally bounded
- (ii) the magnitude of the output is proportional to the size of perturbations:

$$\int_t^{t+T} y_1^2(\tau) d\tau \leq g + c \int_t^{t+T} (p_r(\tau)^2 + \dot{p}_r(\tau)^2) d\tau \quad (4.14)$$

$$\int_t^{t+T} x_1^2(\tau) d\tau \leq g + c \int_t^{t+T} (p_a(\tau)^2 + \dot{p}_a(\tau)^2) d\tau \quad (4.15)$$

Error variables

$$z_1 = y - y_r, \quad z_2 = v_{2,2} - \hat{\varrho} \dot{y}_r - \alpha_1$$

Stabilizing functions

$$\begin{aligned} \alpha_1 &= \hat{\varrho} \bar{\alpha}_1 + \Upsilon_1 \\ \bar{\alpha}_1 &= -(c_1 + d_1) z_1 - \xi_2 - \bar{\omega}^T \hat{\theta} \\ \alpha_2 &= -\hat{b}_2 z_1 - \left[c_2 + d_2 \left(\frac{\partial \alpha_1}{\partial y} \right)^2 \right] z_2 + \beta_2 + \frac{\partial \alpha_1}{\partial \hat{\theta}} \Gamma \tau_2 + \Upsilon_2 \\ \beta_2 &= \frac{\partial \alpha_1}{\partial y} (\xi_2 + \omega^T \hat{\theta}) + \frac{\partial \alpha_1}{\partial \eta} (A_0 \eta + e_4 y) + \frac{\partial \alpha_1}{\partial y_r} \dot{y}_r + k_2 v_{2,1} \\ &\quad + \frac{\partial \alpha_1}{\partial \lambda_1} (-k_1 \lambda_1 + \lambda_2) + \frac{\partial \alpha_1}{\partial \lambda_2} (-k_2 \lambda_1 + \lambda_3) + \frac{\partial \alpha_1}{\partial \lambda_3} (-k_3 \lambda_1 + \lambda_4) \\ &\quad - \left(\dot{y}_r + \frac{\partial \alpha_1}{\partial \hat{\varrho}} \right) \gamma \operatorname{sgn}(b_2) (\dot{y}_r + \bar{\alpha}_1) z_1 \\ \Upsilon_1 &= -g_0 \operatorname{sgn}(b_2) (\dot{y}_r + \bar{\alpha}_1)^2 z_1 \\ \Upsilon_2 &= -\frac{\partial \alpha_1}{\partial \hat{\theta}} \Gamma \sigma_\theta \hat{\theta} - \left(\dot{y}_r + \frac{\partial \alpha_1}{\partial \hat{\varrho}} \right) \gamma \sigma_\varrho \hat{\varrho} \end{aligned}$$

Tuning functions

$$\tau_1 = (\omega - \hat{\varrho} (\dot{y}_r + \bar{\alpha}_1) e_1) z_1, \quad \tau_2 = \tau_1 - \frac{\partial \alpha_1}{\partial y} \omega z_2$$

Parameter update laws

$$\dot{\hat{\theta}} = \Gamma \tau_2 - \Gamma \sigma_\theta \hat{\theta}, \quad \dot{\hat{\varrho}} = -\gamma \operatorname{sgn}(b_2) (\dot{y}_r + \bar{\alpha}_1) z_1 - \gamma \sigma_\varrho \hat{\varrho}$$

Switching σ -modification

$$\sigma_\theta = \begin{cases} 0, & \|\hat{\theta}\| \leq M_\theta \\ \sigma_{s\theta}, & \|\hat{\theta}\| \geq 2M_\theta \\ -\frac{2\sigma_{s\theta}}{M_\theta^3} \|\hat{\theta}\|^3 + \frac{9\sigma_{s\theta}}{M_\theta^2} \|\hat{\theta}\|^2 - \frac{12\sigma_{s\theta}}{M_\theta} \|\hat{\theta}\| + 5\sigma_{s\theta}, & \text{otherwise} \end{cases}$$

$$\sigma_\varrho = \begin{cases} 0, & |\hat{\varrho}| \leq M_\varrho \\ \sigma_{s\varrho}, & |\hat{\varrho}| \geq 2M_\varrho \\ -\frac{2\sigma_{s\varrho}}{M_\varrho^3} |\hat{\varrho}|^3 + \frac{9\sigma_{s\varrho}}{M_\varrho^2} |\hat{\varrho}|^2 - \frac{12\sigma_{s\varrho}}{M_\varrho} |\hat{\varrho}| + 5\sigma_{s\varrho}, & \text{otherwise} \end{cases}$$

Adaptive control law

$$u = \alpha_2 - v_{2,3} + \hat{\varrho} \ddot{y}_r$$

Figure 4.3. The control law and the parameter update laws are designed in $\rho = 2$ steps.

4.4.4 Transient bounds

In this section we give explicit \mathcal{L}_∞ bounds on the magnitude of the outputs, as a direct application of Theorem 5 in Chapter 3.

Consider the system (4.11) (resp. 4.12) and the adaptive controller composed of the control law and the parameter update law described in Figure 4.3. Then we have:

$$\|y_1(t)\|_\infty \leq \frac{1}{\sqrt{c_0 d_0}} f_r + \frac{1}{\sqrt{c_0 g_0}} g_r \quad (4.16)$$

$$\|x_1(t)\|_\infty \leq \frac{1}{\sqrt{c_0 d_0}} f_a + \frac{1}{\sqrt{c_0 g_0}} g_a \quad (4.17)$$

where f_r, g_r, f_a and g_a are scalar functions that depends only on the process parameters a_i, b_i , the observer parameters, $\|p_r\|_\infty$ and $\|\dot{p}_r\|_\infty$ (resp. $\|p_a\|_\infty$ and $\|\dot{p}_a\|_\infty$). c_0 and d_0 are defined as

$$c_0 = \min_{i=1,2} c_i, \quad d_0 = \left(\sum_{i=1}^2 \frac{1}{d_i} \right)^{-1}$$

4.5 Numerical simulations

In order to investigate the efficiency of the proposed control and to establish a comparison between the relative and absolute coordinates strategies, we consider the 1952 Taft and the 1989 Loma Prieta earthquakes.

In our simulation, the structure is modeled as a single-degree-of-freedom system, whose parameters are listed in Table 4.1. The hysteretic parameters are also described in Table 4.2. We remark that this particular choice of the hysteretic parameters satisfies $A > 0, \beta + \bar{\gamma} > 0$ and $\beta - \bar{\gamma} \geq 0$, that is, the hysteretic component $z(t)$ will be always bounded [IMR04].

	base	structure
mass	$m_1 = 6 \times 10^5 \text{ kg}$	$m_2 = 6 \times 10^5 \text{ kg}$
stiffness	$k_1 = 0.1185 \times 10^8 \text{ N/m}$	$k_2 = 9 \times 10^8 \text{ N/m}$
damping	$\bar{c}_1 = 0.1067 \times 10^7 \text{ Ns/m}$	$\bar{c}_2 = 0.2324 \times 10^7 \text{ Ns/m}$

Table 4.1. Model coefficients of the single-degree-of-freedom system.

$\alpha = 0.5$	$A = 1$
$k_0 = 61224.49 \text{ N/m}$	$\beta = 0.5$
$D = 0.0245 \text{ m}$	$\bar{\gamma} = 0.5$

Table 4.2. Parameters of the hysteresis model.

We note that the responses of the floors in open loop experiments are practically identical, because, in general, base isolated buildings behave as rigid body systems concentrating the maximum displacements at the isolators. Consequently, single degree of freedom approximations are useful to simulate their response for the purpose of comparing the performance of different control strategies.

We use an index (μ) in order to evaluate the response improvement due to active control with respect to the response where only passive control is applied. The index is defined as follows. For a fixed norm (in this chapter both the infinity and the root-mean-square norm are used) and a fixed system representation (in relative or absolute coordinates), we compute the ratio between the norms of the controlled and the uncontrolled response. For example, as can be seen in Table 4.4, in the uncontrolled case the infinity norm of the relative base displacement is

$$r_u = \|y_1\|_\infty = 1.9845 \cdot 10^{-2} \text{ m}$$

and the norm in the controlled case with design parameters $c_0 = d_0 = g_0 = 5$ is

$$r_c = \|y_1\|_\infty = 1.0452 \cdot 10^{-2} \text{ m}.$$

This way, we define the index μ_∞ of response improvement as

$$\mu_\infty = \frac{r_c}{r_u} \cdot 100 = 52.67\% \quad (4.18)$$

Equivalently, the root-mean-square norm of the relative base displacement is

$$r_u = \|y_1\|_{RMS} = 8.0442 \cdot 10^{-3} \text{ m}$$

and the norm in the controlled case with design parameters $c_0 = d_0 = g_0 = 5$ is

$$r_c = \|y_1\|_{RMS} = 3.7167 \cdot 10^{-3} \text{ m}.$$

This way, we define the index μ_{RMS} of response improvement as

$$\mu_{RMS} = \frac{r_c}{r_u} \cdot 100 = 46.20\% \quad (4.19)$$

The infinity norm of a signal w is defined as

$$\|w\|_\infty = \max_{t \in [t_0, t_1]} |w(t)|.$$

Thus, the infinity norm will be useful in considering the maximum absolute values of the signals we are analyzing. On the other hand, a measure of a signal that reflects its eventual, average size is its root-mean-square value (in a finite interval), defined by

$$\|w\|_{RMS} = \sqrt{\frac{1}{t_1 - t_0} \int_{t_0}^{t_1} w^2(t)}.$$

This is a classical notion of the size of a signal, widely used in many areas of engineering and, in our analysis, this norm can give us a measure of the reduction of the structure oscillations.

4.5.1 Results

Two sets of numerical experiments have been performed. In the first one, the system is excited by the 1952 Taft earthquake. Figure 4.4 shows the ground acceleration, velocity and displacement for this earthquake. The second set of experiments corresponds to the excitation of the 1989 Loma Prieta earthquake, whose ground motion is shown in Figure 4.12. Table 4.3 summarizes the results presented in this section.

For the Taft case, Figure 4.5 displays the time histories of the base and the structure motions (displacement, velocity and interstory drift) and the control signal acceleration for the control designed using the relative coordinates. Figure 4.6 gives the same information for the case with absolute coordinates.

TAFT EARTHQUAKE		LOMA PRIETA EARTHQUAKE	
Figure	Content	Figure	Content
4.4	Taft earthquake	4.12	Taft earthquake
4.5	Time histories in rel. coord.	4.13	Time histories in rel. coord.
4.6	Time histories in abs. coord.	4.14	Time histories in abs. coord.
4.7	index μ_∞ in rel. coord.	4.15	index μ_∞ in rel. coord.
4.8	index μ_∞ in abs. coord.	4.16	index μ_∞ in abs. coord.
4.9	index μ_{RMS} in rel. coord.	4.17	index μ_{RMS} in rel. coord.
4.10	index μ_{RMS} in abs. coord.	4.18	index μ_{RMS} in abs. coord.
4.11	norm of the control	4.19	norm of the control

Table 4.3. List of figures.

In both cases the following control parameters have been selected:

$$c_0 = d_0 = g_0 = \gamma = 30, \quad \Gamma = \gamma I, \quad \sigma_{s\theta} = \sigma_{s\rho} = 40.$$

In order to check the influence of the control parameters, the same experiments of the cases of Figures 4.5 and 4.6 have been performed for different values of the parameters c_0, d_0 and g_0 . For each experiment, we compute the indices μ_∞ and μ_{RMS} defined in equations (4.18) and (4.19). Figures 4.7 and 4.8 shows the index μ_∞ for both relative and absolute coordinate cases respectively. Figures 4.9 and 4.10 shows the index μ_{RMS} for both relative and absolute coordinate cases respectively. Finally, Figure 4.11 shows the infinity and the root-mean-square norms of the control accelerations in both the relative and absolute coordinate cases.

For the Loma Prieta earthquake, Figures 4.12-4.19 show the same kind of results.

Table 4.4 gives the peak values ($\|\cdot\|_\infty$) of the base and structure relative displacements and the interstory drift for the cases in Figure 4.7. Table 4.5 gives the peak values of the base and structure absolute displacements and the interstory drift for the cases in Figure 4.8. Tables 4.6 and 4.7 gives the same kind of results as in Tables 4.4 and 4.5, but with respect to the root-mean-square norm.

4.5.2 Discussion of the results

Looking at Figure 4.5, we may observe that the controlled relative displacement and velocity, both for the base and the structure, are significantly reduced compared to the uncontrolled case. The controlled interstory drift is increased but it remains within acceptable small values. Figure 4.6 shows that the controlled absolute displacements and velocities are also significantly reduced. In this case the interstory drift is reduced in contrast with the interstory behavior of the relative case in Figure 4.5. By comparing the control action in Figures 4.5 and 4.6, this action is clearly smaller and smoother in the case of using absolute coordinates.

By analyzing the plots of the indices μ in Figures 4.7-4.11, we get a more detailed insight on the performance of the control. To help to this analysis, let us consider the Laplace transform of the dynamical equations Σ_s^r and Σ_s^a (see equations (4.2) and (4.4)):

$$y_2(s) = \frac{\bar{c}_2 s + \bar{k}_2}{m_2 s^2 + \bar{c}_2 s + \bar{k}_2} y_1(s) + \frac{m_2 s^2}{m_2 s^2 + \bar{c}_2 s + \bar{k}_2} d(s) \quad (4.20)$$

$$x_2(s) = \frac{\bar{c}_2 s + \bar{k}_2}{m_2 s^2 + \bar{c}_2 s + \bar{k}_2} x_1(s) \quad (4.21)$$

and using norms we have:

$$\|y_2(t)\| = \left\| \frac{\bar{c}_2 s + \bar{k}_2}{m_2 s^2 + \bar{c}_2 s + \bar{k}_2} y_1(t) + \frac{m_2 s^2}{m_2 s^2 + \bar{c}_2 s + \bar{k}_2} d(t) \right\| \quad (4.22)$$

$$\|x_2(t)\| = \left\| \frac{\bar{c}_2 s + \bar{k}_2}{m_2 s^2 + \bar{c}_2 s + \bar{k}_2} x_1(t) \right\| \quad (4.23)$$

Looking at Figures 4.7-4.10, we observe that, by increasing the control design parameters, the indices μ of response of the system (displacements and velocities of the structure and the base) are decreasing in both relative and absolute coordinates. By comparing Figures 4.7-4.8 (resp. Figures 4.9-4.10), we note that the interstory drift increases with the control action in the case of relative coordinates, while it decreases in the case of absolute coordinates.

We recall that the control objective is the regulation of the base displacement, y_1 in the relative case and x_1 in the absolute case. The structure relative displacement y_2 and absolute displacement x_2 are not directly controlled. According to this, it is normal that in Figures 4.7-4.10 the indices μ are lower for x_1 than for x_2 and also lower for y_1 than for y_2 .

As can be seen in equations (4.22)-(4.23), any improvement in the absolute base displacement x_1 leads to a direct improvement of the absolute structure displacement x_2 . Nevertheless, the improvement in the relative base displacement y_1 influences y_2 but it is also affected by the presence of the perturbation earthquake term d which is not zero during the ground motion. When the design parameters are augmented in order to improve these indices (see equations (4.16)-(4.17)), the improvements of the base and the structure in the relative case are sensibly uncoupled whereas in the absolute case both floors move as a single unit. This is also more evident in the index μ representations of the relative velocities. Roughly speaking, in equation (4.22) we may see that, when $y_1(t)$ goes to zero, the structure displacement $y_2(t)$ tends to be in open loop under the effect of the earthquake $d(t)$.

It is also remarkable in Figures 4.7-4.10 that improvements in the absolute case are bigger than those of the relative case. The absolute coordinates based scheme makes use of advantages introduced by base isolation by seeking to keep the building stationary relative to its undisturbed configuration, rather than attempting to move it with the ground to keep relative motion small.

Figure 4.11 shows the infinity and the root-mean-square norm of the control signal in the absolute and the relative cases. Both the infinity and root-mean-square norm in the absolute case are practically constant when the design parameters are augmented whereas the norm in the relative case increases almost linearly with those parameters. This means that, in the absolute case, the responses can be reduced without increasing the peak and the root-mean-square values of the control force. However, in relative coordinates, reducing the response is achieved with the cost of increasing the control effort.

The same results have been obtained with the Loma Prieta earthquake. We have then showed that our adaptive backstepping control has dealt with these two earthquakes with different characteristics. This way, we consider that this strategy can be applied to a wide class of earthquakes.

	$\ y_1\ _\infty$	$\ y_2\ _\infty$	$\ y_2 - y_1\ _\infty$
uncontrolled	$1.9845 \cdot 10^{-2}$	$1.9987 \cdot 10^{-2}$	$1.4490 \cdot 10^{-4}$
$c_0 = d_0 = g_0 = 5$	$1.0452 \cdot 10^{-2}$	$1.0767 \cdot 10^{-2}$	$3.3969 \cdot 10^{-4}$
$c_0 = d_0 = g_0 = 10$	$6.7747 \cdot 10^{-3}$	$6.8965 \cdot 10^{-3}$	$4.6492 \cdot 10^{-4}$
$c_0 = d_0 = g_0 = 15$	$5.0135 \cdot 10^{-3}$	$5.0869 \cdot 10^{-3}$	$5.6237 \cdot 10^{-4}$
$c_0 = d_0 = g_0 = 20$	$4.0826 \cdot 10^{-3}$	$4.2223 \cdot 10^{-3}$	$6.2589 \cdot 10^{-4}$
$c_0 = d_0 = g_0 = 25$	$3.4416 \cdot 10^{-3}$	$3.6495 \cdot 10^{-3}$	$7.1248 \cdot 10^{-4}$
$c_0 = d_0 = g_0 = 30$	$2.9699 \cdot 10^{-3}$	$3.2397 \cdot 10^{-3}$	$7.8056 \cdot 10^{-4}$

Table 4.4. Peak values of the base and structure relative displacements and the interstory drift for the cases in Figure 4.7.

	$\ x_1\ _\infty$	$\ x_2\ _\infty$	$\ x_2 - x_1\ _\infty$
uncontrolled	$5.9997 \cdot 10^{-2}$	$6.0083 \cdot 10^{-2}$	$1.4467 \cdot 10^{-4}$
$c_0 = d_0 = g_0 = 5$	$7.1816 \cdot 10^{-3}$	$7.2513 \cdot 10^{-3}$	$9.4010 \cdot 10^{-5}$
$c_0 = d_0 = g_0 = 10$	$3.9191 \cdot 10^{-3}$	$3.9812 \cdot 10^{-3}$	$6.9284 \cdot 10^{-5}$
$c_0 = d_0 = g_0 = 15$	$2.6517 \cdot 10^{-3}$	$2.6885 \cdot 10^{-3}$	$5.6743 \cdot 10^{-5}$
$c_0 = d_0 = g_0 = 20$	$1.9928 \cdot 10^{-3}$	$2.0169 \cdot 10^{-3}$	$4.8190 \cdot 10^{-5}$
$c_0 = d_0 = g_0 = 25$	$1.5920 \cdot 10^{-3}$	$1.6107 \cdot 10^{-3}$	$4.1966 \cdot 10^{-5}$
$c_0 = d_0 = g_0 = 30$	$1.3244 \cdot 10^{-3}$	$1.3397 \cdot 10^{-3}$	$3.6834 \cdot 10^{-5}$

Table 4.5. Peak values of the base and structure absolute displacements and the interstory drift for the cases in Figure 4.8.

	$\ y_1\ _{RMS}$	$\ y_2\ _{RMS}$	$\ y_2 - y_1\ _{RMS}$
uncontrolled	$8.0442 \cdot 10^{-3}$	$8.0979 \cdot 10^{-3}$	$5.6761 \cdot 10^{-5}$
$c_0 = d_0 = g_0 = 5$	$3.7167 \cdot 10^{-3}$	$3.8174 \cdot 10^{-3}$	$1.2670 \cdot 10^{-4}$
$c_0 = d_0 = g_0 = 10$	$2.3630 \cdot 10^{-3}$	$2.4540 \cdot 10^{-3}$	$1.3924 \cdot 10^{-4}$
$c_0 = d_0 = g_0 = 15$	$1.7106 \cdot 10^{-3}$	$1.7972 \cdot 10^{-3}$	$1.5492 \cdot 10^{-4}$
$c_0 = d_0 = g_0 = 20$	$1.3342 \cdot 10^{-3}$	$1.4195 \cdot 10^{-3}$	$1.7007 \cdot 10^{-4}$
$c_0 = d_0 = g_0 = 25$	$1.0909 \cdot 10^{-3}$	$1.1770 \cdot 10^{-3}$	$1.8394 \cdot 10^{-4}$
$c_0 = d_0 = g_0 = 30$	$9.2174 \cdot 10^{-4}$	$1.0102 \cdot 10^{-3}$	$1.9653 \cdot 10^{-4}$

Table 4.6. Root-mean-square norms of the base and structure relative displacements and the interstory drift for the cases in Figure 4.9.

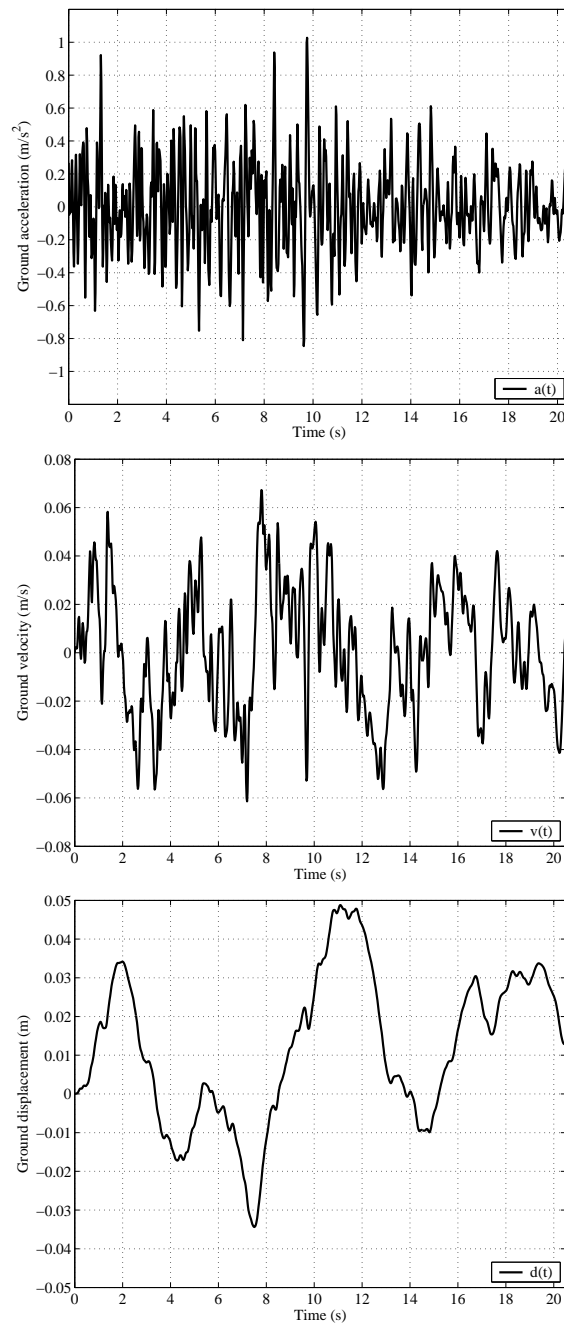


Figure 4.4. 1952 Taft earthquake, ground acceleration (up), velocity (middle) and displacement (down).

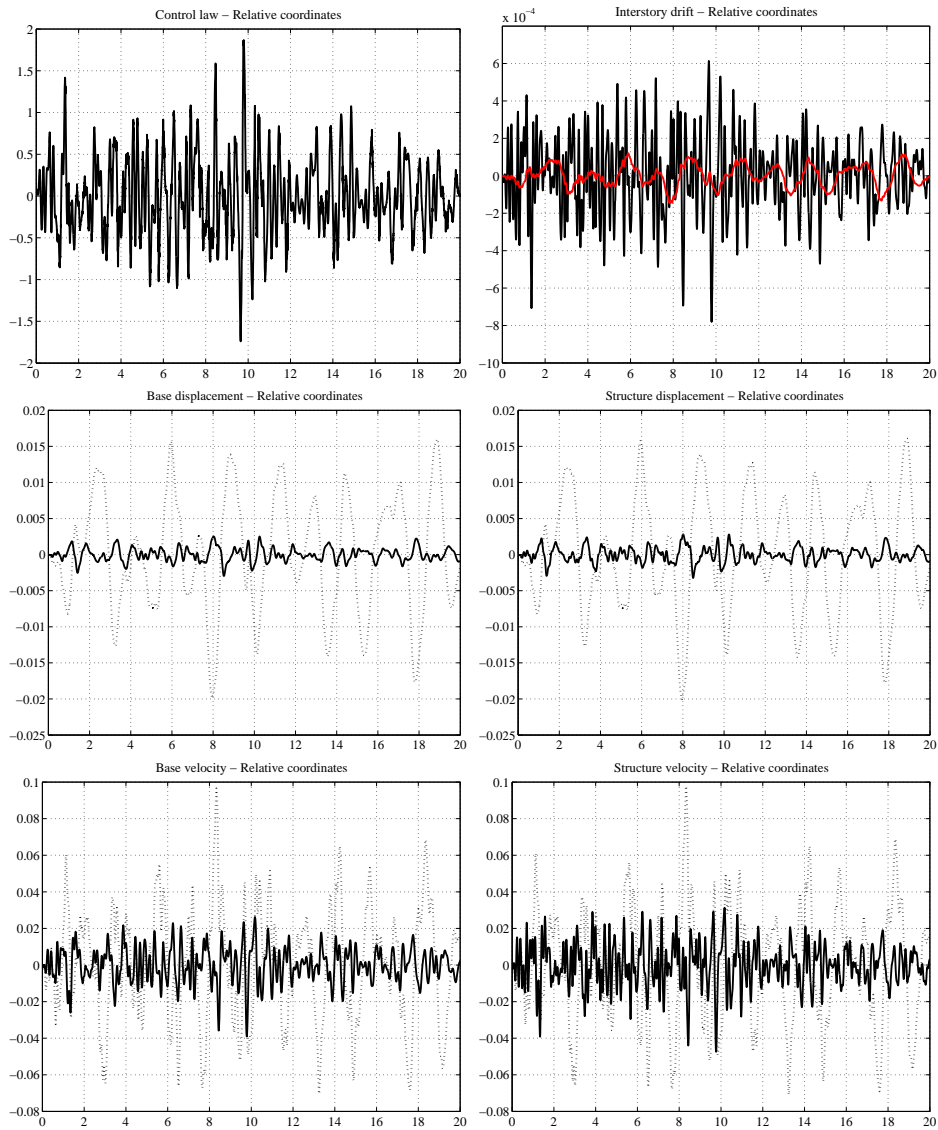


Figure 4.5. 1952 Taft earthquake. Model based in relative coordinates. From left to right and top to bottom: control signal acceleration, $u(t)/m_1$ (m/s^2); closed loop interstory drift (black) and open loop interstory drift (red) (m); closed loop base displacement (solid) and open loop base displacement (dashed) (m); closed loop structure displacement (solid) and open loop structure displacement (dashed) (m); closed loop base velocity (solid) and open loop base velocity (dashed) (m); closed loop structure velocity (solid) and open loop structure velocity (dashed) (m).

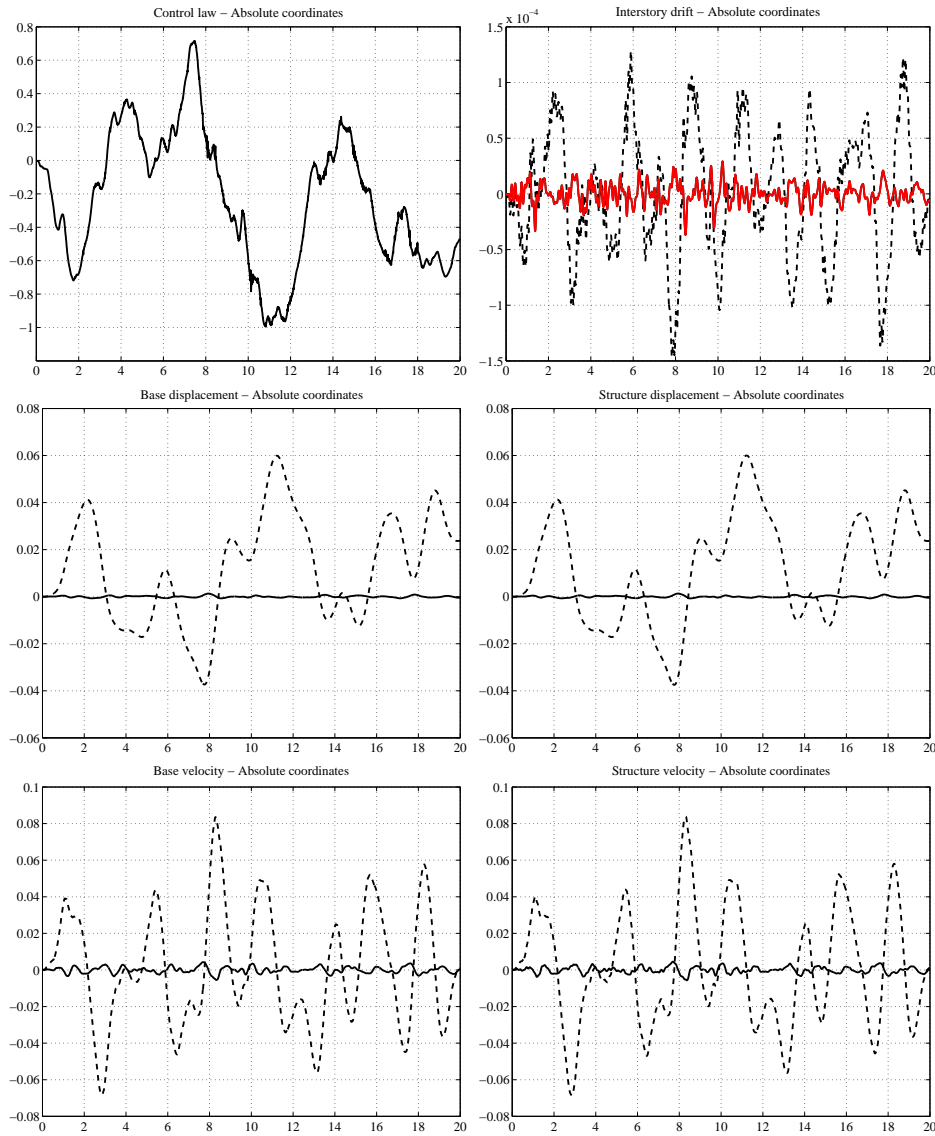


Figure 4.6. 1952 Taft earthquake. Model based in absolute coordinates. From left to right and top to bottom: control signal acceleration, $u(t)/m_1$ (m/s²); closed loop interstory drift (black) and open loop interstory drift (red) (m); closed loop base displacement (solid) and open loop base displacement (dashed) (m); closed loop structure displacement (solid) and open loop structure displacement (dashed) (m); closed loop base velocity (solid) and open loop base velocity (dashed) (m); closed loop structure velocity (solid) and open loop structure velocity (dashed) (m).

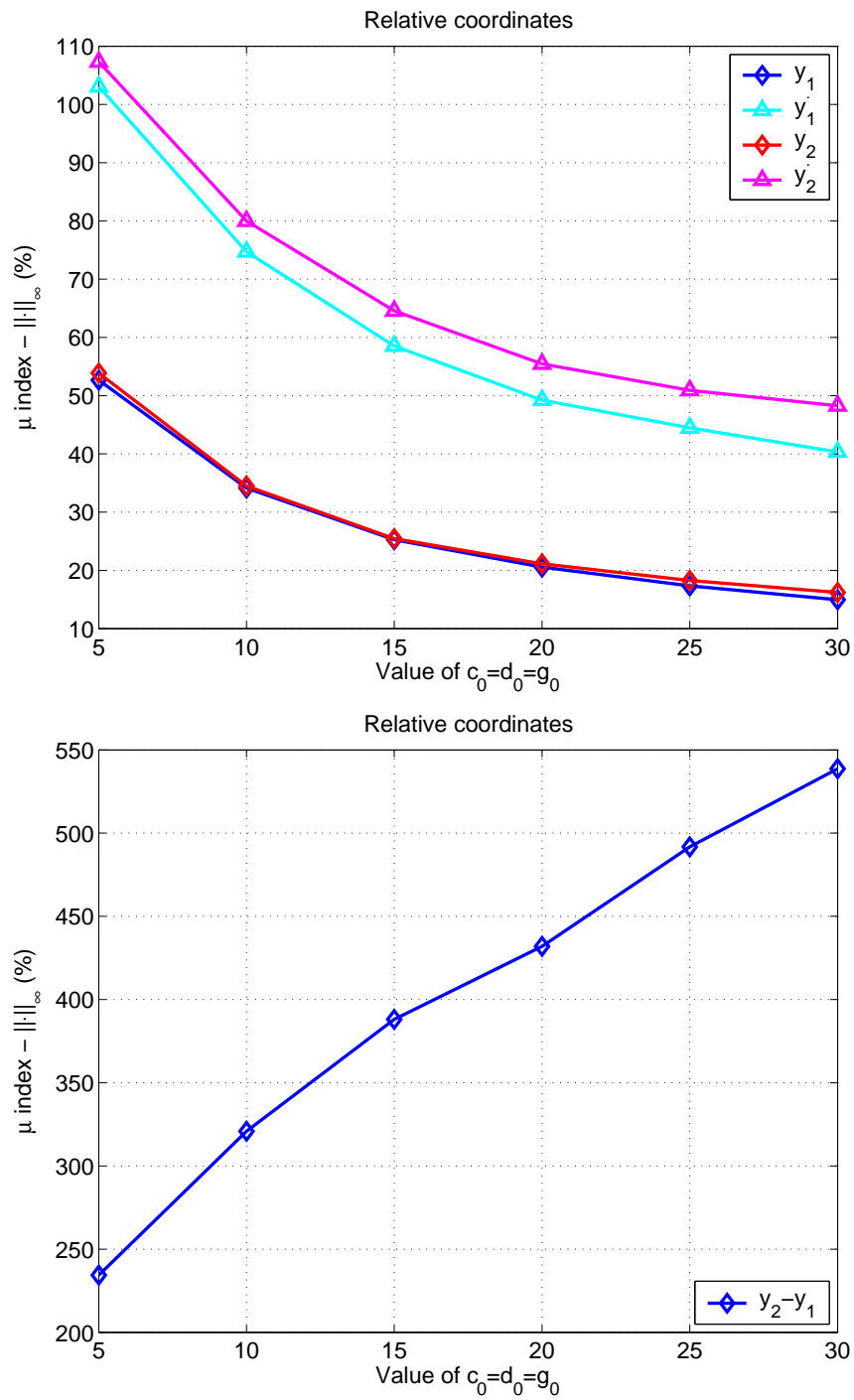


Figure 4.7. Taft earthquake. Index μ_{∞} for some design parameters for the case of relative coordinates.

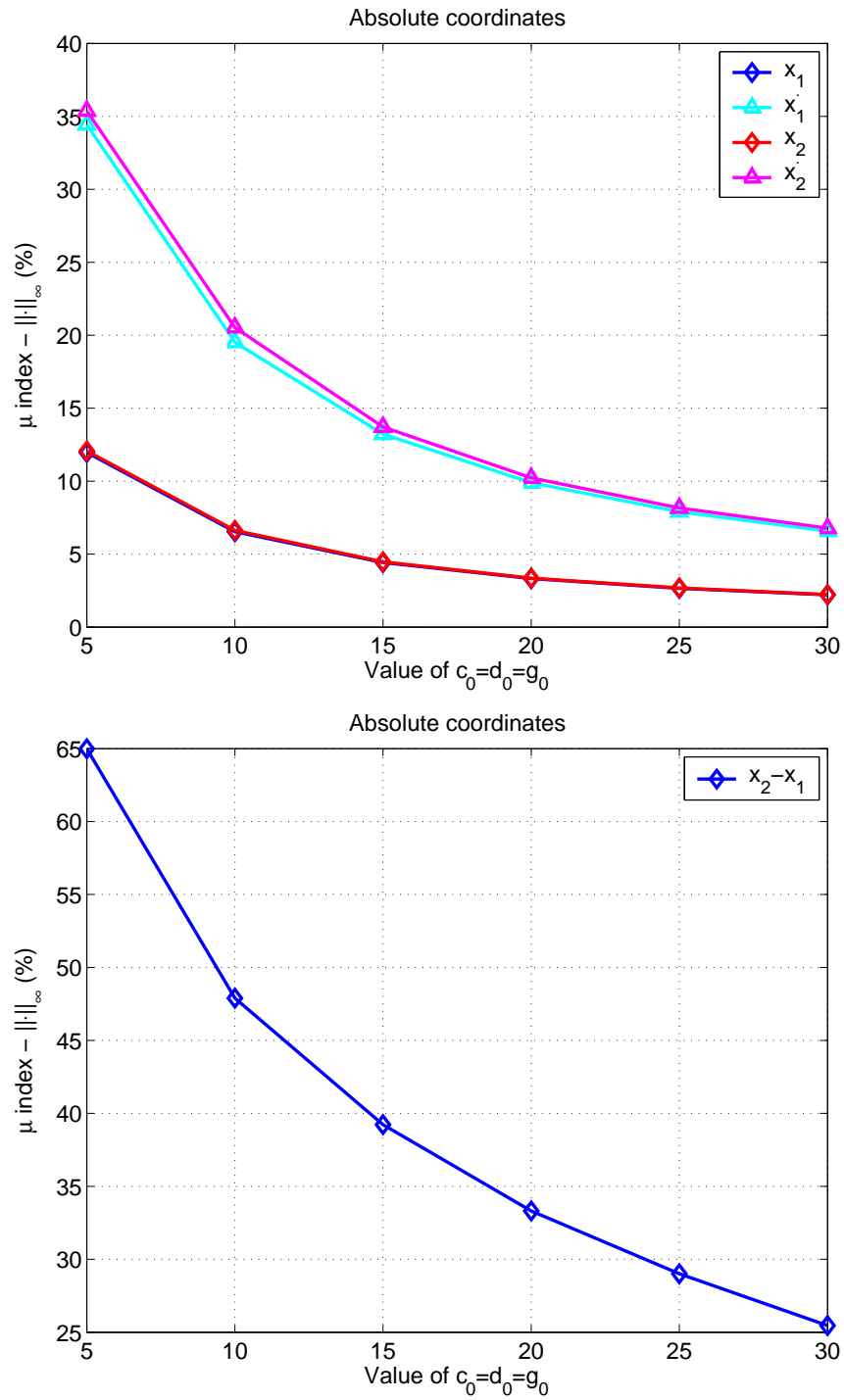


Figure 4.8. Taft earthquake. Index μ_{∞} for some design parameters for the case of absolute coordinates.

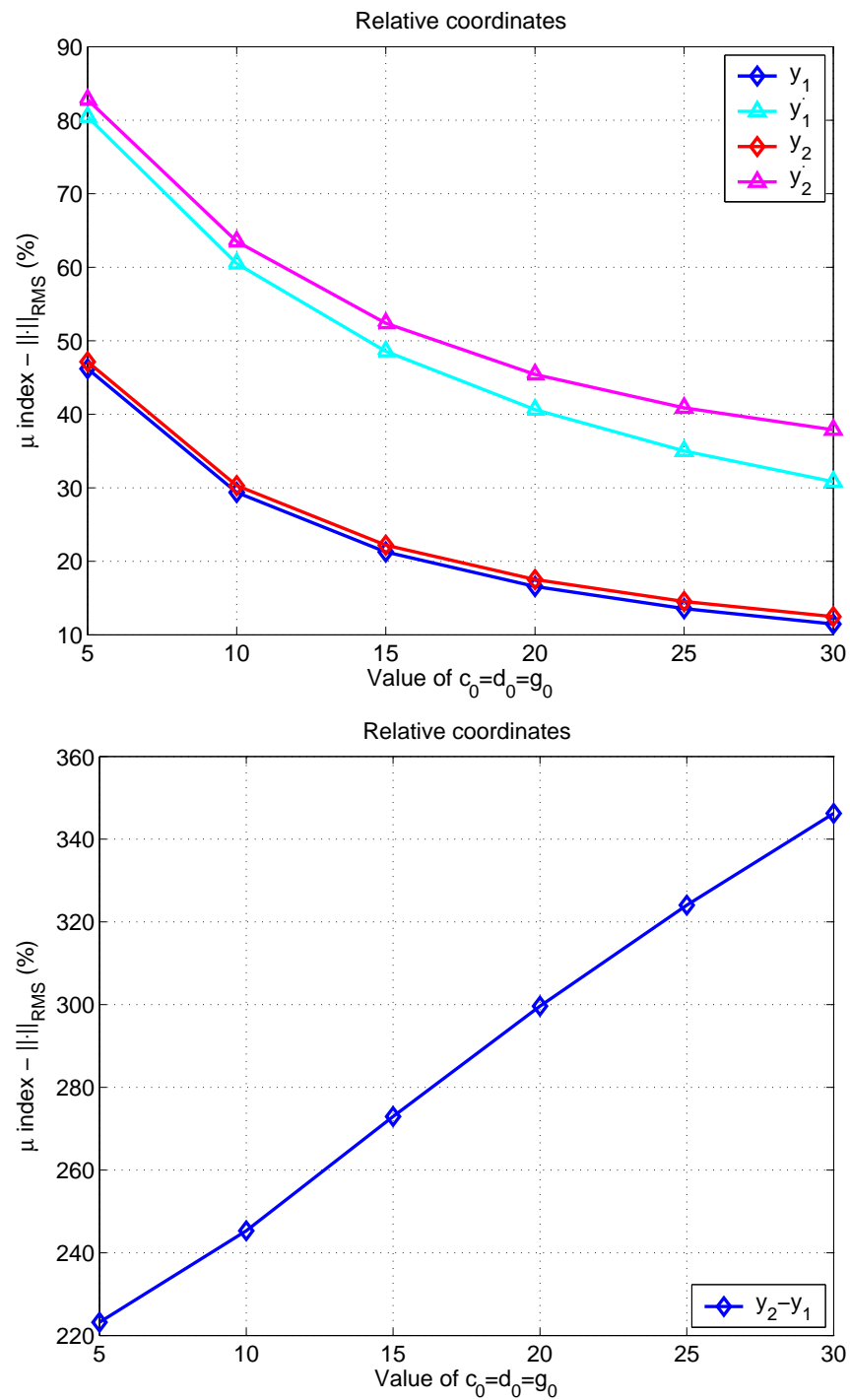


Figure 4.9. Taft earthquake. Index μ_{RMS} for some design parameters for the case of relative coordinates.

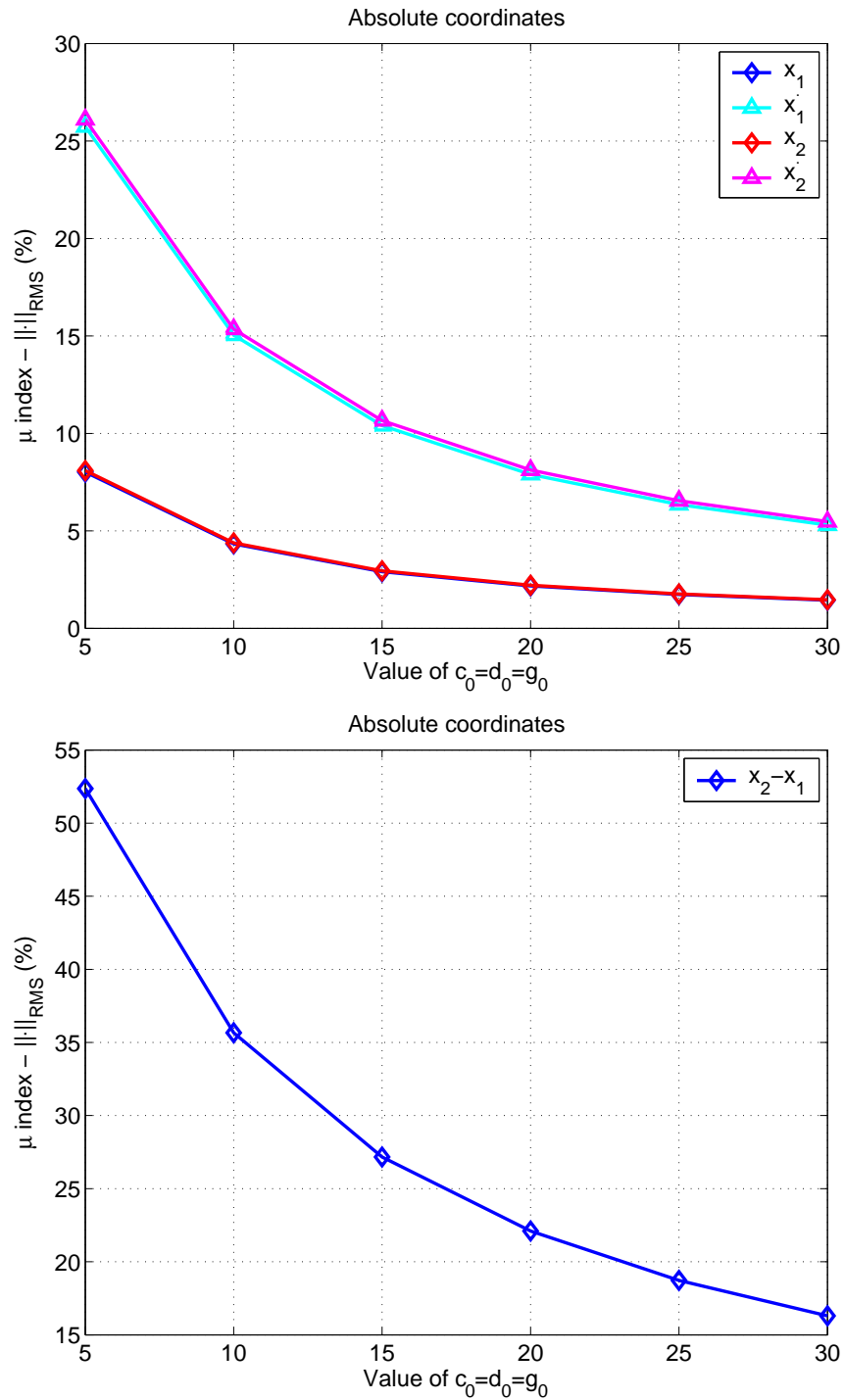


Figure 4.10. Taft earthquake. Index μ_{RMS} for some design parameters for the case of absolute coordinates.

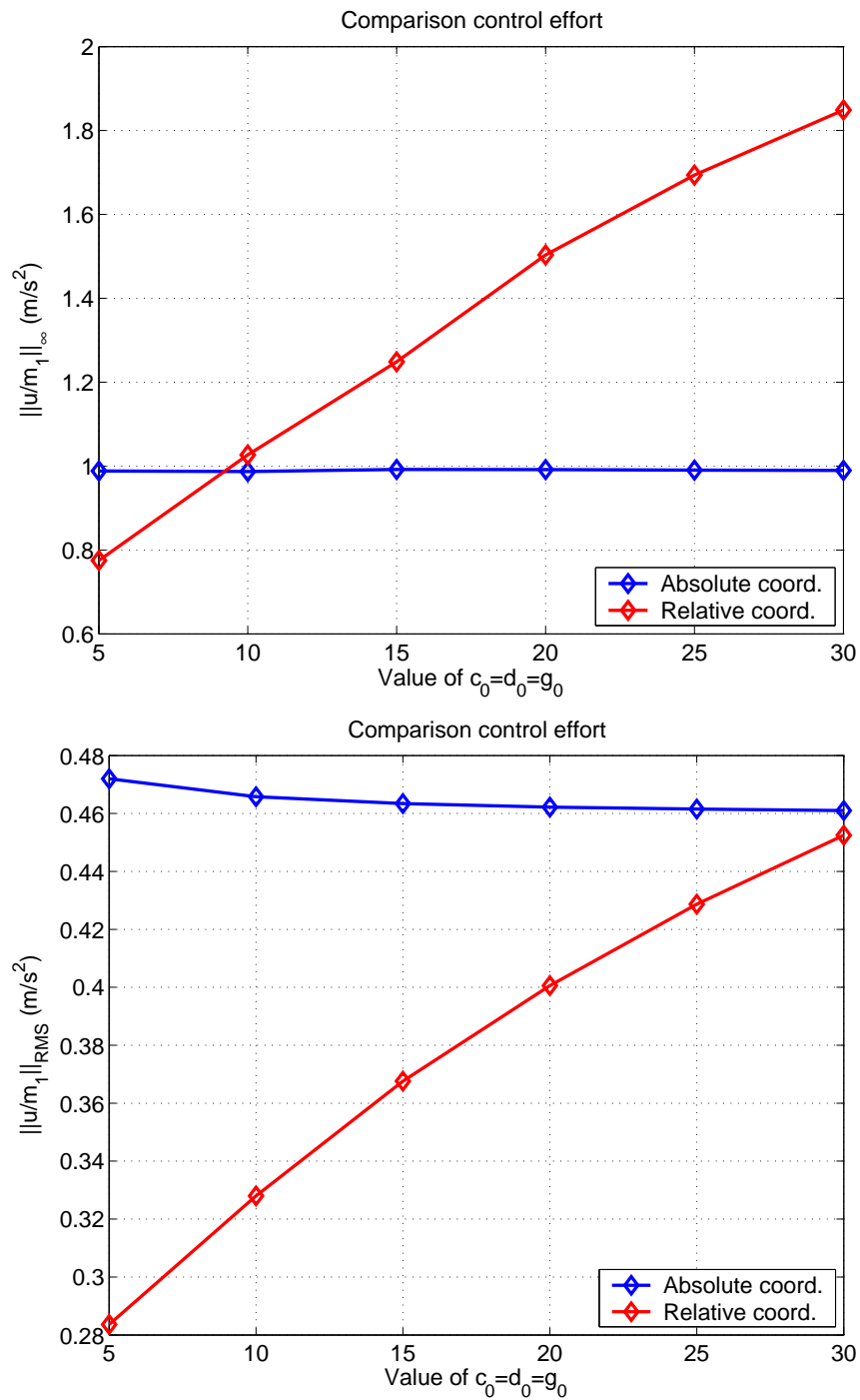


Figure 4.11. Taft earthquake. Infinity norm (up) and root-mean-square norm (down) of the control signal acceleration in both the relative and the absolute coordinates cases.

	$\ x_1\ _{RMS}$	$\ x_2\ _{RMS}$	$\ x_2 - x_1\ _{RMS}$
uncontrolled	$2.5625 \cdot 10^{-2}$	$2.5651 \cdot 10^{-2}$	$5.6761 \cdot 10^{-5}$
$c_0 = d_0 = g_0 = 5$	$2.0534 \cdot 10^{-3}$	$2.0755 \cdot 10^{-3}$	$2.9725 \cdot 10^{-5}$
$c_0 = d_0 = g_0 = 10$	$1.1099 \cdot 10^{-3}$	$1.1241 \cdot 10^{-3}$	$2.0244 \cdot 10^{-5}$
$c_0 = d_0 = g_0 = 15$	$7.4547 \cdot 10^{-4}$	$7.5564 \cdot 10^{-4}$	$1.5422 \cdot 10^{-5}$
$c_0 = d_0 = g_0 = 20$	$5.5832 \cdot 10^{-4}$	$5.6620 \cdot 10^{-4}$	$1.2545 \cdot 10^{-5}$
$c_0 = d_0 = g_0 = 25$	$4.4552 \cdot 10^{-4}$	$4.5193 \cdot 10^{-4}$	$1.0629 \cdot 10^{-5}$
$c_0 = d_0 = g_0 = 30$	$3.7025 \cdot 10^{-4}$	$3.7564 \cdot 10^{-4}$	$9.2508 \cdot 10^{-6}$

Table 4.7. Root-mean-square norms of the base and structure absolute displacements and the interstory drift for the cases in Figure 4.10.

	Relative coordinates		Absolute coordinates	
	$\ u/m_1\ _{\infty}$	$\ u/m_1\ _{RMS}$	$\ u/m_1\ _{\infty}$	$\ u/m_1\ _{RMS}$
$c_0 = d_0 = g_0 = 5$	$7.7510 \cdot 10^{-1}$	$2.8360 \cdot 10^{-1}$	$9.8850 \cdot 10^{-1}$	$4.7200 \cdot 10^{-1}$
$c_0 = d_0 = g_0 = 10$	1.0269	$3.2800 \cdot 10^{-1}$	$9.8690 \cdot 10^{-1}$	$4.6580 \cdot 10^{-1}$
$c_0 = d_0 = g_0 = 15$	1.2487	$3.6760 \cdot 10^{-1}$	$9.9210 \cdot 10^{-1}$	$4.6340 \cdot 10^{-1}$
$c_0 = d_0 = g_0 = 20$	1.5035	$4.0060 \cdot 10^{-1}$	$9.9180 \cdot 10^{-1}$	$4.6220 \cdot 10^{-1}$
$c_0 = d_0 = g_0 = 25$	1.6938	$4.2870 \cdot 10^{-1}$	$9.9040 \cdot 10^{-1}$	$4.6150 \cdot 10^{-1}$
$c_0 = d_0 = g_0 = 30$	1.8487	$4.5250 \cdot 10^{-1}$	$9.8960 \cdot 10^{-1}$	$4.6100 \cdot 10^{-1}$

Table 4.8. Control effort.

4.6 Conclusions

From a structural engineering point of view, the objective of an active control component, as part of a hybrid seismic control system for building structures, is to keep the base displacement relative to the ground and the relative displacement between the structure and the base (interstory drift) within a reasonable range according to the design of the base isolator. In this work, we have proposed a backstepping adaptive control formulated using two alternative coordinates: relative to the ground and relative to an inertial frame (absolute). In order to establish a comparison between both alternatives two control strategies have been considered: (a) measure y_1 and regulate y_1 (in the relative case); and (b) measure x_1 and regulate x_1 (absolute coordinates). In order to investigate the efficacy of the proposed control and to establish a comparison between the relative and the absolute coordinates strategies, the 1952 Taft and the 1989 Loma Prieta earthquakes have been considered. If we consider the following items for our analysis:

- ▶ base displacement relative to the ground
- ▶ interstory drift
- ▶ control effort and smoothness of the control signal

we may summarize the following from the results discussed in Section 4.5.2:

- ▶ the base displacement y_1 in the relative case is clearly reduced with respect the strict passive control. This has been the objective for the backstepping control.
- ▶ in the absolute coordinates case, the backstepping control objective has been stated in reducing the absolute base displacement x_1 and this has been achieved. The relative base displacement $y_1 = x_1 - d$ is augmented but it is still within an acceptable range.
- ▶ the interstory drift $x_2 - x_1$ in the absolute case is significantly reduced whereas in the relative case, $y_2 - y_1$ is augmented with respect the uncontrolled situation. Anyhow, both interstories are considered acceptable.
- ▶ the control signal in the absolute case is relatively smooth. The control signal in the relative case contains high-frequencies. The control effort is larger in the relative coordinates strategy.

From these issues we recommend the use of the absolute coordinates strategy. Besides, the choice of a backstepping adaptive control has allowed to consider that the parameters of the models are uncertain and to have computable bounds on the transient behavior. Finally, the error can be made arbitrarily small by sufficiently increasing the design gains. When using the absolute coordinates, it has been shown that this increase does not lead to an increased of the peak and the root-mean-square norm of the control forces. This behavior of the control forces can also be observed in the simulation results in [IRG97].

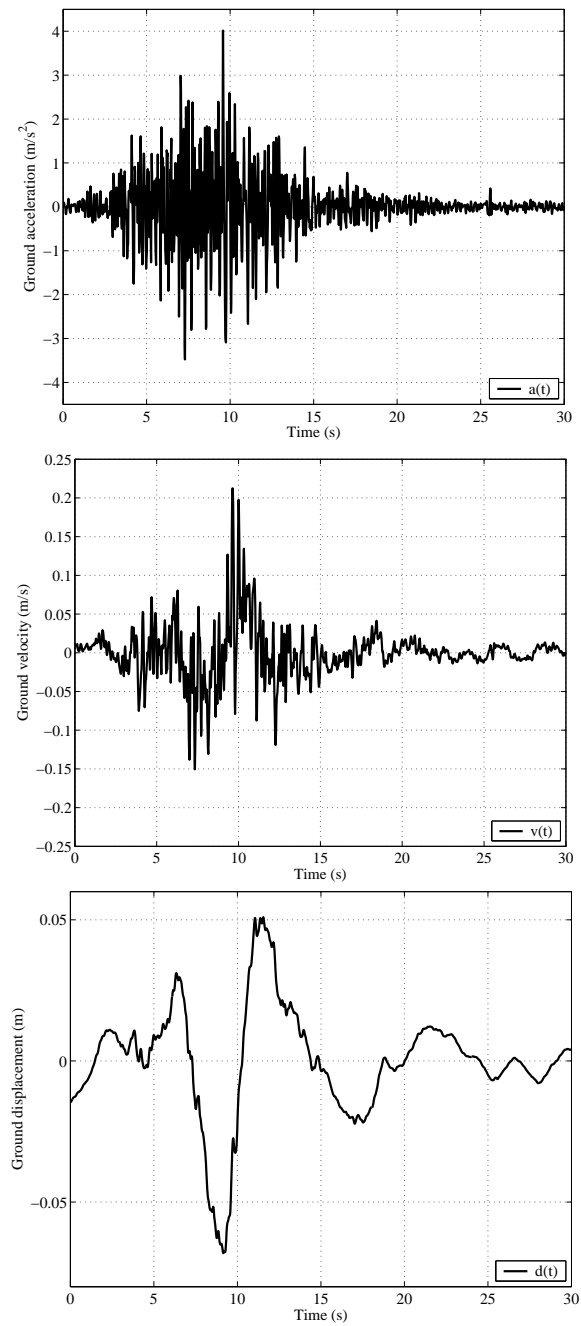


Figure 4.12. 1989 Loma Prieta earthquake, ground acceleration (up), velocity (middle) and displacement (down).

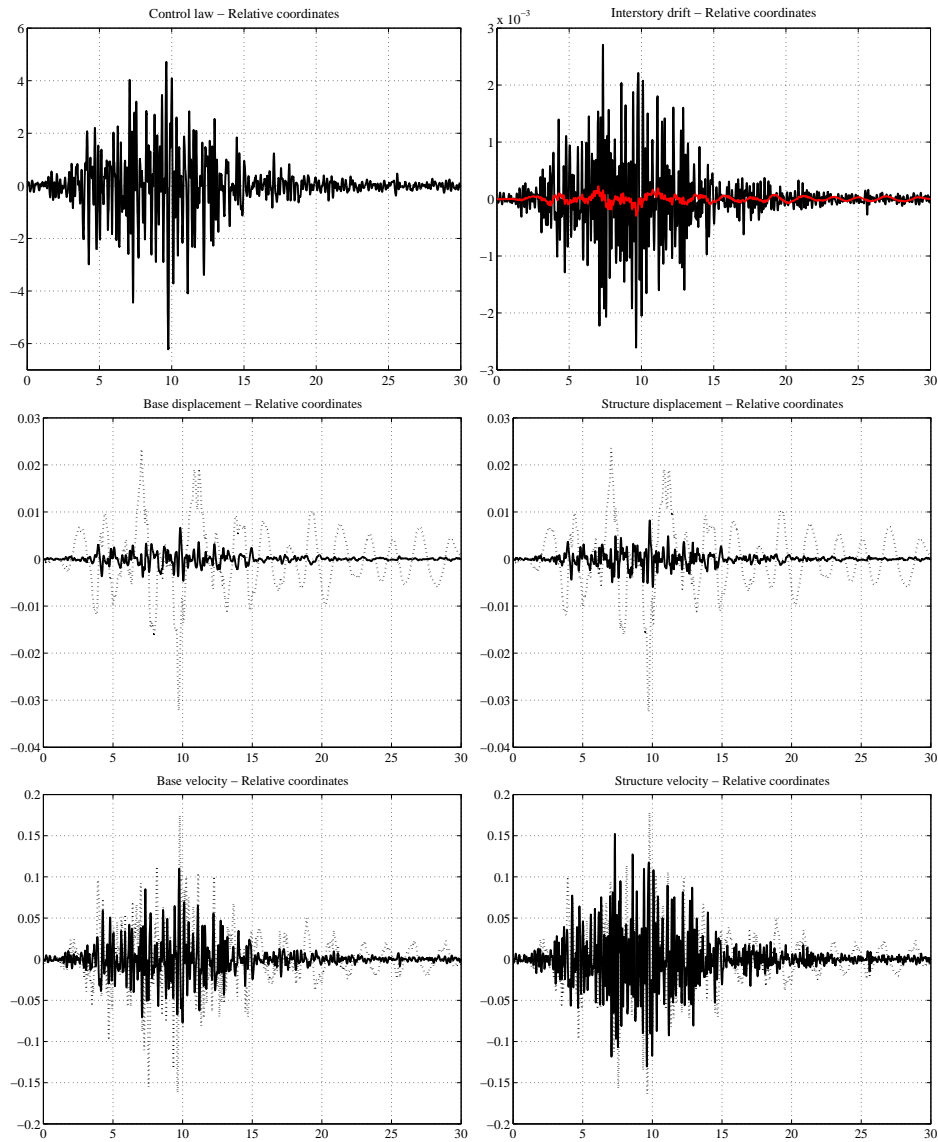


Figure 4.13. 1989 Loma Prieta earthquake. Model based in relative coordinates. From left to right and top to bottom: control signal acceleration, $u(t)/m_1$ (m/s^2); closed loop interstory drift (black) and open loop interstory drift (red) (m); closed loop base displacement (solid) and open loop base displacement (dashed) (m); closed loop structure displacement (solid) and open loop structure displacement (dashed) (m); closed loop base velocity (solid) and open loop base velocity (dashed) (m); closed loop structure velocity (solid) and open loop structure velocity (dashed) (m).

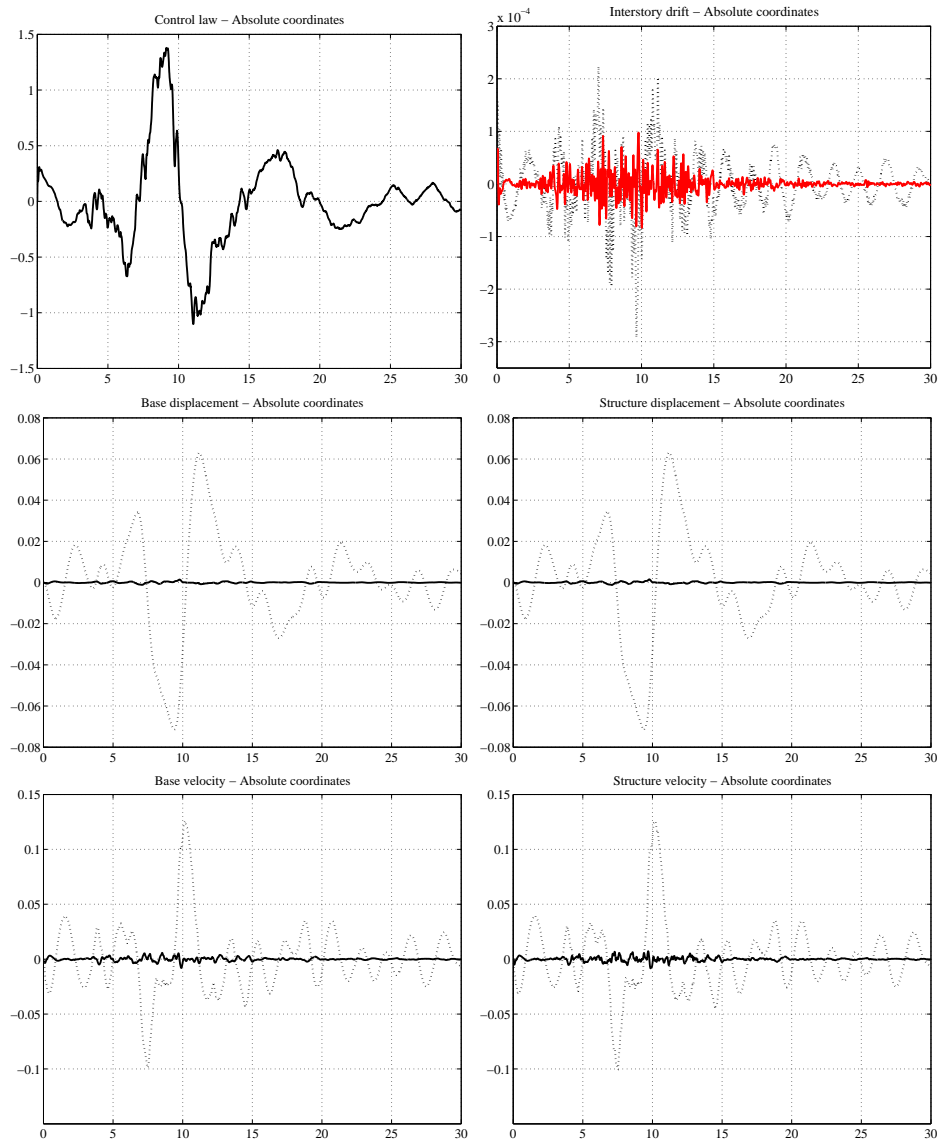


Figure 4.14. 1989 Loma Prieta earthquake. Model based in absolute coordinates. From left to right and top to bottom: control signal acceleration, $u(t)/m_1$ (m/s^2); closed loop interstory drift (black) and open loop interstory drift (red) (m); closed loop base displacement (solid) and open loop base displacement (dashed) (m); closed loop structure displacement (solid) and open loop structure displacement (dashed) (m); closed loop base velocity (solid) and open loop base velocity (dashed) (m); closed loop structure velocity (solid) and open loop structure velocity (dashed) (m).

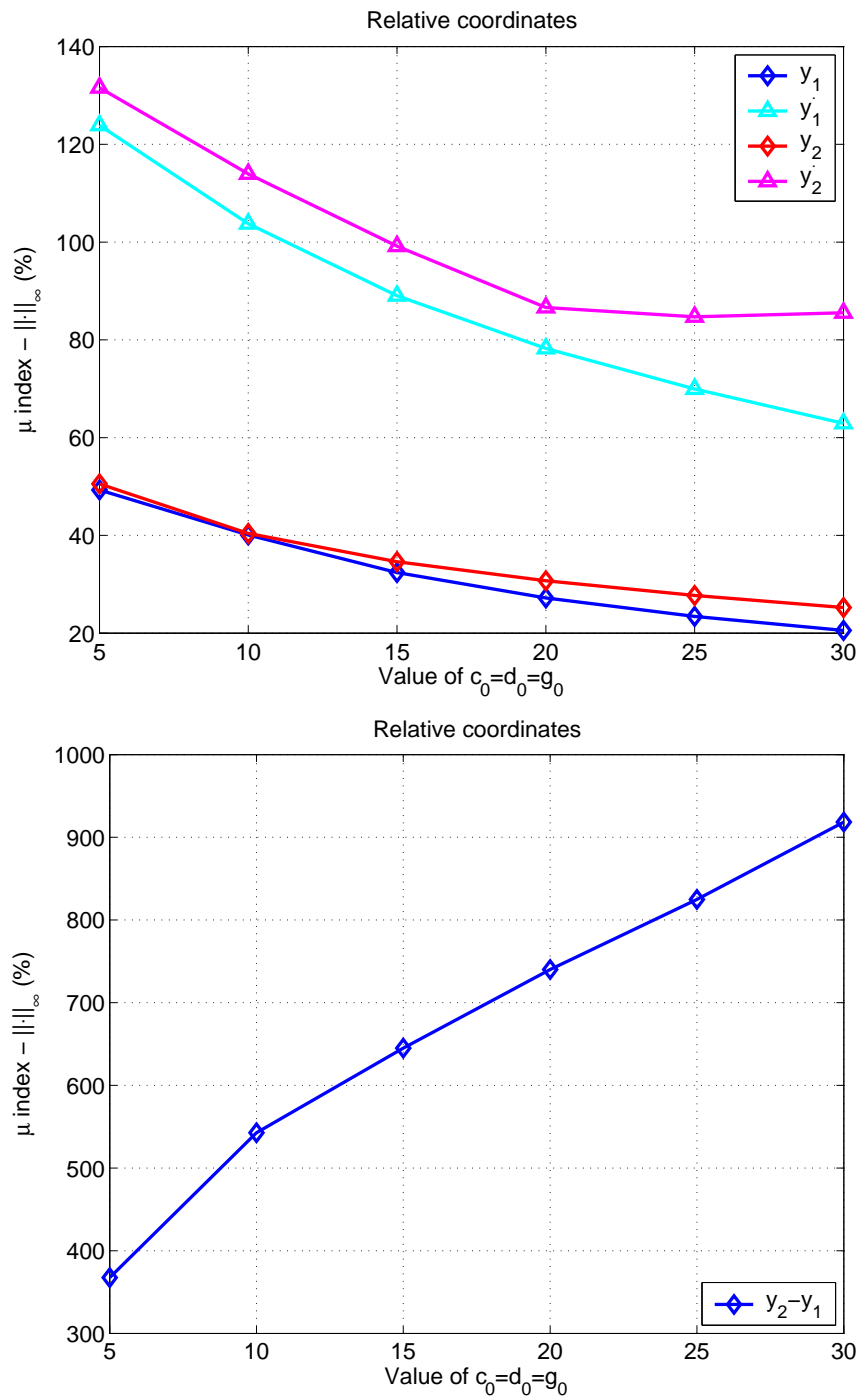


Figure 4.15. Loma Prieta earthquake. Index μ_{∞} for some design parameters for the case of relative coordinates.

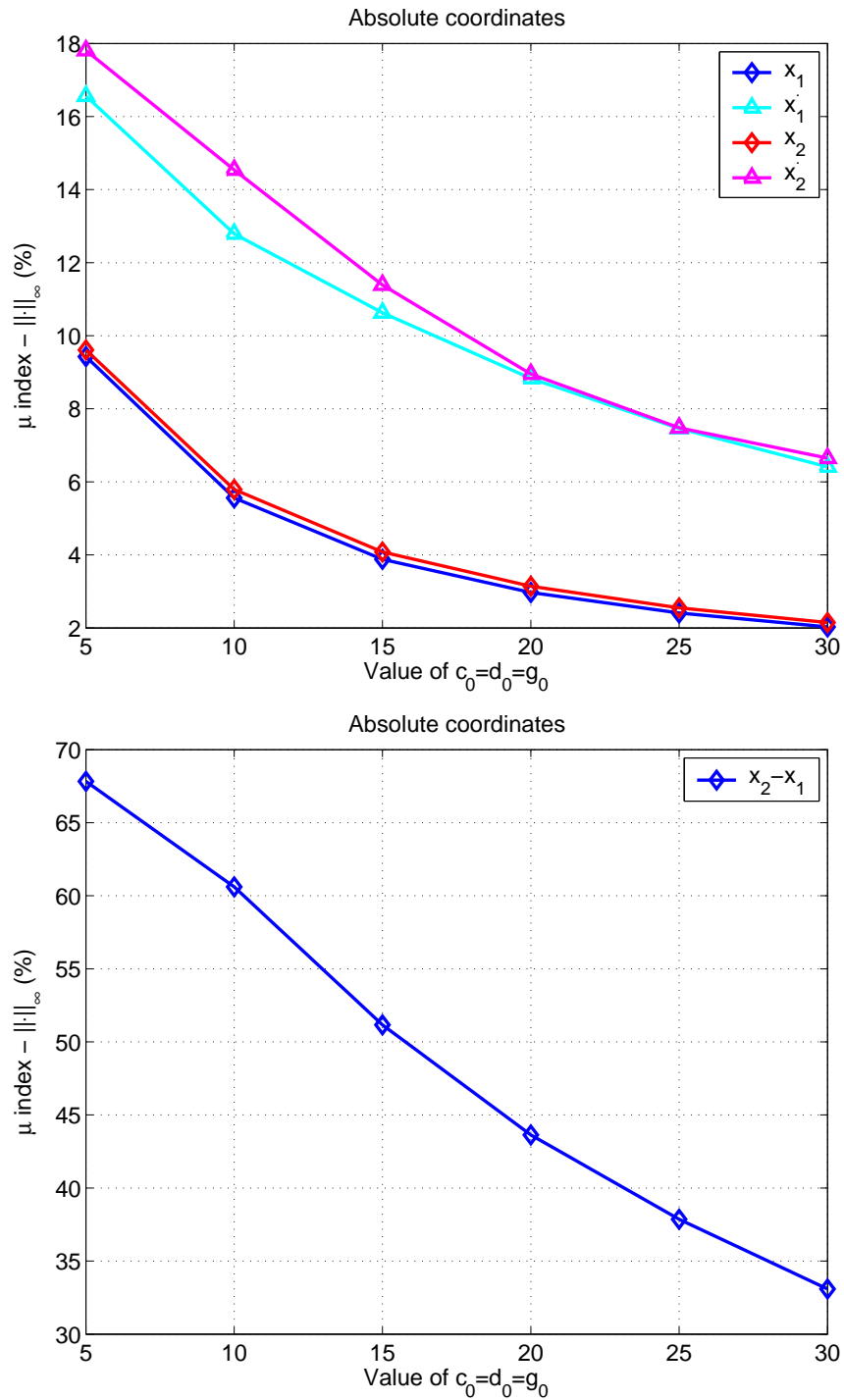


Figure 4.16. Loma Prieta earthquake. Index μ_{∞} for some design parameters for the case of absolute coordinates.

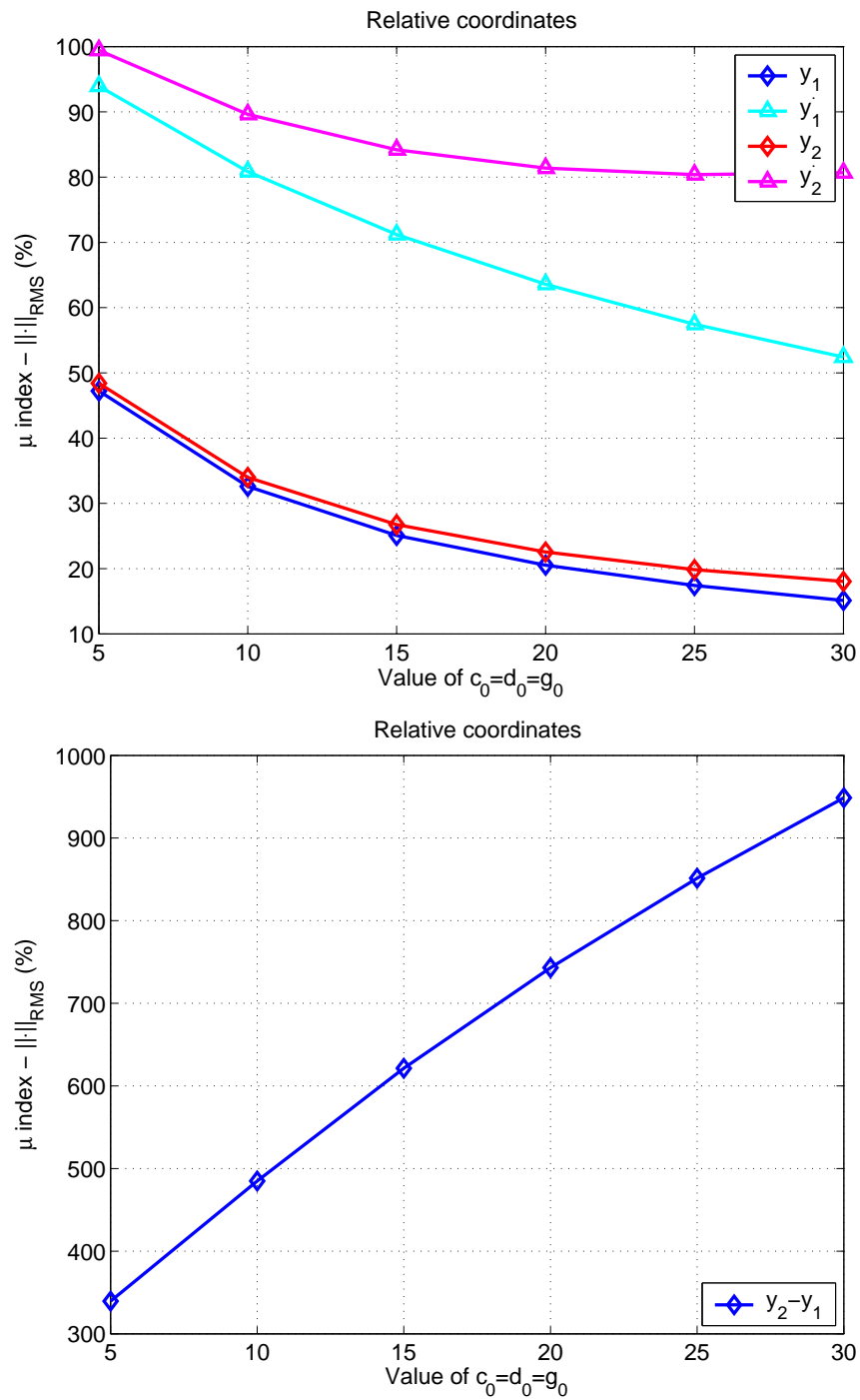


Figure 4.17. Loma Prieta earthquake. Index μ_{RMS} for some design parameters for the case of relative coordinates.

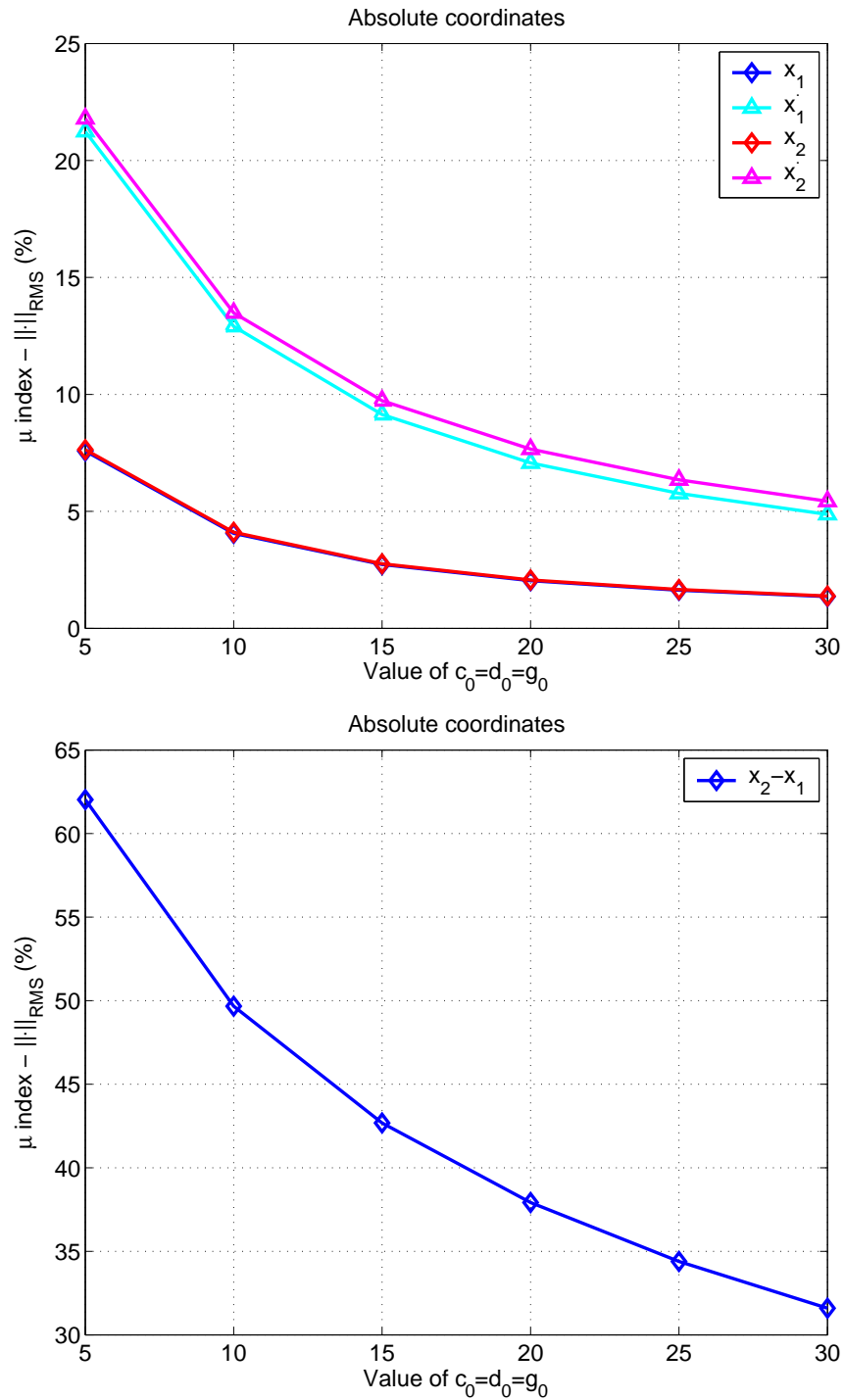


Figure 4.18. Loma Prieta earthquake. Index μ_{RMS} for some design parameters for the case of absolute coordinates.

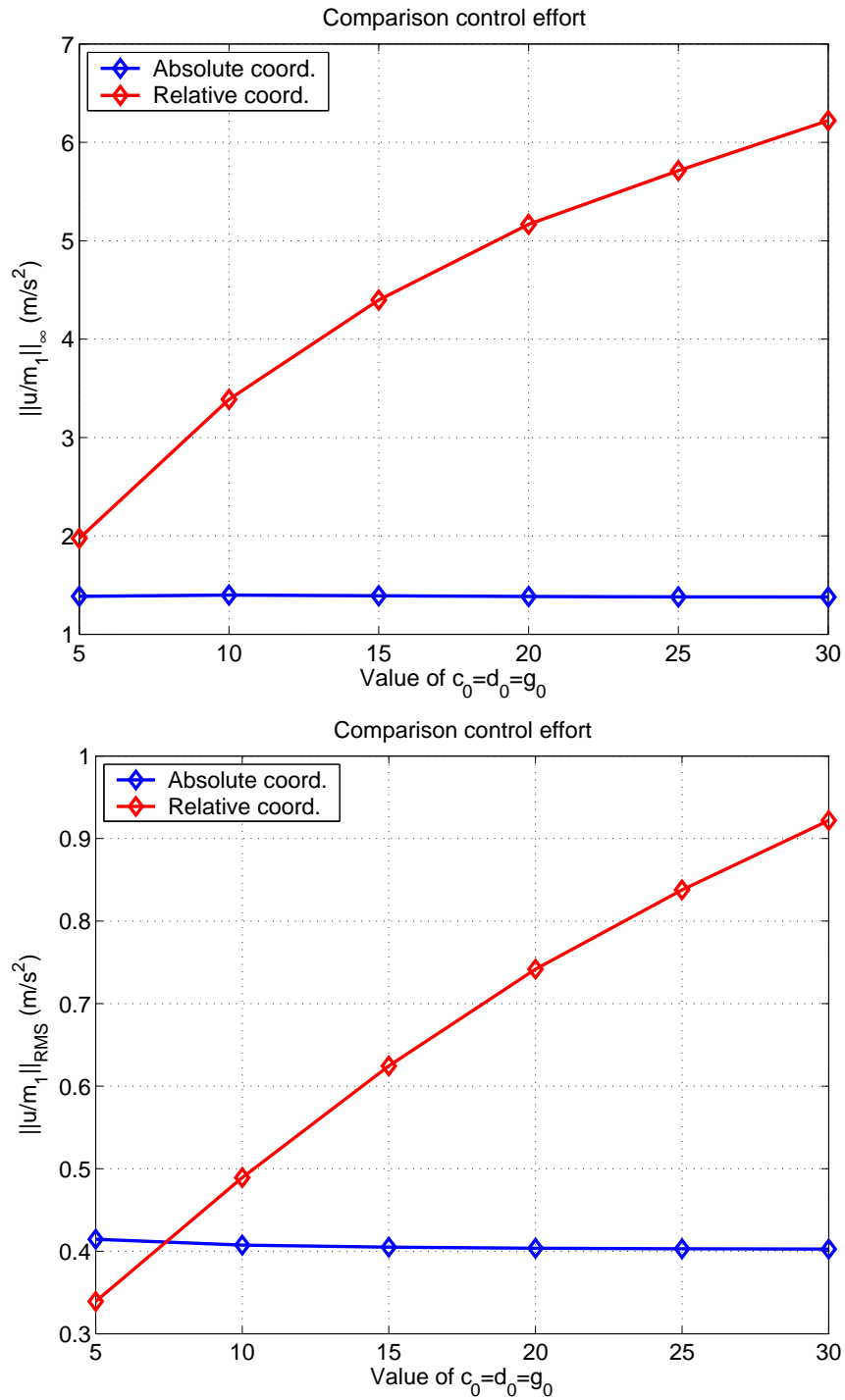
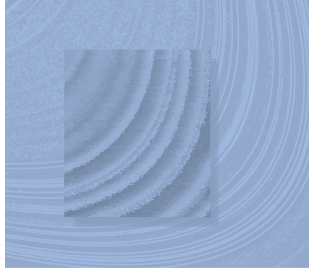


Figure 4.19. Loma Prieta Earthquake. Infinity norm (up) and root-mean-square norm (down) of the control signal acceleration in both the relative and the absolute coordinates cases.



Chapter 5

Sensitivity analysis of the backstepping adaptive tuning functions control design

The backstepping-based adaptive tuning functions design is a control scheme for uncertain systems that ensures reasonably good stability and performance properties of the closed loop. The complexity of the controller makes inevitable the use of digital computers to perform the calculation of the control signal. This chapter addresses the issue of the numerical sensitivity of the adaptive tuning functions. It is shown that while the increase of the design parameters may be desirable to achieve a good transient performance, it harms the control signal as this increase introduces large high-frequency components due to the numerical errors.

5.1 Introduction

The last few years witnessed an increasing interest in the backstepping based designs for control of uncertain systems, especially their adaptive version [KKK95]. Unlike most certainty-equivalence designs [IS96], the adaptive tuning functions offers the designer explicit bounds on the transient behavior of the closed loop [KKK95, Chapter 10]. Since the publication of adaptive tuning functions design applied to linear systems [KKK94], research in this field has focused mainly on robustness issues with respect to unmodelled dynamics and/or external disturbances [IK98a, IK98b, IRG97, NV01b, OIG01, ZI98, WS96, WZS99].

The digital implementation of the continuous backstepping adaptive counterpart has been considered in [RIG99]. A modified tuning functions scheme that borrows elements from the certainty-equivalence controllers have been proposed in [ZI00]. The parameter variation has been treated in [GRI99] and schemes that do not assume the knowledge of the high-frequency gain were proposed in [Miy00b, ZWS00]. A multivariable version of the tuning functions design was proposed in [LT96, WY98, CHIK03].

With respect to numerically reliable algorithms for solving control problems, we cannot forget that there is a continuing and growing need in the systems and control community for good algorithms and robust numerical software for increasingly challenging applications [Var04]. This way, in order to contribute to the accurate and efficient numerical solution of problems in control systems analysis and design we must focus on algorithm development, sensitivity and accuracy issues, large-scale computations and high-performance software [HKMP04, Doo04].

In our case, the complexity of the resulting nonlinear controller makes inevitable the use of a computer to deliver the control signal. Due to the representation of real numbers on a finite number of digits, numerical errors propagate during the process of computing the control law. A crucial question that arises naturally is: how sensitive is the control signal to the numerical errors that are generated by the computational process?

This question was considered for the first time in [PIR04b] by means of numerical simulations. The sensitivity of the control law with respect to the numerical errors and the influence of the design parameters are analyzed in this chapter. For simplicity, we consider a third order linear system with unknown parameters in closed loop with the standard adaptive tuning functions design [KKK95, Chapter 10]. With reasonable design parameters, it has been observed that the control signal is corrupted by large high-frequency components.

5.2 Plant and controller design

Consider here a specific system as a prototype. For this system we summarize the control law to be implemented and analyzed.

5.2.1 Plant

We consider the linear single-input single-output system

$$y(s) = \frac{b_0}{s(s^2 + a_2s + a_1)}u(s), \quad (5.1)$$

where the coefficients $a_1 = 5$, $a_2 = 1$, $b_0 = 1$ are unknown.

The control objective is to ensure the output $y(t)$ to asymptotically track a given smooth reference signal with the specific form

$$y_r(t) = \frac{1}{p_1(s)p_2(s)}r(t),$$

where $p_i(s) = \frac{s^2}{\omega_i^2} + \frac{2\xi_i s}{\omega_i} + 1$, $\xi_i = 0.7$, $\omega_i = 4.9$ ($i = 1, 2$) and $r(t)$ is the unit step.

5.2.2 Design procedure

We use the standard tuning functions design developed in Chapter 2, which is schematically outlined in the following control algorithm.

Error variables

$$z_1 = y - y_r \quad (5.2)$$

$$z_2 = \lambda_2 - \hat{\rho}\dot{y}_r - \alpha_1 \quad (5.3)$$

$$z_3 = \lambda_3 - \hat{\rho}\ddot{y}_r - \alpha_2 \quad (5.4)$$

Stabilizing functions

$$\alpha_1 = \hat{\rho} \bar{\alpha}_1 \quad (5.5)$$

$$\bar{\alpha}_1 = -(c_1 + d_1)z_1 - \xi_2 - \bar{\omega}^T \hat{\theta} \quad (5.6)$$

$$\begin{aligned} \alpha_2 = & -\hat{b}_0 z_1 - \left[c_2 + d_2 \left(\frac{\partial \alpha_1}{\partial y} \right)^2 \right] z_2 \\ & + \beta_2 + \frac{\partial \alpha_1}{\partial \hat{\theta}} \Gamma \tau_2 \end{aligned} \quad (5.7)$$

$$\begin{aligned} \alpha_3 = & -z_2 - \left[c_3 + d_3 \left(\frac{\partial \alpha_2}{\partial y} \right)^2 \right] z_3 + \beta_3 \\ & + \frac{\partial \alpha_2}{\partial \hat{\theta}} \Gamma \tau_3 - \frac{\partial \alpha_1}{\partial \hat{\theta}} \Gamma \frac{\partial \alpha_2}{\partial y} z_2 \omega \end{aligned} \quad (5.8)$$

$$\begin{aligned} \beta_2 = & \frac{\partial \alpha_1}{\partial y} (\xi_2 + \omega^T \hat{\theta}) + \frac{\partial \alpha_1}{\partial \eta} (A_0 \eta + e_3 y) \\ & + \frac{\partial \alpha_1}{\partial y_r} \dot{y}_r + k_2 \lambda_1 + \frac{\partial \alpha_1}{\partial \lambda_1} (-k_1 \lambda_1 + \lambda_2) \\ & + \left(\dot{y}_r + \frac{\partial \alpha_1}{\partial \hat{\rho}} \dot{\hat{\rho}} \right) \dot{\hat{\rho}} \end{aligned} \quad (5.9)$$

$$\begin{aligned} \beta_3 = & \frac{\partial \alpha_2}{\partial y} (\xi_2 + \omega^T \hat{\theta}) + \frac{\partial \alpha_2}{\partial \eta} (A_0 \eta + e_3 y) + \frac{\partial \alpha_2}{\partial y_r} \dot{y}_r \\ & + \frac{\partial \alpha_2}{\partial \dot{y}_r} \ddot{y}_r + k_3 \lambda_1 + \frac{\partial \alpha_2}{\partial \lambda_1} (-k_1 \lambda_1 + \lambda_2) \\ & + \frac{\partial \alpha_2}{\partial \lambda_2} (-k_2 \lambda_1 + \lambda_3) + \left(\ddot{y}_r + \frac{\partial \alpha_2}{\partial \hat{\rho}} \dot{\hat{\rho}} \right) \dot{\hat{\rho}} \end{aligned} \quad (5.10)$$

Tuning functions

$$\tau_1 = (\omega - \hat{\rho}(\dot{y}_r + \bar{\alpha}_1)e_1)z_1 \quad (5.11)$$

$$\tau_2 = \tau_1 - \frac{\partial \alpha_1}{\partial y} \omega z_2 \quad (5.12)$$

$$\tau_3 = \tau_2 - \frac{\partial \alpha_2}{\partial y} \omega z_3 \quad (5.13)$$

Parameter update laws

$$\dot{\hat{\theta}} = \Gamma \tau_3 \quad (5.14)$$

$$\dot{\hat{q}} = -\gamma_1 \text{sgn}(b_0)(\dot{y}_r + \bar{\alpha}_1)z_1 \quad (5.15)$$

K-filters

$$\dot{\eta} = A_0 \eta + e_3 y \quad (5.16)$$

$$\dot{\lambda} = A_0 \lambda + e_3 u \quad (5.17)$$

Adaptive control law

$$u = \alpha_3 + \hat{q} y_r^{(3)} \quad (5.18)$$

We present in Figure 5.1 simulations results of the closed-loop system (5.1) for two different values of the design parameters. The propagated errors are not significant for $c_i = d_i = 0.5$, $i = 1, 2, 3$ neither in the tracking error $z_1 = y - y_r$ or in the control law u . On the contrary, the control signal is clearly corrupted for $c_i = d_i = 2$, $i = 1, 2, 3$. We will give, in the following lines, a more detailed insight into these numerical issues.

5.3 Sensitivity analysis

As is well known, a mathematical model comprises independent variables, dependent variables, and relationships (for instance, equations or differential equations) between these quantities.

With respect to the algorithm described in Section 5.2, the numerical methods needed to solve the differential equations of the K -filters (5.16)-(5.17) and the parameter update laws (5.14)-(5.15) introduce themselves numerical errors. The effects of such errors must be quantified in order to assess the respective model's range of validity.

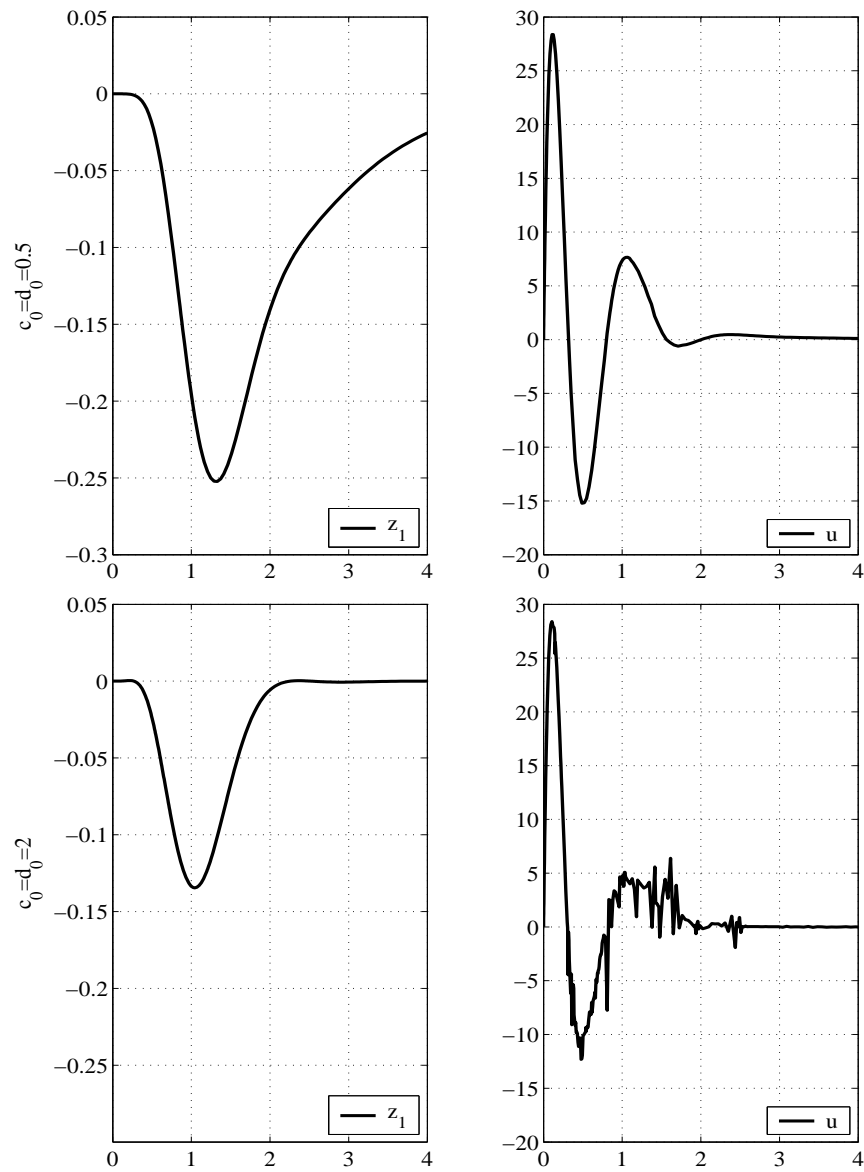


Figure 5.1. The propagated errors are not significant for $c_i = d_i = \kappa = 0.5$, $i = 1, 2, 3$, in u (up), but the control signal is clearly corrupted for $c_i = d_i = \kappa = 2$, $i = 1, 2, 3$ (down).

As considered in [Cac03], the most common procedure for assessing the effects of parameter variations on a model is to vary selected input parameters, rerun the code, and record the corresponding changes in the results, or responses, calculated by the code. The model parameters responsible for the largest relative changes in a response are then considered to be the most important for the respective response.

As can be seen in Section 5.2, for any time t and for fixed design parameters $c_i, d_i > 0$, $i = 1, 2, 3$ and $\gamma > 0$ —these design parameters are chosen by the designer to achieve a good transient performance—, the control signal u can be computed as a function of the reference signal y_r and its derivatives, the K -filters $\eta = (\eta_1, \eta_2, \eta_3)^T$ and $\lambda = (\lambda_1, \lambda_2, \lambda_3)^T$, the estimated parameters $\hat{\theta} = (\hat{\theta}_1, \hat{\theta}_2, \hat{\theta}_3)^T$ and $\hat{\rho}$ and the output signal y . We can then write

$$u(t) = f(y_r, \dot{y}_r, \ddot{y}_r, y_r^{(3)}, \eta^T, \lambda^T, \hat{\theta}^T, \hat{\rho}, y). \quad (5.19)$$

The variables $\eta, \lambda, \hat{\theta}, \hat{\rho}$ and y are explicitly related as can be seen in (5.14)-(5.17), that is, these variables are not independent and, for instance, any perturbation ε in the measure of the output y is immediately propagated through the filters and the estimated parameters. However, we are not analyzing the error propagation through the different signals. We are interested in the sensitivity analysis of the control law $u = f$ with respect to small variations in the value of its variables, although they are clearly dependent.

The influence of the perturbed variables with respect to the control signal will be different, as we will see in the next subsections.

5.3.1 Elements of the analysis

It has been shown that the control signal u is a function of 15 variables, see equation (5.19). However, the reference signal y_r and its derivatives are external signals so that they will be assumed to be exactly known.

In order to fully understand the sensitivity of the control law u , let us consider a *perturbation function*

$$\varepsilon : [a, b] \subset \mathbb{R}^+ \rightarrow \mathbb{R}, \quad 0 < a < b.$$

We consider the ideal case when the control problem is solved ideally without numerical errors. We consider then that $u(t)$ is the control law, $\eta(t)$ and $\lambda(t)$ are the K -filters, $\hat{\theta}(t)$ and $\hat{\rho}(t)$ are the estimated parameters and $y(t)$ is the output signal.

Consider now any of the variables of the function f , for instance y . For any time $t \in [a, b]$ we define the function \tilde{u}_y as

$$\tilde{u}_y(t) = f(y_r(t), \dots, \hat{\rho}(t), y(t) + \varepsilon(t)).$$

For any time t , $\tilde{u}_y(t)$ can be considered as the perturbed control generated if *only* the variable $y(t)$ is perturbed by a quantity defined by $\varepsilon(t)$.

Finally, we define the sensitivity function, $Dy(t)$ of u with respect to y and associated to the perturbed function $\varepsilon(t)$ as

$$Dy(t) = \frac{|u(t) - \tilde{u}_y(t)|}{m},$$

where m is the maximum absolute value of the control signal u ,

$$m = \max_{t \in [a, b]} |u(t)|.$$

The function $\varepsilon(t)$ can be considered as a function that, for any $t \in [a, b]$, contains random numerical errors that are generated by the computational process. This way, $Dy(t)$ is a certain measure of the relative error with respect to the control signal and can be considered as a time-dependent function:

$$\begin{aligned} Dy : \mathbb{R}^+ &\rightarrow \mathbb{R} \\ t &\rightarrow Dy(t) \end{aligned}$$

5.3.2 First consideration

Let x be any of the 15 variables of the control law $u = f$. We have considered its sensitivity function Dx defined as

$$\begin{aligned} Dx : \mathbb{R}^+ &\rightarrow \mathbb{R} \\ t &\rightarrow Dx(t) = \frac{|u(t) - \tilde{u}_x(t)|}{m} \end{aligned}$$

For each $t \in [0, 4]$, we have rerun the code (that is, the control algorithm in Section 5.2.2) and computed $Dx(t)$. In Figure 5.2 they are depicted the time history representations of the sensitivity functions $D\eta_1, D\eta_2, D\eta_3, D\lambda_1, D\lambda_2, D\lambda_3, D\hat{\theta}_1, D\hat{\theta}_2, D\hat{\theta}_3, D\hat{c}$ and Dy in a semilogarithmic scale, with the choice of a constant perturbed function $\varepsilon(t) = 10^{-7}$ and design parameters $c_i = d_i = \gamma = 2$, $i = 1, 2, 3$.

Even for very small values of $\varepsilon(t)$, the sensitivity of the variable η is considerable, specially η_1 .

The same results have been obtained for different choices of a_1, a_2 and b_0 —see equation (5.1)— and even for unstable systems, as can be seen in Tables 5.3.2 and 5.3.2.

As a conclusion, although all the variables have a certain influence, the variable η_1 is the responsible for the largest relative changes in the control law, and it must be then considered to be the most important for the sensitivity analysis.

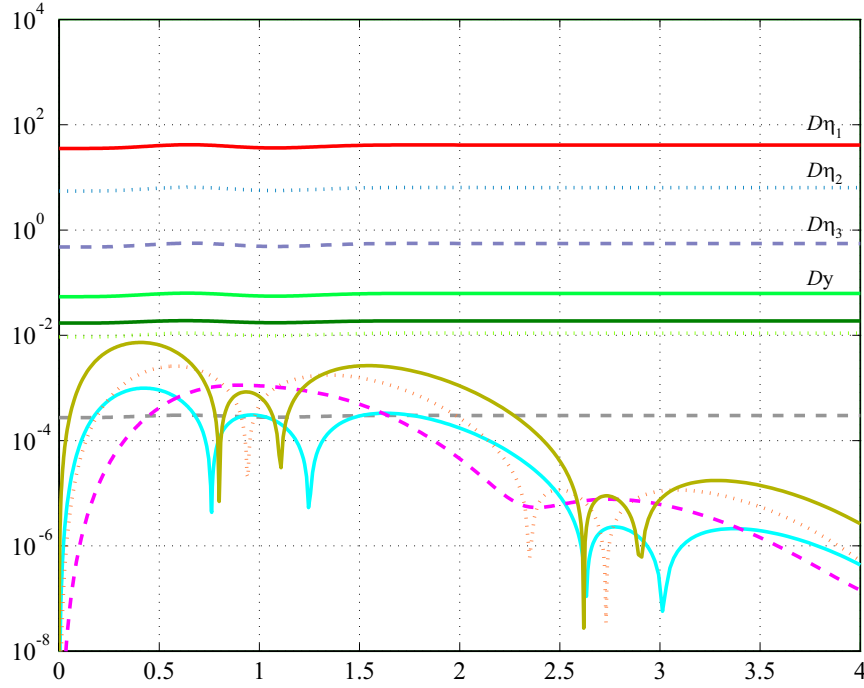


Figure 5.2. Time history representation of $D\eta_1$, $D\eta_2$, $D\eta_3$, $D\lambda_1$, $D\lambda_2$, $D\lambda_3$, $D\hat{\theta}_1$, $D\hat{\theta}_2$, $D\hat{\theta}_3$, $D\hat{\theta}$ and D_y in a semilogarithmic scale, with $\varepsilon(t) = 10^{-7}$, $t \in [0, 4]$ and $c_i = d_i = \gamma = 2$, $i = 1, 2, 3$.

5.3.3 Second consideration

A question that can arise naturally at this point is: how is the influence of the choice of the design parameters in the control signal u ?

For any time instant t , fixed *equal* design parameter $c_i = d_i = \gamma = \kappa > 0$, $i = 1, 2, 3$, (so as to simplify the analysis), and if we consider the perturbed control

$$\tilde{u}_{\eta_1}(t) = f(y_r, \dot{y}_r, \ddot{y}_r, y_r^{(3)}, \eta^T + e_1^T \varepsilon(t), \lambda^T, \hat{\theta}^T, \hat{\theta}, y),$$

the absolute error of the control design $|u(t) - \tilde{u}_{\eta_1}(t)|$ can be expressed as a function of $\varepsilon(t)$ and κ ,

$$|u(t) - \tilde{u}_{\eta_1}(t)| = \sum_{i=1}^9 \varepsilon(t)^i \sum_{j=0}^{12} \nu_{ij}(t) \kappa^j. \quad (5.20)$$

variable	$\max_{t \in [0,4]} Dx(t)$	
	$c_i = d_i = \gamma = 0.5$	$c_i = d_i = \gamma = 2$
x		
η_1	$5.9634 \cdot 10^{-2}$	$4.1743 \cdot 10^{+1}$
η_2	$1.9197 \cdot 10^{-2}$	$6.4881 \cdot 10^{+0}$
η_3	$3.8149 \cdot 10^{-3}$	$5.6228 \cdot 10^{-1}$
λ_1	$4.6353 \cdot 10^{-4}$	$1.8945 \cdot 10^{-2}$
λ_2	$9.8813 \cdot 10^{-6}$	$1.1022 \cdot 10^{-2}$
λ_3	$7.4611 \cdot 10^{-6}$	$3.0353 \cdot 10^{-4}$
$\hat{\theta}_1$	$6.6353 \cdot 10^{-6}$	$9.9091 \cdot 10^{-4}$
$\hat{\theta}_2$	$5.1341 \cdot 10^{-6}$	$2.5940 \cdot 10^{-3}$
$\hat{\theta}_3$	$2.4707 \cdot 10^{-6}$	$1.1271 \cdot 10^{-3}$
$\hat{\rho}$	$2.8861 \cdot 10^{-5}$	$7.3046 \cdot 10^{-3}$
y	$4.8361 \cdot 10^{-4}$	$6.3120 \cdot 10^{-2}$

Table 5.1. Maximum values of the sensitivity functions $Dx(t)$, for $\varepsilon(t) = 10^{-7}$ and $a_1 = 5, a_2 = b_0 = 1$ (stable system).

variable	$\max_{t \in [0,4]} Dx(t)$	
	$c_i = d_i = \gamma = 0.5$	$c_i = d_i = \gamma = 2$
x		
η_1	$5.8476 \cdot 10^{-2}$	$4.0583 \cdot 10^{+1}$
η_2	$1.8739 \cdot 10^{-2}$	$6.2983 \cdot 10^{+0}$
η_3	$3.7151 \cdot 10^{-3}$	$5.4416 \cdot 10^{-1}$
λ_1	$4.5985 \cdot 10^{-4}$	$1.8632 \cdot 10^{-2}$
λ_2	$1.0446 \cdot 10^{-5}$	$1.0809 \cdot 10^{-2}$
λ_3	$7.4021 \cdot 10^{-6}$	$2.9852 \cdot 10^{-4}$
$\hat{\theta}_1$	$8.0584 \cdot 10^{-6}$	$1.0365 \cdot 10^{-3}$
$\hat{\theta}_2$	$5.6264 \cdot 10^{-6}$	$2.8132 \cdot 10^{-3}$
$\hat{\theta}_3$	$2.9390 \cdot 10^{-6}$	$1.2153 \cdot 10^{-3}$
$\hat{\rho}$	$3.9099 \cdot 10^{-5}$	$7.9106 \cdot 10^{-3}$
y	$4.7352 \cdot 10^{-4}$	$6.1479 \cdot 10^{-2}$

Table 5.2. Maximum values of the sensitivity functions $Dx(t)$, for $\varepsilon(t) = 10^{-7}$ and $a_1 = -1, a_2 = b_0 = 1$ (unstable).

The explicit analytical expression of equation (5.20) in function of the perturbation function $\varepsilon(t)$ and the design parameters $c_i, d_i, i = 1, 2, 3$, and γ , are generated using the symbolic calculus software Maple². The complete analytical expression of equation (5.20) has been omitted for space reasons, but we have shown its structure.

²Maple is a trademark of Waterloo Maple Inc.

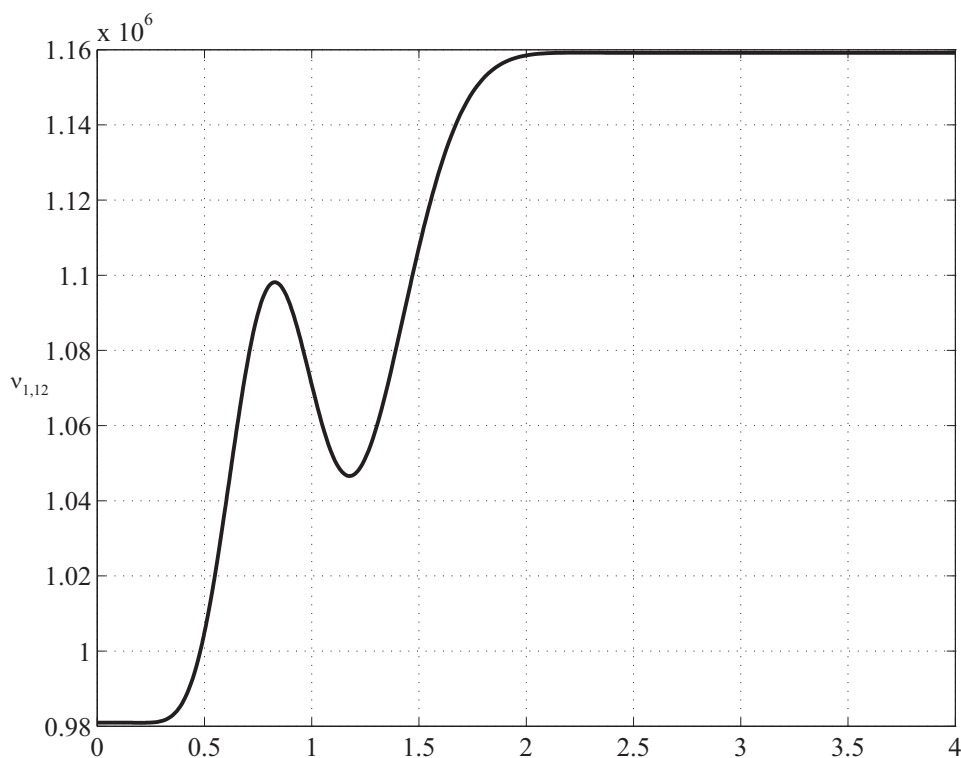


Figure 5.3. Time history of the coefficient $\nu_{1,12}$.

We are interested in the magnitude of the coefficient $\nu_{1,12}$ of the term $\varepsilon\kappa^{12}$, which is the most important term responsible of the error propagation. Using again the symbolic calculus software Maple, the explicit expression of this coefficient is:

$$\begin{aligned}
 \nu_{1,12}(t) = & \hat{\varrho}^9 \left(9.81 \cdot 10^5 - 8.24 \cdot 10^8 (y - y_r) \eta_1 \right. \\
 & - 8.07 \cdot 10^7 (y - y_r) \eta_2 \\
 & - 1.28 \cdot 10^5 (y - y_r) \eta_3 \\
 & - 3.23 \cdot 10^6 y y_r + 2.26 \cdot 10^6 y^2 \\
 & + 9.70 \cdot 10^5 y_r^2 - 1.62 \cdot 10^5 \hat{\theta}_2 \\
 & \left. + 1.60 \cdot 10^4 \hat{\theta}_3 \right) \quad (5.21)
 \end{aligned}$$

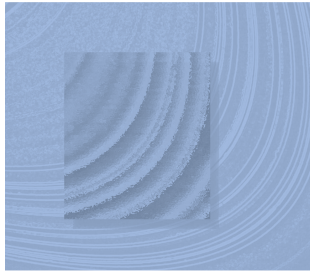
The time history of the coefficient $\nu_{1,12}$ is depicted in Figure 5.3. It can be seen that $\nu_{1,12} \approx 10^6$. Therefore only with a choice of $0 < \kappa < 1$ the term $\nu_{1,12}\varepsilon\kappa^{12}$ can be made small. In the same sense, a choice of $\kappa > 1$ leads to a big absolute error of the control signal. This phenomenon can be appreciated in Figure 5.1 for two different values of the design parameters, $\kappa = 0.5 < 1$ and $\kappa = 2 > 1$. In fact, when $\kappa = 0.5$, the backstepping control signal is smooth according to what is expected from the theory presented in Chapter 2. However, when $\kappa = 2$, the control signal is clearly corrupted.

5.4 Conclusions

This chapter has focused on a analysis via numerical simulations and with the help of symbolic calculus of the sensitivity of the adaptive backstepping tuning functions control design for a relative degree three linear system—in both stable and unstable plants. Improving the transient behavior is done generally by increasing the design gains c_0 , d_0 and γ . It has been observed that for $c_0 = d_0 = \gamma < 1$ the effect of small numerical error propagation remains negligible, while for $c_0 = d_0 > 1$ the control signal is corrupted by noise arising from the computational process.

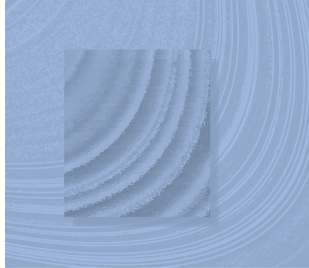
The analysis of the phenomenon led to the following conclusion: to improve the tracking error performance $y - y_r$, an increase of the gains c_0 and d_0 is desirable. However, this enlarges the effect of the numerical errors in the inherent computations. The effect of the error propagation leads to an unnecessary actuator effort and a large control amplitude. The tuning function design has thus shown to be sensitive to the numerical errors that are generated by the computational process.

The need for reliable algorithms for solving complex control problems, such as the backstepping one, has made necessary to focus on sensitivity and accuracy issues. In our case, the complexity of the control algorithm makes indispensable a certain compromise between the choice of the design parameters and the sensitivity of the control law.



Part II

CONTROL SYNTHESIS BY SUM OF SQUARES OPTIMIZATION



Chapter 6

Control synthesis of polynomial and rational systems

We introduce in this chapter a recently developed computational approach to nonlinear control synthesis [Par00]. The basis is a recent convergence criterion that can be viewed as a dual to Lyapunov's second theorem. The criterion is stated in terms of a function which can be interpreted as the stationary density of a substance that is generated all over the state-space and flows along the system trajectories toward the equilibrium. This criterion has a remarkable convexity property, which is used for controller synthesis of polynomial and rational vector fields via convex optimization. Recent numerical methods for verification of positivity of multivariate polynomials based on sum of squares decompositions are used.

6.1 Introduction

Analysis and control of nonlinear systems are among the most challenging problems in systems and control theory. Despite many years of research, there is still no universal methodology for analyzing stability and performance of nonlinear systems, let alone constructing controllers that stabilize such systems.

Various approaches based on Lyapunov and storage functions for analysis as well as control Lyapunov functions (CLFs) for synthesis have been proposed [Kha96]. However, these approaches suffer from the following drawback: constructing such functions is hard, and moreover, no coherent and tractable computational method exists to aid us in constructing them.

On one hand, there has also been a strong development of computational tools based on Lyapunov functions. Many such methods are based on convex optimization and solution of matrix inequalities, exploiting the fact that the set of Lyapunov functions for a given system is convex.

On the other hand, a serious obstacle in the controller synthesis is however that the joint search for a controller $u(x)$ and a Lyapunov function $V(x)$ is not convex. Consider the synthesis problem for the affine nonlinear system

$$\dot{x} = f(x) + g(x)u.$$

The set of u and V satisfying the condition

$$\frac{\partial V}{\partial x}[f(x) + g(x)u(x)] < 0$$

is not convex. In fact, for some systems the set of u and V satisfying the inequality is not even connected.

Given the difficulties with Lyapunov based controller synthesis, it is most striking to find that the convergence criterion presented here as Theorem 6, based on the so-called density function ρ has a remarkable convexity property. Indeed, the set of (ρ, u) satisfying the *dual criterion* or *divergence inequality*

$$\nabla \cdot [\rho(f + gu)] > 0 \tag{6.1}$$

is convex. This convexity property will be exploited in the computation of stabilizing controllers in the case of polynomial or rational vector fields. Recent numerical methods for verification of positivity of multivariate polynomials based on sum of squares decompositions are used.

6.2 Control synthesis of linear systems via LMI

The synthesis of linear systems is a problem completely solved via the computational methods using semidefinite programming or linear matrix inequalities (LMI). In this section we introduce the basic notation for the LMI methods. The problem of the joint search of a controller $K(x)$ and a Lyapunov function $V(x)$ for a linear system is solved using this methodology and the linearized inverted pendulum is controlled in an example.

6.2.1 Linear matrix inequalities

A linear matrix inequality (LMI) has the form

$$F(x) \triangleq F_0 + \sum_{i=1}^m x_i F_i > 0, \quad (6.2)$$

where $x \in \mathbb{R}^m$ is the variable and the symmetric matrices $F_i = F_i^T \in \mathbb{R}^{n \times n}$, $i = 0, \dots, m$, are given. The inequality symbol in (6.2) means that $F(x)$ is positive-definite, i.e., $u^T F(x) u > 0$ for all nonzero $u \in \mathbb{R}^n$. Of course, the LMI (6.2) is equivalent to a set of n polynomial inequalities in x , i.e., the leading principal minors of $F(x)$ must be positive.

We will also encounter nonstrict LMIs, which have the form

$$F(x) \geq 0. \quad (6.3)$$

The LMI (6.2) is a convex constraint on x , i.e., the set $\{x \mid F(x) > 0\}$ is convex. Although the LMI (6.2) may seem to have specialized form, it can represent a wide variety of convex constraints on x . In particular, linear inequalities, (convex) quadratic inequalities, matrix norm inequalities, and constraints that arise in control theory, such as Lyapunov and convex quadratic matrix inequalities, can all be cast in the form of an LMI.

For a more extended development of the LMI techniques and its applications see [BGFB94, GNLC95, SW].

6.2.2 Synthesis of linear systems via LMI

Consider the linear system

$$\dot{x} = Ax + Bu, \quad (6.4)$$

where $x \in \mathbb{R}^n$, $A \in \mathbb{R}^{n \times n}$, $B \in \mathbb{R}^{n \times 1}$ and $u \in \mathbb{R}$. To find a stabilizing controller $u = Kx$, we need a Lyapunov function $V(x) := x^T P x$ with P positive definite such that $A + BK$ is stable, i.e.,

$$P(A + BK) + (A + BK)^T P < 0. \quad (6.5)$$

The objective is to find, at the same time, both the controller K and the matrix P , but this condition is not affine in both P and K , so it cannot be expressed as a linear matrix inequality.

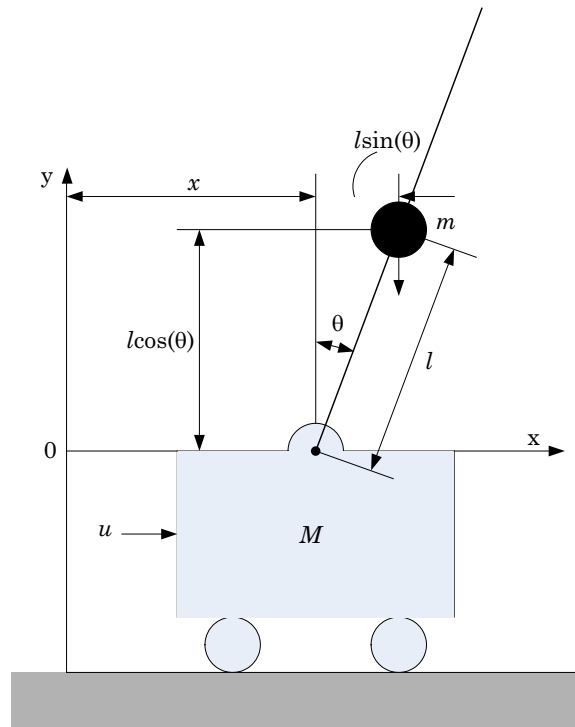


Figure 6.1. Inverted pendulum.

By multiplying the expression above by $Q := P^{-1}$ (we can invert P thanks to its positive definiteness), and defining a new variable $L := KQ$, we obtain

$$\begin{aligned}
 & P^{-1}P(A+BK)P^{-1} + P^{-1}(A+BK)^T P P^{-1} = \\
 & = (A+BK)Q + Q(A+BK)^T \\
 & = AQ + BKQ + (AQ + BKQ)^T \\
 & = AQ + BL + (AQ + BL)^T < 0, \tag{6.6}
 \end{aligned}$$

which is affine in both Q and L . Since $Q > 0$, we can always find the controller K as $K = LQ^{-1}$.

Example 6.1 In this example we shall consider the design of an inverted pendulum control system via linear matrix inequalities. We shall design a controller to keep the pendulum upright at steady state after transient periods are over.

Consider the inverted pendulum mounted on a motor-driven cart as shown in Figure 6.1. The inverted pendulum is unstable in that it may fall over any time in any direction unless a suitable control force is applied. Here we consider only a two-dimensional problem in which the pendulum moves only in the plane of the page. Assume that the pendulum mass is concentrated at the center of the rod, as shown in the Figure 6.1. Assume that the rod is massless. The control force u is applied to the cart. Define the angle of the rod from the vertical line as θ . Since we want to keep the inverted pendulum vertical, angle θ is assumed to be small.

The nonlinear dynamic equations of the system are

$$\frac{4}{3}m\ell^2\ddot{\theta} + m\ell \cos\theta\ddot{x} - mgl \sin\theta = 0 \quad (6.7)$$

$$(M + m)\ddot{x} + m\ell \cos\theta\ddot{\theta} - m\ell \sin\theta\dot{\theta}^2 = u, \quad (6.8)$$

where m is the mass of the ball, M the mass of the cart and 2ℓ the total length of the rod.

Since we must keep the inverted pendulum vertical, we can assume that $\theta(t)$ and $\dot{\theta}(t)$ are small quantities such that $\sin\theta \approx \theta$, $\cos\theta \approx 1$, and $\theta\dot{\theta}^2 \approx 0$. Then, equations (6.7)-(6.8) can be linearized as follows:

$$\frac{4}{3}m\ell^2\ddot{\theta} + m\ell\ddot{x} - mgl\theta = 0, \quad (6.9)$$

$$(M + m)\ddot{x} + m\ell\ddot{\theta} = u. \quad (6.10)$$

Define state variables x_1, x_2, x_3 and x_4 by

$$x_1 = x,$$

$$x_2 = \dot{x},$$

$$x_3 = \theta,$$

$$x_4 = \dot{\theta}.$$

In terms of vector-matrix equations, we have

$$\begin{bmatrix} \dot{x}_1 \\ \dot{x}_2 \\ \dot{x}_3 \\ \dot{x}_4 \end{bmatrix} = \begin{bmatrix} 0 & 1 & 0 & 0 \\ 0 & 0 & -\frac{3mg\ell}{4M\ell+m\ell} & 0 \\ 0 & 0 & 0 & 1 \\ 0 & 0 & \frac{3(M+m)g}{4M\ell+m\ell} & 0 \end{bmatrix} \begin{bmatrix} x_1 \\ x_2 \\ x_3 \\ x_4 \end{bmatrix} + \begin{bmatrix} 0 \\ \frac{4\ell}{4M\ell+m\ell} \\ 0 \\ -\frac{3}{4M\ell+m\ell} \end{bmatrix} u.$$

In this example, we assume the following numerical values for M , m , and ℓ :

$$M = 2 \text{ kg}, \quad m = 0.1 \text{ kg}, \quad \ell = 0.5 \text{ m}.$$

We assume that all the states are available for feedback, and therefore we can consider a control of the form

$$u = Kx = \begin{bmatrix} k_1 & k_2 & k_3 & k_4 \end{bmatrix} \begin{bmatrix} x_1 \\ x_2 \\ x_3 \\ x_4 \end{bmatrix} = k_1x_1 + k_2x_2 + k_3x_3 + k_4x_4$$

We are now interested in to find a symmetric positive definite matrix P and a vector K that stabilizes the equations of the inverted pendulum. We know that $Q = P^{-1}$ is also symmetric and positive definite, i.e.,

$$Q > 0, \quad Q = Q^T. \quad (6.11)$$

Using equation (6.6) we have that

$$AQ + BL + (AQ + BL)^T < 0 \quad (6.12)$$

In order to apply the Matlab LMI toolbox, we need to express these linear matrix inequalities in a single linear matrix inequality. This way, we obtain the matrix

$$\begin{bmatrix} AQ + BL + (AQ + BL)^T & 0 \\ 0 & -Q \end{bmatrix} < 0. \quad (6.13)$$

After solving the LMI, we obtain

$$L = \begin{bmatrix} -10.9142 & -5.2440 & 9.2310 & -9.5140 \end{bmatrix},$$

$$Q = \begin{bmatrix} 3.6858 & -1.1346 & -0.3346 & 0.1540 \\ -1.1346 & 5.1372 & 0.0110 & -3.0648 \\ -0.3346 & 0.0110 & 0.1945 & -0.6203 \\ 0.1540 & -3.0648 & -0.6203 & 4.8183 \end{bmatrix}.$$

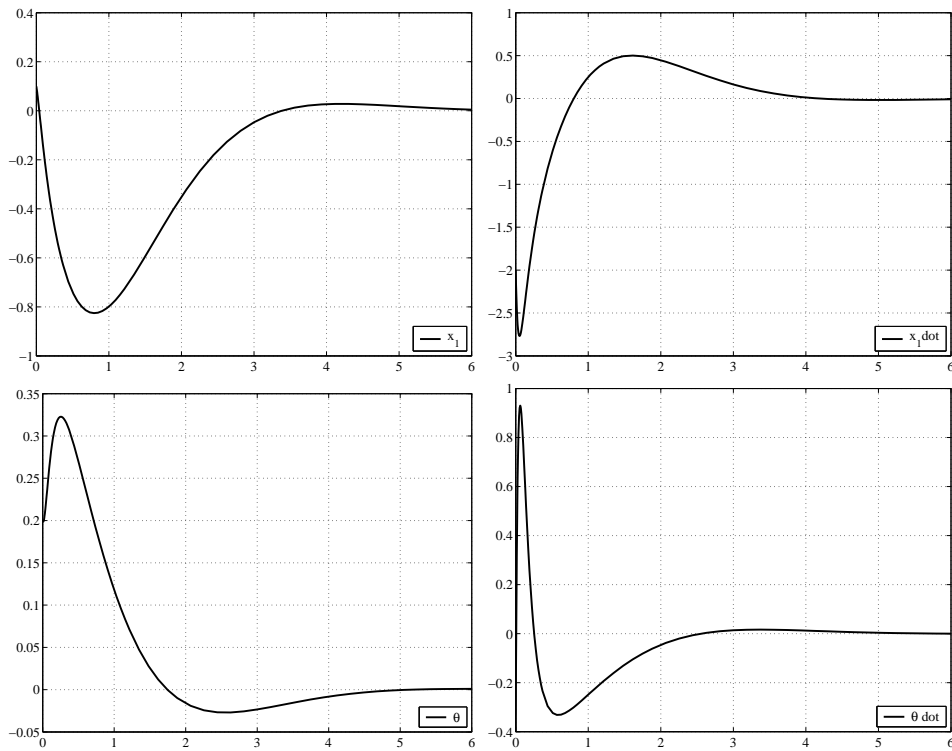


Figure 6.2. Simulation of the linearized inverted pendulum with initial conditions $(x, \dot{x}, \theta, \dot{\theta}) = (0.1, -2, 0.2, -0.4)$.

Using $P = Q^{-1}$ and $K = LP$ the final expressions for these matrices are

$$P = \begin{bmatrix} 1.9100 & 2.0958 & 12.2560 & 2.8499 \\ 2.0958 & 2.8247 & 15.2049 & 3.6872 \\ 12.2560 & 15.2049 & 93.2442 & 21.2839 \\ 2.8499 & 3.6872 & 21.2839 & 5.2019 \end{bmatrix},$$

$$K = [54.3317 \quad 67.7675 \quad 445.8293 \quad 96.7857].$$

In other words, the controller is

$$u = 54.3317x_1 + 67.7675x_2 + 445.8293x_3 + 96.7857x_4$$

and the related Lyapunov function of the closed-loop is

$$\begin{aligned} V(x) = & 1.9100x_1^2 + 4.1916x_1x_2 + 24.5120x_1x_3 \\ & + 5.6998x_1x_4 + 2.8247x_2^2 + 30.4098x_2x_3 \\ & + 7.3744x_2x_4 + 93.2442x_3^2 + 42.5678x_3x_4 + 5.2019x_4^2. \end{aligned}$$

Simulation results can be found in Figure 6.2. ■

Extending this procedure to the nonlinear case does not seem feasible, at least in a reasonably straightforward way. Consider an affine nonlinear system

$$\dot{x} = f(x) + g(x)u.$$

While the condition

$$\frac{\partial V}{\partial x} [f(x) + g(x)k(x)] < 0$$

is clearly the nonlinear equivalent of equation (6.5) above, there does not seem to be an efficient way of searching simultaneously over the Lyapunov function V and the controller $k(x)$.

Nevertheless, in Section 6.3 we introduce a partial solution of this problem in the case where $f(x)$ and $g(x)$ are polynomial or rational vector fields via two computational relaxations.

6.3 Control synthesis of polynomial systems

6.3.1 Hilbert's 17th problem

The history of the problem of expressing nonnegative polynomials as a sum of squares dates back to before the beginning of the 20th century. We define some notation that we use throughout the following chapters. Let \mathcal{P}_+ denote the set of polynomials (the underlying polynomial ring is understood from the context) that are globally nonnegative, $\mathcal{P}_+(K)$ the set of polynomials nonnegative on a set $K \subseteq \mathbb{R}^n$, and Σ^2 the set of polynomials that can be expressed as the sum of squares of other polynomials. Starting with the observation that any univariate polynomial that is nonnegative on all of \mathbb{R} may be written as the sum of squares of other polynomials (in fact, of two other polynomials), Hilbert asked whether this fact generalizes to higher dimensions, that is, to multivariate polynomials. In other words, having seen that

$$\Sigma^2 = \mathcal{P}_+ \text{ in } \mathbb{R}[x],$$

Hilbert asked whether this equality is always true, or whether the inclusion is ever strict. Hilbert gave the negative answer himself with a nonconstructive proof. At the Paris Congress in 1900, he then posed his famous 17th question, now known as Hilbert's 17th problem, of whether a nonnegative polynomial can be expressed as the sum of squares of *rational* functions.

In 1927, Artin developed, and then used what is now known as the Artin-Schreier theory of closed fields, to give an affirmative answer to Hilbert's 17th problem: Any polynomial, nonnegative on all \mathbb{R}^n , may be expressed as the sum of quotients of polynomials.

While Hilbert proved that the inclusion $\Sigma^2 \subseteq \mathcal{P}_+$ is in general strict, the proof was not constructive. Motzkin is the first credited to have written down a concrete example, and this did not happen until the 1960's. Motzkin's famous example is the homogeneous polynomial (or form) in three variables:

$$M(x, y, z) = x^4y^2 + x^2y^4 + z^6 - 3x^2y^2z^2.$$

While this is nonnegative for any $(x, y, z) \in \mathbb{R}^3$, it cannot be written as a sum of squares of other polynomials.

The connection between \mathcal{P}_+ and polynomial optimization has begun to be exploited, due to the computational tractability of Σ^2 , as described in the following sections.

6.3.2 First relaxation: the sum of squares approach

In order to understand the possibilities and limitations of computational approaches to nonlinear stability, an issue that has to be addressed is how to deal numerically with functional inequalities such as the standard Lyapunov one, or the divergence inequality (6.15).

Even in the restricted case of polynomial functions, it is well-known that the problem of checking global nonnegativity of a polynomial of quartic (or higher) degree is computationally hard. For this reason, we need tractable sufficient conditions that guarantee nonnegativity, and that are not overly conservative. A particularly interesting sufficient condition is given by the existence of a sum of squares decomposition: can the polynomial $p(x)$ be written as

$$p(x) = \sum_i p_i^2(x),$$

for some polynomials $p_i(x)$? Obviously, if this is the case, then $p(x)$ takes only nonnegative values. Notice that in the case of quadratic forms, for instance, the two conditions (nonnegativity and sum of squares) are equivalent.

In this respect, it is interesting to notice that many methods used in control theory for constructing Lyapunov functions (for example, backstepping, as can be seen in Part I) use either implicitly or explicitly a sum of squares approach.

The problem of checking if a given polynomial can be written as a sum of squares can be solved via convex optimization, in particular semidefinite programming. For our purposes, however, it will enough to know that while the standard semidefinite programming machinery can be interpreted as searching for a semidefinite element over an affine family of quadratic forms, the new tools provide a way of finding a sum of squares, over an affine family of polynomials. For instance, these tools can be used in the computation of Lyapunov functions for proving that a nonlinear system is stable.

6.3.3 Second relaxation: the dual theorem of Lyapunov

Lyapunov's second theorem has long been recognized as one of the most fundamental tools for analysis and synthesis of nonlinear systems. The importance of the criterion stems from the fact that it allows stability of a system to be verified without solving the differential equation explicitly.

Lyapunov functions play a role similar to potential functions and energy functions. Moreover, when asymptotic stability of an equilibrium has been proved using Lyapunov's theorem, input-output stability can often be proved using the Lyapunov function as a "storage function".

Lyapunov's theorem has a close relative, Theorem 6. The relationship between the two theorems can be considered as an analogous to the duality that has been used since 1940s for closely related problems in calculus of variations.

The notation

$$\nabla V = \left[\frac{\partial V}{\partial x_1} \cdots \frac{\partial V}{\partial x_n} \right], \quad V : \mathbb{R}^n \rightarrow \mathbb{R},$$

$$\nabla \cdot f = \frac{\partial f_1}{\partial x_1} + \cdots + \frac{\partial f_n}{\partial x_n}, \quad f : \mathbb{R}^n \rightarrow \mathbb{R}^n$$

will be used throughout the chapter.

The proof of the Theorem 6 relies on the following lemma, which can be viewed as a version on Liouville's theorem.

Lemma 2 Let $f \in \mathcal{C}^1(D, \mathbb{R}^n)$ where $D \subset \mathbb{R}^n$ is open and let $\rho \in \mathcal{C}^1(D, \mathbb{R})$ be integrable. For $x_0 \in \mathbb{R}^n$, let $\phi_t(x_0)$ be the solution $x(t)$ of $\dot{x} = f(x)$, $x(0) = x_0$. For a measurable set Z , assume that $\phi_\tau(Z) = \{\phi_\tau(x) \mid x \in Z\}$ is a subset of D for all τ between 0 and t . Then

$$\int_{\phi_t(Z)} \rho(x) dx - \int_Z \rho(z) dz = \int_0^t \int_{\phi_\tau(Z)} [\nabla \cdot (f\rho)](x) dx d\tau$$

Proof. Note that for every \mathcal{C}^1 matrix function $M(t)$ with $M(0) = I$

$$\left. \frac{\partial}{\partial t} \det M(t) \right|_{t=0} = \text{trace} M'(0).$$

This follows by direct expansion of the determinant, since the first-order terms in t correspond to the diagonal elements of $M(t)$.

Let $M(t) = \left(\frac{\partial \phi_t}{\partial z} \right) (z)$ and use $|\cdot|$ to denote determinant. The differentiability of f gives that $\phi_t(z)$ is of class \mathcal{C}^1 in z and \mathcal{C}^2 in t . Hence

$$\begin{aligned} \left[\frac{\partial}{\partial t} \left| \frac{\partial \phi_t}{\partial z} (z) \right| \right]_{t=0} &= \left[\text{trace} \frac{\partial^2}{\partial t \partial z} \phi_t(z) \right]_{t=0} \\ &= \text{trace} \frac{\partial f}{\partial z} (z) = [\nabla \cdot f](z) \end{aligned}$$

and with the notation $\rho_t(z) = \rho(\phi_t(z)) \left| \left(\frac{\partial \phi_t}{\partial z} (z) \right) \right|$

$$\begin{aligned} \left. \frac{\partial}{\partial t} \rho_t(z) \right|_{t=0} &= \nabla \rho \cdot f + \rho(\nabla \cdot f) = [\nabla \cdot (f\rho)](z), \\ \left. \frac{\partial}{\partial t} \rho_t(z) \right|_{t=\tau} &= \frac{\partial}{\partial h} \left\{ \rho_h(\phi_\tau(z)) \left| \frac{\partial \phi_\tau}{\partial z} (z) \right| \right\} \Big|_{h=0} \\ &= [\nabla \cdot (f\rho)](\phi_\tau(z)) \left| \frac{\partial \phi_\tau}{\partial z} (z) \right|. \end{aligned}$$

Let $\chi(\cdot)$ be the characteristic function of Z . Then

$$\begin{aligned}
\int_{\phi_t(Z)} \rho(x) dx - \int_Z \rho(z) dz &= \int_{\mathbb{R}^n} \rho(x) \chi(\phi_t^{-1}(x)) dx - \int_Z \rho(z) dz \\
&= \int_{\mathbb{R}^n} \rho(\phi_t(z)) \chi(z) \left| \frac{\partial \phi_t(z)}{\partial z} \right| dz - \int_Z \rho(z) dz \\
&= \int_Z [\rho_t(z) - \rho(z)] dz \\
&= \int_Z \int_0^t [\nabla \cdot (f\rho)](\phi_\tau(z)) \left| \frac{\partial \phi_\tau(z)}{\partial z} \right| d\tau dz \\
&= \int_0^t \int_{\phi_\tau(Z)} [\nabla \cdot (f\rho)](x) dx d\tau.
\end{aligned}$$

□

Theorem 6 Given the equation

$$\dot{x}(t) = f(x(t)),$$

where $f \in \mathcal{C}^1(\mathbb{R}^n, \mathbb{R}^n)$ and $f(0) = 0$, suppose there exists a non-negative $\rho \in \mathcal{C}^1(\mathbb{R}^n - \{0\}, \mathbb{R})$ such that

$$\blacktriangleright \frac{\rho(x)f(x)}{|x|} \text{ is integrable on } \{x \in \mathbb{R}^n : |x| \geq 1\} \text{ and} \quad (6.14)$$

$$\blacktriangleright [\nabla \cdot (f\rho)] > 0 \text{ for almost all } x. \quad (6.15)$$

Then, for **almost all** initial states $x(0)$ the trajectory $x(t)$ exists for $t \in [0, \infty)$ and tends to zero as $t \rightarrow \infty$.

Moreover, if the equilibrium $x = 0$ is stable, then the conclusion remains valid even if ρ takes negative values.

Proof. (*Second statement*). Here it is assumed that $x = 0$ is a stable equilibrium while ρ may take negative values.

Rather than exploiting that $f \in \mathcal{C}^1(\mathbb{R}^n, \mathbb{R}^n)$, we will actually prove the result under the weaker condition that $f \in \mathcal{C}^1(\mathbb{R}^n - \{0\}, \mathbb{R}^n)$ and $f(x)/|x|$ is bounded near $x = 0$. Given any $x_0 \in \mathbb{R}^n$, let $\phi_t(x_0)$ for $t \geq 0$ be the solution $x(t)$ of $\dot{x}(t) = f(x(t))$, $x(0) = x_0$. Assume first that ρ is integrable on $\{x \in \mathbb{R}^n \mid |x| \geq 1\}$ and $|f(x)|/|x|$ is bounded, that is, $f(x)$ is Lipschitz. Then, thanks to the Picard's existence theorem, ϕ_t is well defined for all t .

Given $r > 0$, define

$$Z = \bigcap_{l=1}^{\infty} \{x_0 : |\phi_t(x_0)| > r \text{ for some } t > l\}.$$

Notice that Z contains all trajectories with $\limsup_{t \rightarrow \infty} |x(t)| > r$. The set Z , being the intersection of a countable number of open sets, is measurable. Moreover, $\phi_t(Z) = \{\phi_t(x) \mid x \in Z\}$ is equal to Z for every t . By stability of the equilibrium $x = 0$, there is a positive lower bound ε on the norms of the elements in Z , so Lemma 2 with $D = \{x : |x| > \varepsilon\}$ gives

$$\begin{aligned} 0 &= \int_{\phi_t(Z)} \rho(x) dx - \int_Z \rho(z) dz \\ &= \int_0^t \int_{\phi_\tau(Z)} [\nabla \cdot (f\rho)](x) dx d\tau. \end{aligned}$$

By assumption in equation (6.15), this implies that Z has measure zero. Consequently, $\limsup_{t \rightarrow \infty} |x(t)| \leq r$ for almost all trajectories. As r was chosen arbitrarily, this proves that $\lim_{t \rightarrow \infty} |x(t)| = 0$ for almost all trajectories.

When $|f(x)|/|x|$ is unbounded and, in particular, it is not a Lipschitz function anymore, there may not exist any non-zero t such that $\phi_t(z)$ is well defined for all z . We then introduce

$$\begin{aligned} \rho_0(x) &= \left[\frac{e^{-|x|}}{1 + |\rho(x)|^2} + \frac{|f(x)|^2}{|x|^2} \right]^{1/2} \rho(x), \\ f_0(x) &= \frac{f(x)\rho(x)}{\rho_0(x)}. \end{aligned}$$

Then $|f_0(x)|/|x|$ is bounded and ρ_0 is integrable on $\{x \in \mathbb{R}^n : |x| \geq 1\}$, so the argument above can be applied to f_0 together with ρ_0 to prove that $\lim_{\tau \rightarrow \infty} |y(\tau)| = 0$ for almost all trajectories of the system $dy/d\tau = f_0(y(\tau))$. However, modulo a transformation of the time axis

$$t = \int_0^\tau \frac{\rho(y(s))}{\rho_0(y(s))} ds$$

the trajectories are identical: $x(t) = y(\tau)$. This, together with the boundedness of $f(x)/|x|$ near $x = 0$, also shows that $x(t)$ exists for $t \in [0, \infty)$ and tends to zero as $t \rightarrow \infty$ provided that $\lim_{\tau \rightarrow \infty} |y(\tau)| = 0$. The proof of the second statement in Theorem 6 is complete. \square

Theorem 7 Consider a measure space (X, \mathcal{A}, μ) , a set $P \subset X$ of finite measure and a measurable map $T : X \rightarrow X$. Suppose that

$$\mu(T^{-1}Y) \leq \mu(Y) \text{ for all measurable } Y \subset X. \quad (6.16)$$

Define Z as the set of elements $x \in P$ such that $T^n(x) \in P$ for infinitely many integers $n \geq 0$. Then $\mu(T^{-1}Z) = \mu(Z)$.

Proof. Note that

$$Z = P \cap \left(\bigcap_{j=1}^{\infty} \bigcup_{k=j}^{\infty} T^{-k}(P) \right),$$

so Z is measurable. Let the superscript c denote the complementary set with respect to X , like $Z^c = X - Z$. Define for $n = 1, 2, \dots$

$$Z_n = \bigcup_{k=1}^n T^{-k}(Z), \quad Z_0 = \emptyset.$$

The set Z_n for $n \geq 1$ consists of those elements of X that are mapped into Z in n or less steps. Let us prove by induction over n that

$$\mu(T^{-1}(Z)) \geq \mu(Z_n \cap Z) + \mu(T^{-n-1}(Z) \cap Z_n^c). \quad (6.17)$$

The inequality holds trivially for $n = 0$. Assuming that it holds for some $n \geq 0$, we get

$$\begin{aligned} \mu(T^{-1}(Z)) &\geq \mu(Z_n \cap Z) + \mu(T^{-n-1}(Z) \cap Z_n^c) \\ &= \mu(Z_n \cap Z) + \mu(T^{-n-1}(Z) \cap Z_n^c \cap Z) \\ &\quad + \mu(T^{-n-1}(Z) \cap Z_n^c \cap Z^c) \\ &\geq \mu((Z_n \cup (T^{-n-1}(Z) \cap Z_n^c)) \cap Z) \\ &\quad + \mu(T^{-1}(T^{-n-1}(Z) \cap Z_n^c \cap Z^c)) \\ &= \mu(Z_{n+1} \cap Z) + \mu(T^{-n-2}(Z) \cap Z_{n+1}^c). \end{aligned}$$

Induction over n therefore proves equation (6.17) for all integers $n \geq 0$. It follows that

$$\mu(Z) \geq \mu(T^{-1}(Z)) \geq \sup_n \mu(Z_n \cap Z) = \mu(Z),$$

where the last equality is due to $Z = \left(\bigcup_{n=1}^{\infty} T^{-n}(Z) \right) \cap P$. \square

Proof. (*First statement of Theorem 6*). We may assume without restriction that ρ is integrable for $|x| \geq 1$ and $|f(x)|/|x|$ is bounded by some constant C so $\phi_t(x_0)$ is well defined for all x_0, t . Define $X = \mathbb{R}^n, P = \{x \in \mathbb{R}^n : |x| > r\}, T(x) = \phi_1(x)$ and

$$\mu(Y) = \int_Y \rho(x) dx \text{ for measurable } Y \subset X.$$

The condition (6.16) holds by Lemma 2. Hence $\mu(T^{-1}Z) = \mu(Z)$ for Z defined as in Theorem 7, so by Lemma 2 with $t = -1$ and $D = \{x \in \mathbb{R}^n : |x| > \varepsilon\}$ for some sufficiently small $\varepsilon > 0$

$$\int_{-1}^0 \int_{\phi_\tau(Z)} [\nabla \cdot (f\rho)](x) dx d\tau = 0.$$

This gives that the Lebesgue measure of $\phi_\tau(Z)$ is zero for almost all $\tau \in [-1, 0]$. Hence, Z must have measure zero and for almost all $x \in P$ there exists $j > 0$ such that

$$|\phi_n(x)| \leq r, \quad \text{for } n > j.$$

The choice of r was arbitrary, so $\lim_{t \rightarrow \infty} |\phi_n(x_0)| = 0$ as $n = 1, 2, \dots$ for almost all x_0 . For a real positive number t , let $[t]$ denote its integer part. The global bound $|f(x)|/|x| < C$ gives $|\dot{x}| < C|x|$ so

$$|x(t)| \leq e^{C|t-[t]|} |x([t])| \leq e^C |x([t])| \rightarrow 0 \quad \text{as } t \rightarrow \infty.$$

Hence $|\phi_t(x_0)| \rightarrow 0$ also for non-integer values of t and the proof is complete. \square

Examples**Example 6.2** The system

$$\begin{bmatrix} \dot{x}_1 \\ \dot{x}_2 \end{bmatrix} = \begin{bmatrix} -2x_1 + x_1^2 - x_2^2 \\ -2x_2 + 2x_1x_2 \end{bmatrix}$$

has two equilibria $(0, 0)$ and $(2, 0)$. Let $f(x)$ be the right-hand side and let $\rho(x) = |x|^{-\alpha}$. Then

$$\begin{aligned} [\nabla \cdot (f\rho)](x) &= \nabla\rho \cdot f + \rho(\nabla \cdot f) \\ &= -\alpha|x|^{-\alpha-2}x^T f + |x|^{-\alpha}(4x_1 - 4) \\ &= -\alpha|x|^{-\alpha-2}(x_1 - 2)|x|^2 + |x|^{-\alpha}(4x_1 - 4) \\ &= |x|^{-\alpha}[(4 - \alpha)x_1 + 2\alpha - 4]. \end{aligned}$$

With $\alpha = 4$ all conditions of Theorem 6 hold, so almost all trajectories tend to $(0, 0)$ as $t \rightarrow \infty$. The exceptional trajectories turn out to be those that start with $x_1 \geq 2, x_2 = 0$. See Figure 6.3 for a phase plane plot of this system. ■

Example 6.3 The system

$$\begin{bmatrix} \dot{x}_1 \\ \dot{x}_2 \end{bmatrix} = \begin{bmatrix} -2x_1 + x_1^2 - x_2^2 \\ -6x_2 + 2x_1x_2 \end{bmatrix}$$

has four equilibria $(0, 0)$, $(2, 0)$ and $(3, \pm\sqrt{3})$. In this case, $\rho(x) = |x|^{-4}$ gives

$$\begin{aligned} [\nabla \cdot (f\rho)](x) &= -4|x|^{-6}x^T f + |x|^{-4}(4x_1 - 8) \\ &= -4|x|^{-6}[(x_1 - 2)|x|^2 - 4x_2^2] + |x|^{-4}(4x_1 - 8) \\ &= 16x_2^2|x|^{-6} \end{aligned}$$

so again Theorem 6 shows that almost all trajectories tend to $(0, 0)$ as $t \rightarrow \infty$. The exceptional trajectories are the three unstable equilibria, the axis $x_2 = 0, x_1 \geq 2$ and the stable manifold of the equilibrium $(2, 0)$, that spirals out from the equilibrium $(3, \pm\sqrt{3})$. ■

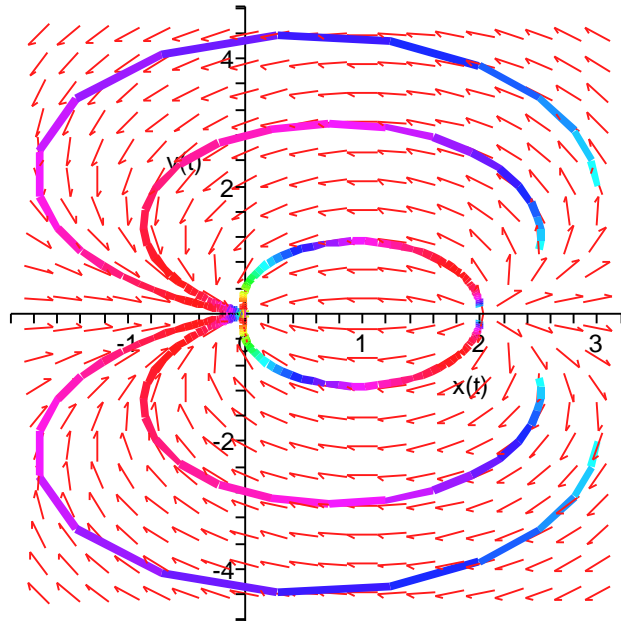


Figure 6.3. Phase plane plot for Example 6.2.

6.3.4 Convexity in nonlinear stabilization

An important application area for Lyapunov function is the synthesis of stabilizing feedback controllers. For a given system, the set of Lyapunov functions is convex. This fact is the basis for many numerical methods, most notably in computation of quadratic Lyapunov functions using linear matrix inequalities, as can be seen in Section 6.2 or in a more detailed way in [BGFB94]. However, when the control law and Lyapunov function are to be found simultaneously, no such convexity property is at hand. In fact, the set of (V, u) satisfying

$$\nabla V \cdot (f + gu) < 0$$

may not even be connected.

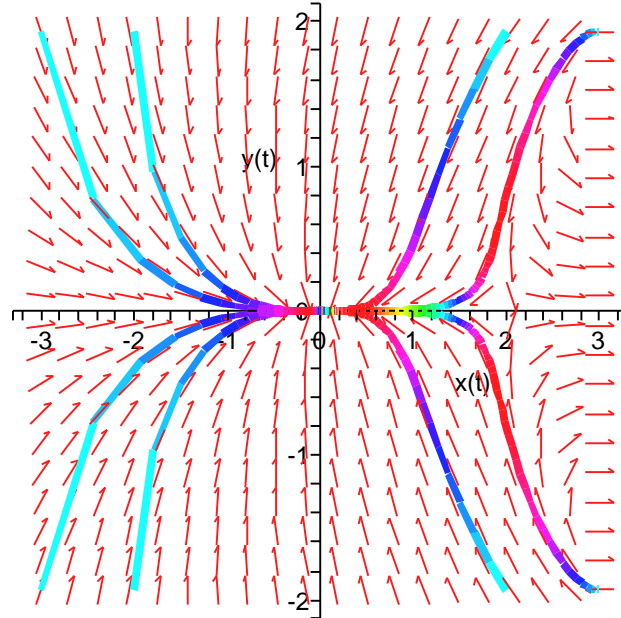


Figure 6.4. Phase plane plot for Example 6.3.

Given this problem, it is most striking to find that the corresponding synthesis problem for the convergence criterion in Theorem 6 is convex. In fact, the divergence criterion

$$\nabla V \cdot [(f + gu)\rho] > 0$$

is convex in the pair $(\rho, u\rho)$.

6.3.5 Polynomial systems

Consider the system

$$\dot{x} = f(x) + g(x)u$$

where $f(x)$ and $g(x)$ are polynomial vectors. To apply the tools presented in the previous sections to the stabilization of this system, consider the following parameterized representation for ρ and $u\rho$:

$$\rho(x) = \frac{a(x)}{b(x)^\alpha}, \quad u(x)\rho(x) = \frac{c(x)}{b(x)^\alpha},$$

where $a(x), b(x), c(x)$ are polynomials, $b(x)$ is positive, and α is chosen large enough so as to satisfy the integrability condition in Theorem 6. Note that by choosing this particular representation, we presuppose that we will be searching for ρ and u that are rationals. In particular, the resulting control law will be

$$u(x) = \frac{c(x)}{a(x)}.$$

In this case, the divergence criterion can be written as

$$\begin{aligned} \nabla \cdot [\rho(f + gu)] &= \nabla \cdot \left[\frac{1}{b^\alpha} (fa + gc) \right] \\ &= -\alpha \frac{1}{b^{\alpha+1}} \nabla b \cdot (fa + gc) + \frac{1}{b^\alpha} \nabla \cdot (fa + gc) \\ &= \frac{1}{b^{\alpha+1}} [b \nabla \cdot (fa + gc) - \alpha \nabla b \cdot (fa + gc)]. \end{aligned}$$

Since b is positive, we only need to satisfy the inequality

$$\boxed{b \nabla \cdot (fa + gc) - \alpha \nabla b \cdot (fa + gc) > 0.} \quad (6.18)$$

For fixed b, α , the inequality is linear in a, c . Instead of checking positivity, we check that the left-hand side is a *sum of squares*, and then the problem can be solved using semidefinite programming.

Example 6.4 A simple numerical example is the following:

$$\begin{aligned} \dot{x}_1 &= x_2 - x_1^3 + x_1^2 \\ \dot{x}_2 &= u. \end{aligned}$$

The function $b(x)$ is chosen based on the linearization of the system. We picked $b(x) = 3x_1^2 + 2x_1x_2 + 2x_2^2$, which is a control Lyapunov function (CLF) for the linearized system and, therefore, $b(x)^{-\alpha}$ (for some α) will be a good choice for a ρ function near the origin. Since we will be using a cubic polynomial for $c(x)$, and $a(x)$ is taken to be a constant, we choose $\alpha = 4$ to satisfy the integrability condition.

In this case, after solving the sum of squares inequality

$$b\nabla \cdot (fa + gc) - \alpha \nabla b \cdot (fa + gc) > 0, \quad (6.19)$$

we obtain an explicit expression for the controller, as a third-order polynomial in x_1 and x_2 . The optimization criterion chosen is the ℓ_1 norm of the coefficients. This way, we approximately try to minimize the number of nonzero terms. The expression for the final controller is

$$u(x_1, x_2) = -1.22x_1 - 0.57x_2 - 0.129x_2^3.$$

A phase plot of the closed-loop system is presented in Figure 6.5. ■

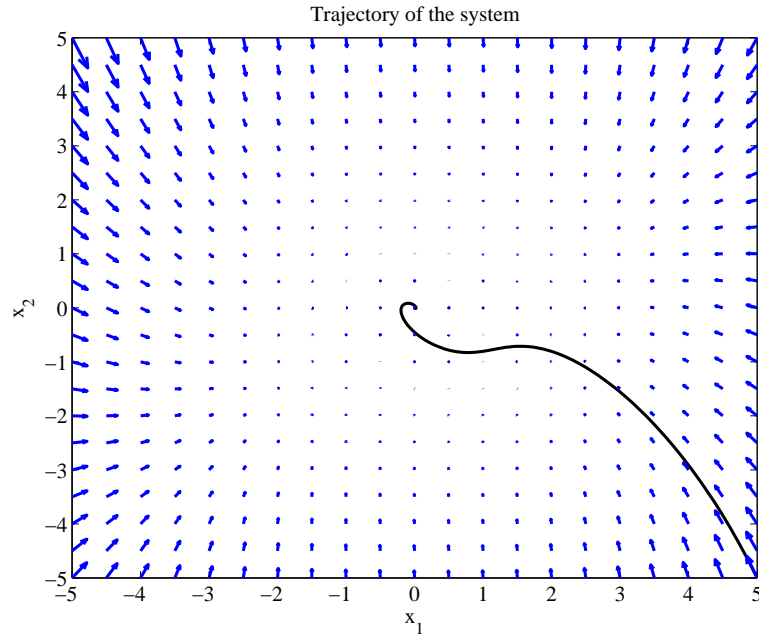


Figure 6.5. Phase plot of the closed-loop system in Example 6.4. The solid curve is the trajectory with initial conditions (5, -5).

Example 6.5 (Attitude control of a body) We will now look at the attitude control of a rigid body using three inputs as a physically motivated example. The complete attitude dynamics of a rigid body can, for example, be described using the following state equations [Shu93]:

$$\dot{\omega} = J^{-1}S(\omega)J\omega + J^{-1}u \quad (6.20)$$

$$\dot{\psi} = H(\psi)\omega \quad (6.21)$$

with $\omega \in \mathbb{R}^3$ the angular velocity vector in a body-fixed frame, $\psi \in \mathbb{R}^3$ the Rodrigues parameter vector, and $u \in \mathbb{R}^3$ the control torque. The matrix J is the positive definite inertia matrix, while $S(\omega)$ and $H(\psi)$ are given by

$$S(\omega) = \begin{bmatrix} 0 & \omega_3 & -\omega_2 \\ -\omega_3 & 0 & \omega_1 \\ \omega_2 & -\omega_1 & 0 \end{bmatrix} \quad (6.22)$$

$$H(\psi) = \frac{1}{2} (I - S(\psi) + \psi\psi^T) \quad (6.23)$$

We will apply the method described in this Chapter to numerically construct a stabilizing controller for this system. Synthesis of stabilizing controller for this system can also be performed using backstepping [KT99]. In our construction, the matrix

$$J = \begin{bmatrix} 4 & 0 & 0 \\ 0 & 2 & 0 \\ 0 & 0 & 1 \end{bmatrix}$$

will be chosen as the inertia matrix. In a state-space representation, the system will be:

$$\begin{aligned} \dot{\omega}_1 &= 4\omega_2\omega_3 + \frac{1}{4}u_1 \\ \dot{\omega}_2 &= -6\omega_1\omega_3 + \frac{1}{2}u_2 \\ \dot{\omega}_3 &= 2\omega_1\omega_2 + u_3 \\ \dot{\psi}_1 &= \frac{1}{2} [(1 + \psi_1^2)\omega_1 + (\psi_1\psi_2 - \psi_3)\omega_2 + (\psi_1\psi_3 + \psi_2)\omega_3] \\ \dot{\psi}_2 &= \frac{1}{2} [(\psi_1\psi_2 + \psi_3)\omega_1 + (1 + \psi_2^2)\omega_2 + (\psi_2\psi_3 - \psi_1)\omega_3] \\ \dot{\psi}_3 &= \frac{1}{2} [(\psi_1\psi_3 - \psi_2)\omega_1 + (\psi_2\psi_3 + \psi_1)\omega_2 + (1 + \psi_3^2)\omega_3] \end{aligned}$$

First, a density function of the following type is used:

$$\rho(\omega, \psi) = \frac{a(\omega, \psi)}{(\|\omega\|^2 + \|\psi\|^2)^\alpha} \quad (6.24)$$

where $a(\omega, \psi)$ will be obtained from convex optimization. Using this density function and $\alpha = 6$, it is possible to obtain a controller of the form

$$u_i(\omega, \psi) = \frac{c_i(\omega, \psi)}{a(\omega, \psi)}, \quad i = 1, 2, 3 \quad (6.25)$$

with $a(\omega, \psi)$ being positive definite. In fact, the function $a(\omega, \psi)$ is a homogeneous polynomial of degree 2, whereas the $c_i(\omega, \psi)$'s are polynomials of degree 5. Since the lowest degree of the monomials in $c_i(\omega, \psi)$ is equal to 3, we have $\lim_{(\omega, \psi) \rightarrow 0} u_i(\omega, \psi) = 0$, and thus we may set $u_i(0, 0) = 0$ to obtain a continuous controller as well as to make the origin an equilibrium of the closed-loop system.

Controllers with simpler expressions can be obtained by choosing a control Lyapunov function (CLF) of the linearized system, such as

$$b(\omega, \psi) = \|\omega + \psi\|^2 + \|\psi\|^2 \quad (6.26)$$

or

$$b(\omega, \psi) = \|\omega + \psi\|^2 + \|\omega\|^2 \quad (6.27)$$

for the denominator of the density function. Using (6.27) as the denominator and α again equal to 6, the controller obtained from convex optimization is given in the next equations:

$$\begin{aligned} u_1(\omega, \psi) = & -0.49\psi_1^3 - 0.86\omega_1^3 - 1.2\omega_1\psi_1^2 - 1.5\omega_1\psi_2^2 - 1.1\omega_1\psi_3^2 \\ & + 0.37\omega_1^2\psi_1 - 2.6\omega_1 - 0.77\psi_1 + 0.035\omega_2\psi_1\psi_2 \end{aligned} \quad (6.28)$$

$$\begin{aligned} u_2(\omega, \psi) = & -0.28\psi_2^3 - 0.29\omega_2^3 - 0.27\omega_2\psi_1^2 + 0.17\omega_2^2 - 0.37\psi_1^2\psi_2 \\ & - 0.69\omega_2\psi_2^2 - 1.1\omega_2\psi_3^2 - 0.45\psi_2\psi_3^2 - 1.1\omega_1^2\omega_2 \\ & - 0.44\omega_1\psi_1\psi_2 - 0.46\psi_2 - 1.1\omega_2 + 0.24\omega_1\omega_2\psi_1 \end{aligned} \quad (6.29)$$

$$\begin{aligned} u_3(\omega, \psi) = & -0.14\psi_3^3 - 0.18\omega_3^3 - 0.44\omega_1^2\omega_3 - 0.34\omega_2^2\omega_3 - 0.55\omega_3\psi_2^2 \\ & + 0.11\omega_1^2\psi_3 + 0.052\omega_3^2\psi_3 - 0.18\psi_1^2\psi_3 - 0.039\psi_2^2\psi_3 \\ & - 0.2\omega_2^2\psi_3 - 0.38\omega_3\psi_3^2 + 0.4\omega_2\omega_3\psi_2 + 0.37\omega_1\omega_3\psi_1 \\ & + 0.43\omega_2\psi_2\psi_3 - 0.69\omega_3 - 0.35\psi_3. \end{aligned} \quad (6.30)$$

A trajectory of the closed-loop system as well as its resulting control law is shown in Figure 6.6. ■

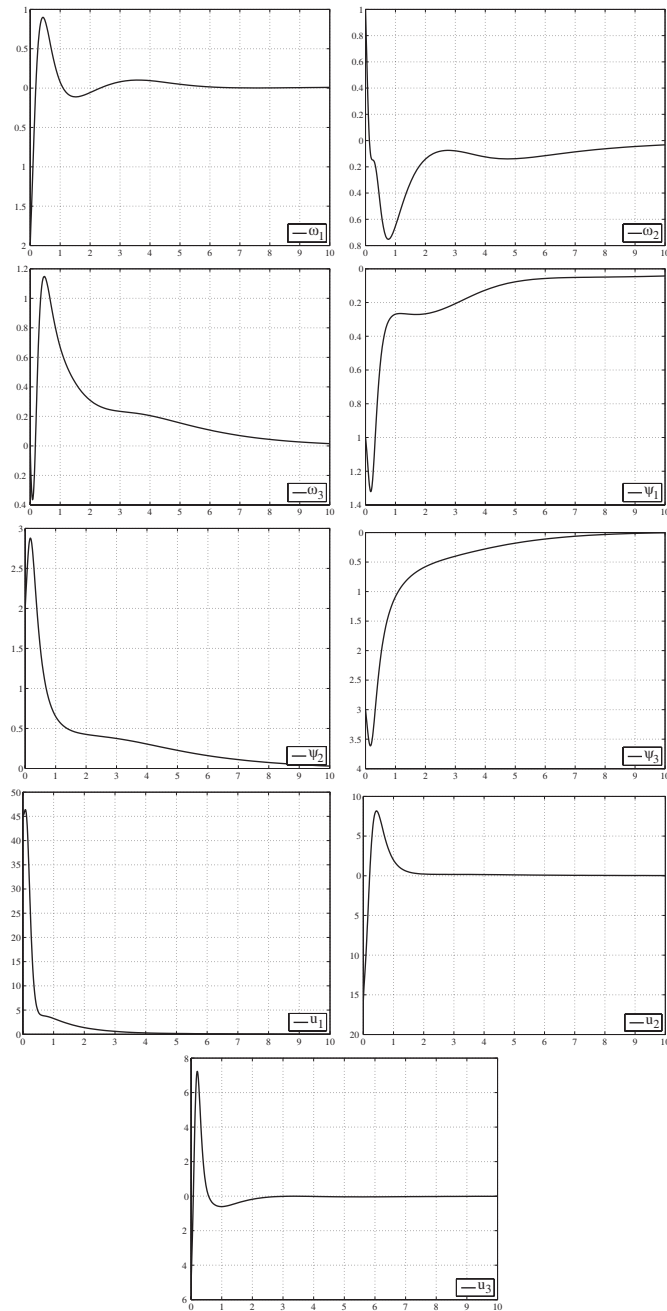


Figure 6.6. Trajectory of the controlled rigid body with initial conditions $(\omega, \psi) = (-1, 1, 0, -1, 2, -3)$ (first and second row) and control law $u(t) = (u_1(t), u_2(t), u_3(t))$ (third row).

6.3.6 Extension to the rational case

Consider the system

$$\dot{x} = f(x) + g(x)u$$

where $f(x)$ and $g(x)$ are *rational* vectors. Without loss of generality, we can consider that

$$f(x) = \frac{\tilde{f}(x)}{h(x)}, \quad g(x) = \frac{\tilde{g}(x)}{h(x)},$$

where $\tilde{f}(x)$, $\tilde{g}(x)$ and $h(x)$ are polynomial expressions.

To apply the tools presented in the previous sections to the stabilization of this system, consider also the following parameterized representation for ρ and $u\rho$:

$$\rho(x) = \frac{a(x)}{b(x)^\alpha}, \quad u(x)\rho(x) = \frac{c(x)}{b(x)^\alpha},$$

where $a(x)$, $b(x)$, $c(x)$ are polynomials, $b(x)$ is positive, and α is chosen large enough so as to satisfy the integrability condition in Theorem 6. Note that by choosing this particular representation, we presuppose that we will be searching for ρ and u that are rationals. In particular, the resulting control law will be

$$u(x) = \frac{c(x)}{a(x)}.$$

In this case, the divergence criterion presented in Theorem 6 can be written as

$$\begin{aligned} \nabla \cdot [\rho(f + gu)] &= \nabla \cdot \left[\frac{1}{b^\alpha h} (\tilde{f}a + \tilde{g}c) \right] \\ &= \frac{bh}{b^{\alpha+1}h^2} \nabla \cdot (\tilde{f}a + \tilde{g}c) + \nabla \frac{1}{b^\alpha h} \cdot (\tilde{f}a + \tilde{g}c) \\ &= \frac{1}{b^{\alpha+1}h^2} \left[bh \nabla \cdot (\tilde{f}a + \tilde{g}c) - (\alpha h \nabla b + b \nabla h) \cdot (\tilde{f}a + \tilde{g}c) \right]. \end{aligned}$$

Since both $b(x)$ and $h(x)^2$ are positive, we only need to satisfy the inequality

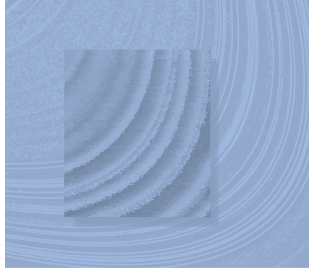
$$\boxed{bh \nabla \cdot (\tilde{f}a + \tilde{g}c) - (\alpha h \nabla b + b \nabla h) \cdot (\tilde{f}a + \tilde{g}c) > 0.} \quad (6.31)$$

For fixed b , α , the inequality is linear in a , c . Instead of checking positivity, we check that the left-hand side is a *sum of squares*, and then the problem can be solved using semidefinite programming.

6.4 Conclusions

A recently derived computational approach to nonlinear control synthesis [Par00] has been outlined here. The basis is a recent convergence criterion which is closely related to earlier work on optimal control and makes it possible to state the synthesis problem in terms of convex optimization. Polynomials are used for parameterization and positivity is verified and certified using the sum of squares relaxation. In general, a controller designed using this approach is only guaranteed to make almost all trajectories of the closed-loop system tend to the origin. In many cases, however, such a controller will actually be globally asymptotically stabilizing.

In this work we have extended the procedures developed in [Par00] to rational systems and we have implemented a special version of the software presented in [PPP02] that uses an alternative semidefinite programming solver. New developments in sum of squares optimization focus on structure-exploiting techniques for sparse and structured polynomials and in extending these procedures to develop techniques in other scientific areas.



Chapter 7

Control synthesis of systems with uncertain parameters

As presented in Chapter 6, there is a recently derived stability criterion for nonlinear systems –which has a remarkable convexity property– and the development of numerical methods for verification of positivity. These tools had allowed the computation –via semidefinite programming– of stabilizing controllers for the case of systems with polynomial or rational vector fields. Using the theory of semialgebraic sets these computational tools are extended in this chapter for the case of polynomial or rational systems with uncertain parameters.

A question that arises naturally at this point is: the computational tools presented in the previous chapter can be employed to stabilize systems with uncertain parameters?

With the help of the theory of semialgebraic sets this can be done by considering the uncertain parameters as new polynomial variables (*pseudo-variables*) and without augmenting the dynamic of the system. This way, our objective is to find a *worst case* controller, in the sense that the system will be stabilized for all the possible values of the uncertain parameters.

In order to formalize all these questions, we must introduce some notation and a key theorem.

7.1 Putinar's theorem

Definition 1 Let $\Sigma^2 \subset \mathbb{R}[x_1, \dots, x_n]$ denote the set of polynomials which can be written as a sum of squares of other polynomials, that is,

$$\Sigma^2 := \{G(x) \in \mathbb{R}[x_1, \dots, x_n] : \exists h_1(x), \dots, h_m(x) \in \mathbb{R}[x_1, \dots, x_n] \\ \text{such that } G(x) = \sum_{i=1}^m h_i(x)^2\}$$

Definition 2 A subset of \mathbb{R}^n which is a finite Boolean combination of sets of the form $\{x = (x_1, \dots, x_n) : p(x) > 0\}$ and $\{x : q(x) = 0\}$, where $p, q \in \mathbb{R}[x_1, \dots, x_n]$ –i.e. a set that is defined by polynomial inequalities, equalities, and nonequalities– is called a semialgebraic set.

Theorem 8 (Putinar) Suppose we are given a set

$$K := \{x \in \mathbb{R}^n : c_i(x) \geq 0, i = 1, \dots, m\} \quad (7.1)$$

that is compact, and furthermore satisfies the condition that there exists a polynomial $h(x)$ of the form

$$h(x) = s_0(x) + \sum_{i=1}^m s_i(x) \cdot c_i(x),$$

where the $s_i \in \Sigma^2$ are sum of squares and $c_i \in \mathbb{R}[x]$, whose level set

$$\{x \in \mathbb{R}^n : h(x) \geq 0\}$$

is compact. Then, for any polynomial $G(x)$ positive on all of K , there exist $s_0, s_1, \dots, s_m \in \Sigma^2$, such that

$$G(x) = s_0(x) + \sum_{i=1}^m s_i(x) \cdot c_i(x).$$

Proof. See [Put93]. □

It is worth noting that for a large host of applications, the additional constraint required for Theorem 8 is easily satisfied by the corresponding sets K . For instance, the following cases fall into this category.

1. Suppose some c_i in the definition of K satisfies, on its own, the condition $\{c_i(x) \geq 0\}$ compact. Then Theorem 8 applies. This includes any instance where we are taking intersections with ellipses, or circles, among others.
2. Perhaps very importantly, any 0–1 integer programming problem falls easily into this framework. The integer constraint is given by polynomial relations $x_i^2 - x_i = 0$. Consider now the polynomial $u(x) = \sum_i (x_i - x_i^2)$. This is of the correct, and indeed satisfies $\{u(x) \geq 0\}$ compact.
3. If K is compact, and is defined only by linear functions, then we can directly apply Theorem 8. Note that this includes all polytopes.
4. If we know that the compact set K lies inside some ball of radius R , we can simply add the interior of the ball, $\sum_i x_i^2 \leq R^2$ as a redundant constraint, thus not changing K , but automatically satisfying Theorem 8, without appreciably changing the size of definition of the problem (especially if we already have a large number of functions defining K).

In what follows we assume that the set K defined as in equation (7.1) satisfies the hypotheses of the Theorem 8. Using this theorem, we translate the pointwise property

$$G(x) > 0, \quad \forall x \in K \quad (7.2)$$

to the algebraic property

$$\exists s_1, \dots, s_m \in \Sigma^2 \text{ such that } \left(G(x) - \sum_{i=1}^m s_i(x)c_i(x) \right) \in \Sigma^2. \quad (7.3)$$

The membership test in equation (7.3) can be performed in time polynomial in the size of the polynomial $G(x)$ using the computational tools presented in [PPP02].

7.2 Synthesis procedure

Consider the nonlinear affine system

$$\dot{x} = f(x, p) + g(x, p)u, \quad (7.4)$$

where $x \in \mathbb{R}^n$ is the state vector, $p = (p_1, \dots, p_m) \in \mathbb{R}^m$ is the uncertainty parameter vector and $f, g : \mathbb{R}^n \times \mathbb{R}^m \rightarrow \mathbb{R}^n$ are polynomial functions describing the system dynamics. We are searching a controller u that stabilizes the system for all the possible values of the parameter p .

We assume that the following intervals are known:

$$\underline{p}_i \leq p_i \leq \bar{p}_i, \quad i = 1, \dots, m. \quad (7.5)$$

Equation (7.5) can be expressed as

$$\begin{aligned} c_1 &= p_1 - \underline{p}_1 \geq 0 \\ c_2 &= \bar{p}_1 - p_1 \geq 0 \\ &\vdots \\ c_{2m-1} &= p_m - \underline{p}_m \geq 0 \\ c_{2m} &= \bar{p}_m - p_m \geq 0 \end{aligned}$$

This way, the set K can be defined as

$$K = \{p \in \mathbb{R}^m : c_1 \geq 0, c_2 \geq 0, \dots, c_m \geq 0\}.$$

Let us define $\tilde{x} = [x, p]^T$. The system (7.4) is now

$$\dot{\tilde{x}} = f(\tilde{x}) + g(\tilde{x})u. \quad (7.6)$$

To apply the tools presented in Chapter 6 to the stabilization of the system (7.6), consider the parameterized representation for ρ and $u\rho$:

$$\rho(x) = \frac{a(x)}{b(x)^\alpha}, \quad u(x)\rho(x) = \frac{c(x)}{b(x)^\alpha},$$

where $a(x), b(x), c(x)$ are polynomials, $b(x)$ is positive, and α is chosen large enough so as to satisfy the integrability condition in Theorem 6.

In this case, the divergence criterion can be written as

$$\begin{aligned} \nabla_n \cdot [\rho(f + gu)] &= \\ &= \nabla_n \cdot \left[\frac{1}{b^\alpha} (fa + gc) \right] \\ &= -\alpha \frac{1}{b^{\alpha+1}} \nabla_n b \cdot (fa + gc) + \frac{1}{b^\alpha} \nabla_n \cdot (fa + gc) \\ &= \frac{1}{b^{\alpha+1}} [b \nabla_n \cdot (fa + gc) - \alpha \nabla_n b \cdot (fa + gc)], \end{aligned}$$

where the following modified versions of the operators gradient and divergence have been considered:

$$\begin{aligned}\nabla_n V &= \left[\frac{\partial V}{\partial x_1} \cdots \frac{\partial V}{\partial x_n} \right], \quad V : \mathbb{R}^n \times \mathbb{R}^m \rightarrow \mathbb{R} \\ \nabla_n \cdot f &= \frac{\partial f_1}{\partial x_1} + \cdots + \frac{\partial f_n}{\partial x_n}, \quad f : \mathbb{R}^n \times \mathbb{R}^m \rightarrow \mathbb{R}^n.\end{aligned}$$

Since b is positive, we only need to satisfy the inequality

$$G(\tilde{x}) := b \nabla_n \cdot (fa + gc) - \alpha \nabla_n b \cdot (fa + gc) > 0, \quad \forall p \in K. \quad (7.7)$$

Although the system contains uncertain parameters, the explicit expressions of the functions f and g are known and so equation (7.7) can be computationally treated.

For fixed b, α , the inequality is linear in a, c . Instead of checking positivity, we check that the left-hand side is a *sum of squares*. Using Theorem 8 and, more precisely, equation (7.3), the pointwise property (7.7) is translated to the algebraic property

$$\begin{aligned}\exists s_1, \dots, s_{2m} \in \Sigma^2 \text{ such that} \\ \left(G(\tilde{x}) - \sum_{i=1}^{2m} s_i(x) c_i \right) \in \Sigma^2,\end{aligned}$$

that can be performed in polynomial time using the computational tools presented in [PPP02].

7.3 A simple example

In order to show the applicability of the computational approach described in Section 7.2, let us consider the following nonlinear system with an uncertain parameter as the coefficient of the linear term in the first equation:

$$\dot{x}_1 = px_2 - x_1^3 + x_1^2, \quad p \in [0.7, 1.3] \quad (7.8)$$

$$\dot{x}_2 = u \quad (7.9)$$

The system is defined by polynomial expressions in the variables x_1, x_2 and, for computational purposes, p can be treated as a third variable.

Our objective is to find a control function u that stabilizes the system for every $p \in [0.7, 1.3]$. Such a control law u for this system can be found using the techniques described in Chapter 6. We only need to satisfy the inequality (7.7) in the case $n = 2$, that is

$$G(x, p) = b \nabla_2 \cdot (fa + gc) - \alpha \nabla_2 b \cdot (fa + gc) > 0, \quad \forall p \in K \quad (7.10)$$

where

$$f(x_1, x_2, p) = \begin{bmatrix} px_2 - x_1^3 + x_1^2 \\ 0 \end{bmatrix},$$

$$g(x_1, x_2, p) = \begin{bmatrix} 0 \\ 1 \end{bmatrix},$$

and b can be chosen as it is described in [PPR04]

$$b(x_1, x_2) = 3x_1^2 + 2x_1x_2 + 2x_2^2$$

$$= (x_1 + x_2)^2 + 2x_1^2 + x_2^2.$$

Since we will be using a cubic polynomial for $c(x_1, x_2)$, and $a(x_1, x_2)$ is taken to be a constant, we choose $\alpha = 4$ to satisfy the integrability condition. We note that $G(x, p)$ can be considered as a polynomial expression in $\mathbb{R}[x_1, x_2, p]$.

K is defined as follows

$$K = \{p \in \mathbb{R} : 1.3 - p \geq 0, p - 0.7 \geq 0\}$$

$$= \{p \in \mathbb{R} : c_1 \geq 0, c_2 \geq 0\}.$$

We translate the equation (7.10) to the algebraic property

$$\exists s_1, s_2 \in \Sigma^2 \text{ such that}$$

$$(G(x, p) - s_1(x)c_1 - s_2(x)c_2) \in \Sigma^2.$$

After solving the sum of squares problem, using the software introduced in [PPP02], the results are

$$u(x) = -1.3446x_1 - 0.9005x_2 - 0.0902x_2^3,$$

$$s_1(x) = 6.2496x_1^2 + 14.695x_2^2 + 19.1664x_1x_2$$

$$= (1.37x_1 + 2.09x_2)^2 + (2.09x_1 + 3.21x_2)^2,$$

$$s_2(x) = 6.2496x_1^2 + 4.695x_2^2 - 10.8336x_1x_2$$

$$= (1.89x_1 - 1.64x_2)^2 + (1.42x_2 - 1.64x_1)^2.$$

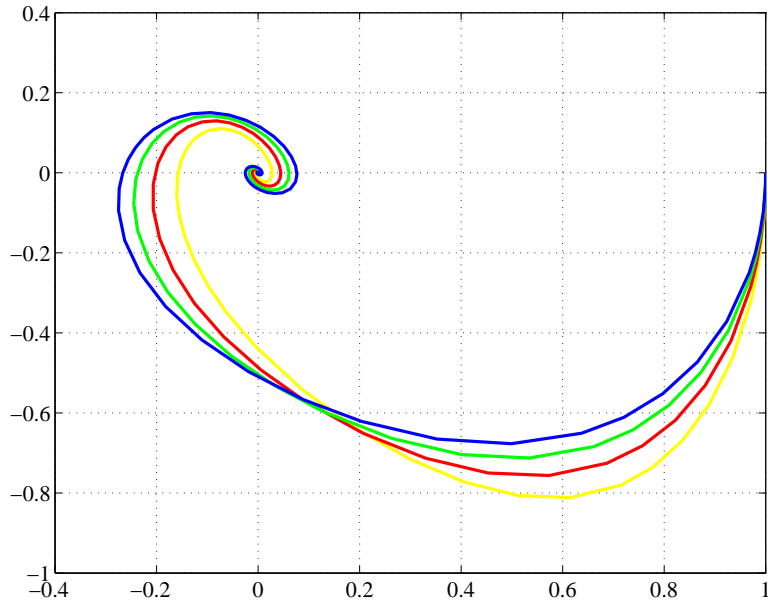


Figure 7.1. Phase plot of the closed-loop system in Section 7.3. Solid curves are trajectories with initial conditions $(x_1, x_2) = (1, 0)$ and for four different values for the parameter p , 0.7, 0.9, 1.1 and 1.3.

In Figure 7.1 we have depicted the trajectories of the closed-loop system in equations (7.8)-(7.9) with initial conditions $(1, 0)$ and for four different values for the parameter p , 0.7, 0.9, 1.1 and 1.3. It can be seen that all the trajectories converge to the origin as it was to be expected.

7.4 Conclusions

In this chapter we have extended, with the help of the theory of semi-algebraic sets, the computational tools presented in Chapter 6 to stabilize polynomial or rational systems with uncertain parameters. We have considered the uncertain parameters as new polynomial variables but we have not augmented the dynamic of the system. Systems with bounded external disturbances can also be considered. The size of the semidefinite programs makes it possible to handle problems that are otherwise too large to solve using state-of-the-art semidefinite programming solvers.

Conclusions and future work

Conclusions

This thesis has dealt with the problem of controlling uncertain systems. Chapter 2 has presented an adaptive version of the backstepping design for linear systems with uncertainties in the parameters developed in [KKK94]. The design needs only the measurement of the output and uses a Kresseilmeier filter to estimate the state of the system. The control law is obtained using a recursive algorithm of as many steps as the relative degree of the linear system. The a-priori knowledge on the linear system is the same as in certainty-equivalence adaptive algorithms; that is the degree and relative degree of the linear system (which is assumed to be minimum phase) and the sign of the high frequency gain. The stability result is global and tracking is assured asymptotically. Furthermore, \mathcal{L}_∞ and \mathcal{L}_2 bounds on the transient behavior can be derived.

Chapter 2 has also presented the main recent developments relative to the tuning functions design. Research has followed several complementary lines: the extension of the technique to multivariable systems has been made in [LT96, WY98] and [CHIK03] while its extension to discrete-time systems and time-varying systems has been done respectively in [RIG99] and [GRI99]. The a-priori knowledge assumption of the high frequency gain has been removed in [Miy00b] using the Nussbaum gain. The robustness of the tuning functions design vis-à-vis unmodelled dynamics and external disturbances has been explored in [IK98a] and [OIG01] using a switching σ -modification, in [IK98b] and [WS96] using a parameter projection, and [ZI98] using signal normalization and σ -modification.

In [NV01b] it has been shown that, contrarily to certainty equivalence algorithms, the tuning functions design does not act as an integrator in the presence of constant disturbances. The robust transient behavior of this adaptive design has been explored in [IRG97] and [WZS99].

Chapter 3 has presented the robust version of the tuning functions design presented in [IRG97]. This design presents two modifications with respect to the standard design of [KKK94]. First it uses a switching σ -modification in the update parameter laws. This prevents parameter drift in the presence of external disturbances and/or unmodelled dynamics. Second, it uses an additional term in the first step of the recursive design to counteract the negative effect of disturbances on asymptotic and transient behavior. These modifications allow the adaptive controller to insure the global boundedness of all closed loop signals in the presence of strictly proper unmodelled dynamics and bounded disturbances. Furthermore, it can be shown that the performance of the closed loop, both asymptotically and in the transient, can be improved arbitrarily by increasing the gains of the controller.

Chapter 4 has focused on the application of the modified version of the tuning functions design presented in Chapter 3 to a problem in the field of Civil Engineering, which consists in a building structure that combines a passive nonlinear base isolator with an active control system.

The objective of the active control component applied to the structural base was to keep the base displacement relative to the ground and the interstory drift within a reasonable range according to the design of the base isolator. The base isolator device exhibits a hysteretic nonlinear behavior which is described analytically by the Bouc-Wen model [Wen76].

The control problem was formulated representing the system dynamics in two alternative coordinates: absolute (with respect to an inertial frame) and relative to the ground. It has been observed by the means of numerical simulations that the base displacement in the relative case is clearly reduced with respect to the strict passive design whereas in the absolute case the relative displacement of the base increases but remains within an acceptable range. Furthermore, it has been observed that the interstory drift is significantly reduced in the absolute case, while it increases in the relative case with respect to the uncontrolled situation.

Finally, it has been observed that the control signal is relatively smooth in the absolute case while this signal contains large high frequency components in the relative coordinate strategy. Thus, we recommend the use of the absolute coordinates. Besides, the choice of a backstepping adaptive control has allowed to consider that the parameters of the models are uncertain and to have computable bounds on the transient behavior.

In Chapter 5, we were interested in an implementation issue of the tuning functions design: that of numerical sensitivity. Indeed, the complexity of the controller makes inevitable the use of digital computers to perform the calculation of the control signal. Our work has addressed the issue of the numerical sensitivity of the adaptive tuning functions using both numerical simulations and an analytical description of the phenomenon. We have considered a relative degree three linear system with unknown parameters and we have used the standard design of [KKK94]. Our methodology was to perturb slightly the signals that the control law uses as inputs and observe the behavior of the closed loop. It has been shown that while the increase of the design parameters may be desirable to achieve a good transient performance, it harms the control signal as this increase introduces large high-frequency components due to the numerical errors. The analytical expression of the effect of the parameters design on the control signal has been obtained using the symbolic calculus software Maple. This expression shows that if the design parameters have values larger than unity, then they act as large high gains which explains the sensitivity of the control to numerical disturbances.

Chapter 6 has extended the problem of synthesis to a class of nonlinear systems by means of computational methods. The basis of this new computational approach is a recent convergence criterion [Ran01] with a remarkable convexity property and the sum of squares optimization which is a computational relaxation that can be used in any problem related to polynomial nonnegativity.

Finally, in Chapter 7, we have considered polynomials and rational vector fields and, thanks to the theory of the semialgebraic sets [Put93], these computational tools have also been extended for the case of polynomial and rational systems with uncertain parameters. This can be done by considering the uncertain parameters as new polynomial variables without augmenting the dynamic of the system. The size of the semidefinite programs makes it possible to handle problems that are otherwise too large to solve using state-of-the-art semidefinite programming solvers. Semidefinite programming, or sum of squares optimization, has a great deal of applications of linear and nonlinear systems analysis and synthesis. Furthermore, these procedures can also be extended to general computational methods in applied mathematics.

Future work

The immediate future work will focus on the following subjects:

Structural control

As an application of the adaptive backstepping control of linear systems in the presence of bounded disturbances, we have developed a hybrid (passive and active) seismic control system for hysteretic base-isolated structures. In this thesis we have considered that the base isolator device exhibits a hysteretic nonlinear behavior which is described analytically by the Bouc-Wen model. The future research in the field of structural control can be precised in the following lines.

From conceptual and potential effectiveness points of view, active control systems have not yet been fully adopted by engineers. This may be due in large part to the requirements in force and power supplies and the risks of keeping systems continuously operative and reliable during earthquakes. As an appealing alternative, semiactive control strategies become very promising. In a semiactive control system, on-line adjustment of the damping and/or stiffness of adaptable devices are done according to feedback signal and control commands.

Moreover, we will consider other hysteretic base-isolated structures and frictional base isolation systems.

We also will evaluate these control algorithms in a benchmark structure fully described in [NNJG04]. The benchmark considered is an eight story building and provides a well defined base isolated building with a broad set of carefully chosen parameter sets, performance measures and guidelines to the control designers.

Backstepping complexity

In the case of the backstepping adaptive tuning functions control design, this thesis has addressed for the first time sensitivity and accuracy issues. As a future work, we will focus on the unexplored field of the complexity (a measure of time or space used by an algorithm) of the backstepping algorithm with respect to the size of the problem (plant order n or the relative degree of the plant ρ) with the help of computational tools and symbolic calculus software.

Sum of squares applications

In the thesis we have presented a computational relaxation to solve the problem of synthesis of nonlinear systems with polynomial or rational vector fields. Using the theory of semialgebraic sets these computational tools have been extended for the case of polynomial or rational systems with uncertain parameters. Semidefinite programming, and more precisely, sum of squares optimization, is a computational relaxation that can be used in any problem related to polynomial nonnegativity. We propose continuing in the field of sum of squares optimization in more applications of linear and nonlinear systems analysis and synthesis (dissipativity analysis, parameter-state dependent LMI, stability of hybrid systems, stability of time-delay systems, estimating domain of attraction, safety verification, robustness analysis and density-based synthesis), and extend these procedures to develop techniques for constructing polynomial functions whose purpose is to provide lower and upper bounds for the functional outputs of the exact solution of partial differential equations.

Analysis, identification and control of systems with friction

Another question that will be considered is the analysis of mechanical systems with frictional elements. Although friction may be a desirable property, as it is for brakes, it is generally an impediment for servo control. We will follow three complementary lines of research: the first one will focus on the analysis of mechanical systems with a more complete model of friction. The second line will deal with developing new methodologies to identify the parameters that appear in the models of friction. Finally, the third line will be devoted to proposing new control algorithms that can cope with the friction present in the mechanical system.

Bibliography

- [ADSKN04] M. Al-Dawod, B. Samali, K. Kwok, and F. Naghdy. Fuzzy controller for seismically excited nonlinear buildings. *Journal of Engineering Mechanics*, 130(4):407–415, 2004.
- [AL04] M.A. Austin and W.J. Lin. Energy balance assessment of base-isolated structures. *Journal of Engineering Mechanics*, 130(3):347–358, 2004.
- [AR04] A.S. Ahlawat and A. Ramaswany. Multiobjective optimal fuzzy logic controller driven active and hybrid control systems for seismically excited nonlinear buildings. *Journal of Engineering Mechanics*, 130(4):416–423, 2004.
- [BB97] A.H. Barbat and L. Bozzo. Seismic analysis of base isolated buildings. *Archives of Computational Methods in Engineering*, 4(2):153–192, 1997.
- [BGFB94] S. Boyd, L. El Ghaoui, E. Feron, and V. Balakrishnan. *Linear Matrix Inequalities in System and Control Theory*. Society for Industrial and Applied Mathematics, 1994.
- [BI89] C.I. Byrnes and A. Isidori. New results and examples in nonlinear feedback stabilization. *Systems and Control Letters*, 12:437–442, 1989.
- [BRRM95] A.H. Barbat, J. Rodellar, E.P. Ryan, and N. Molinares. Active control of nonlinear base-isolated buildings. *Journal of Engineering Mechanics*, 121(6):676–684, 1995.
- [Cac03] D.G. Cacuci. *Sensitivity and Uncertainty Analysis*. Chapman and Hall, 2003.

- [CC04] G. Chen and C. Chen. Semiactive control of the 20-story benchmark building with piezoelectric friction dampers. *Journal of Engineering Mechanics*, 130(4):393–400, 2004.
- [CHIK03] R.R. Costa, L. Hsu, A.K. Imai, and P. Kokotovic. Lyapunov-based adaptive control of MIMO systems. *Automatica*, 39:1251–1257, 2003.
- [DB01] R.C. Dorf and R.H. Bishop. *Modern Control Systems*. Prentice Hall, 2001.
- [Doo04] P.V. Dooren. The basics of developing numerical algorithms. *IEEE Control Systems Magazine*, 24(1):18–27, 2004.
- [FG98] T.I. Fossen and A. Grovlen. Nonlinear output feedback control of dynamically positioned ships using vectorial observer backstepping. *IEEE Transactions on Control Systems Technology*, 6(1):121–128, 1998.
- [Gha94] R. Ghanadan. Computer algebra tools for recursive design of robust and adaptive nonlinear controllers. Technical Report CCEC-06-09-94, University of California, Santa Barbara, 1994.
- [GNLC95] P. Gahinet, A. Nemirovski, A.J. Laub, and M. Chilali. *LMI Control Toolbox*. The Mathworks Incorporated, 1995.
- [GRI99] F. Giri, A. Rabeh, and F. Ikhouane. Backstepping adaptive control of time-varying plants. *Systems and Control Letters*, 36:245–252, 1999.
- [HBC⁺97] G.W. Housner, L.A. Bergman, T.K. Caughey, A.G. Chasiakos, R.O. Claus, S.F. Masri, R.E. Skelton, T.T. Soong, B.F. Spencer, and J.T.P. Yao. Structural control: past, present and future. *Journal of Engineering Mechanics*, 124:897–971, 1997.
- [Hig02] N.J. Higham. *Accuracy and Stability of Numerical Algorithms*. SIAM, 2002.
- [HKL00] S.L. Hung, C.Y. Kao, and J.C. Lee. Active pulse structural control using artificial neural networks. *Journal of Engineering Mechanics*, 126(8):839–849, 2000.

- [HKMP04] N.J. Higham, M. Konstantinov, V. Mehrmann, and P. Petkov. The sensitivity of computational control problems. *IEEE Control Systems Magazine*, 24(1):28–43, 2004.
- [IK98a] F. Ikhouane and M. Krstić. Adaptive backstepping with parameter projection: robustness and asymptotic performance. *Automatica*, 34(4):429–435, 1998.
- [IK98b] F. Ikhouane and M. Krstić. Robustness of the tuning functions adaptive backstepping design for linear systems. *IEEE Transactions on Automatic Control*, 43(3):431–437, 1998.
- [IMR04] F. Ikhouane, V. Mañosa, and J. Rodellar. Bounded and dissipative solutions of the Bouc-Wen model for hysteretic structural systems. In *Proceedings of the American Control Conference*, 2004.
- [IRG97] F. Ikhouane, A. Rabeh, and F. Giri. Transient performance analysis in robust nonlinear adaptive control. *Systems and Control Letters*, 31:21–31, 1997.
- [IS96] P.A. Ioannou and J. Sun. *Robust Adaptive Control*. Prentice Hall, 1996.
- [ISGS96] K. Ida, H. Saiyou, Y. Gatade, and K. Seto. A study on servo-type velocity and displacement sensor for vibration control. In *Proceedings of the Third International Conference on Motion and Vibration Control*, 1996.
- [Isi95] A. Isidori. *Nonlinear Control Systems*. Springer-Verlag, third edition, 1995.
- [ISK98] H. Irschik, K. Schlacher, and A. Kugi. Control of earthquake excited nonlinear structures using Lyapunov’s theory. *Computers and Structures*, 67:83–90, 1998.
- [JD00] L.M. Jansen and S.J. Dyke. Semiactive control strategies for MR dampers: comparative study. *Journal of Engineering Mechanics*, 126(8):795–803, 2000.
- [Kel86] J.M. Kelly. Aseismic base isolation: review and bibliography. *Soil Dynamics and Earthquake Engineering*, 5(4):202–216, 1986.

- [Kha96] H.K. Khalil. *Nonlinear systems*. Upper Saddle River, NJ. Prentice-Hall, Inc., second edition, 1996.
- [KIS98] T. Kobori, Y. Inoue, and K. Seto, editors. *Proceedings of the Second World Conference on Structural Control*, 1998.
- [KK03] K.S. Kim and Y. Kim. Robust backstepping control for slew maneuver using nonlinear tracking function. *IEEE Transactions on Control Systems Technology*, 11(6):822–829, 2003.
- [KKK94] M. Krstić, I. Kanellakopoulos, and P. Kokotović. Nonlinear design of adaptive controllers for linear systems. *IEEE Transactions on Automatic Control*, 39(4):738–752, 1994.
- [KKK95] M. Krstić, I. Kanellakopoulos, and P. Kokotović. *Nonlinear and Adaptive Control Design*. John Wiley & Sons, Inc., 1995.
- [KLS87] J.M. Kelly, G. Leitmann, and A.G. Soldatos. Robust control of base-isolated structures under earthquake excitation. *Journal of Optimization Theory and Applications*, 53(2):159–180, 1987.
- [KS89] P.V. Kokotović and H.J. Sussmann. A positive real condition for global stabilization of nonlinear systems. *Systems and Control Letters*, 13:125–133, 1989.
- [KT99] M. Krstić and P. Tsiotras. Inverse optimal stabilization of a rigid spacecraft. *IEEE Transactions on Automatic Control*, 42:1042–1049, 1999.
- [LISR98] N. Luo, M. De la Sen, and J. Rodellar. Composite adaptive SMC of nonlinear base isolated buildings with actuator dynamics. *Applied Mathematics and Computer Science*, 8(1):183–197, 1998.
- [LRVIS01] N. Luo, J. Rodellar, J. Vehí, and M. De la Sen. Composite semiactive control of a class of seismically excited structures. *Journal of the Franklin Institute*, 338:225–240, 2001.

- [LSLT01] T.C. Lee, K.T. Song, C.H. Lee, and C.C. Teng. Tracking control of unicycle-modeled mobile robots using a saturation feedback controller. *IEEE Transactions on Control Systems Technology*, 9(2):305–318, 2001.
- [LT96] Y. Ling and G. Tao. Adaptive backstepping control design for linear multivariable plants. In *Proceedings of the 35th Conference on Decision and Control*, pages 2438–2443, December 1996.
- [Miy00a] Y. Miyasato. A design method of universal adaptive stabilizer. *IEEE Transactions on Automatic Control*, 45(12):2368–2373, 2000.
- [Miy00b] Y. Miyasato. A model reference adaptive controller for systems with uncertain relative degrees $r, r + 1$ or $r + 2$ and unknown signs of high-frequency gains. *Automatica*, 36:889–896, 2000.
- [MS97] L. Meirovitch and T.J. Stemple. Nonlinear control of structures in earthquakes. *Journal of Engineering Mechanics*, 123(10):1090–1095, 1997.
- [NNJG04] S. Narasimhan, S. Nagarajaiah, E.A. Johnson, and H.P. Gavin. Smart base isolated benchmark building. Part I: problem definition. *Journal of Structural Control and Health Monitoring*, 2004.
- [NV01a] V.O. Nikiforov and K.V. Voronov. Adaptive backstepping with a high-order tuner. *Automatica*, 37:1953–1960, 2001.
- [NV01b] V.O. Nikiforov and K.V. Voronov. Nonlinear adaptive controller with integral action. *IEEE Transactions on Automatic Control*, 46(12):2035–2037, 2001.
- [Oga98] K. Ogata. *Modern Control Engineering*. Prentice Hall, 1998.
- [OIG01] H. Ouardi, F. Ikhouane, and F. Giri. Robustness of backstepping adaptive control with respect to inverse multiplicative uncertainty. In *Proceedings of the American Control Conference*, pages 4172–4177, June 2001.

- [Par00] P.A. Parrilo. *Structured semidefinite programs and semialgebraic geometry methods in robustness and optimization*. PhD thesis, California Institute of Technology, 2000.
- [PIR04a] F. Pozo, F. Ikhouane, and J. Rodellar. Adaptive backstepping control of hysteretic base-isolated structures. In *Proceedings of the Third European Conference on Structural Control*, 2004.
- [PIR04b] F. Pozo, F. Ikhouane, and J. Rodellar. Condicionamiento numérico del diseño de sistemas de control mediante backstepping adaptativo. In *Proceedings of the Congresso de Métodos Computacionais em Engenharia*, 2004.
- [PMKL98] W.N. Patten, C. Mo, J. Kuehn, and J. Lee. A primer on design of semiactive vibration absorber. *Journal of Engineering Mechanics*, 124:61–68, 1998.
- [PP99] C. Prieur and L. Praly. Uniting local and global controllers. In *Proceedings of the Conference on Decision and Control*, 1999.
- [PP02] A. Papachristodoulou and S. Prajna. On the construction of Lyapunov functions using the sum of squares decomposition. In *Proceedings of the Conference on Decision and Control*, 2002.
- [PPP02] S. Prajna, A. Papachristodoulou, and P.A. Parrilo. Introducing SOSTOOLS: a general purpose sum of squares programming solver. In *Proceedings of the Conference on Decision and Control*, 2002.
- [PPR04] S. Prajna, P.A. Parrilo, and A. Rantzer. Nonlinear control synthesis by convex optimization. *IEEE Transactions on Automatic Control*, 49(2):310–314, 2004.
- [PPW04] S. Prajna, A. Papachristodoulou, and F. Wu. Nonlinear control synthesis by sum of squares optimization: a Lyapunov-based approach. In *Proceedings of the Asian Control Conference*, 2004.
- [PSH94] W.N. Patten, R.L. Sack, and Q. He. Controlled semiactive hydraulic vibration absorber for bridges. *Journal of Engineering Mechanics*, 122:187–192, 1994.

- [Put93] M. Putinar. Positive polynomials on compact semi-algebraic sets. *Indiana University Mathematical Journal*, 42(3), 1993.
- [Ran01] A. Rantzer. A dual to Lyapunov’s stability theorem. *Systems and Control Letters*, 42:161–168, 2001.
- [RIG99] A. Rabeh, F. Ikhouane, and F. Giri. An approach to digital implementation of continuous backstepping adaptive control for linear systems. *International Journal of Adaptive Control and Signal Processing*, 13:327–346, 1999.
- [RJS02] J.C. Ramallo, E.A. Johnson, and B.F. Spencer. “Smart” base isolation systems. *Journal of Engineering Mechanics*, 128:1088–1099, 2002.
- [RR01] A. Ralston and P. Rabinowitz. *A first Course in Numerical Analysis*. McGraw-Hill, 2001.
- [Shu93] M.D. Shuster. A survey of attitude representations. *Journal of Astronautical Sciences*, 41(3):439–517, 1993.
- [SKS90] A. Saberi, P.V. Kokotović, and H.J. Sussmann. Global stabilization of partially linear composite systems. *SIAM Journal of Control and Optimization*, 28:1491–1503, 1990.
- [SM98] F. Sadek and B. Mohraz. Semiactive control algorithms for structures with variable dampers. *Journal of Engineering Mechanics*, 124:981–990, 1998.
- [SS89] E.D. Sontag and H.J. Sussmann. Further comments on the stabilizability on the angular velocity of a rigid body. *Systems and Control Letters*, 12:213–217, 1989.
- [SW] C. Scherer and S. Weiland. Linear Matrix Inequalities in Control. Web page <http://>.
- [TK03] H.G. Tanner and K.J. Kyriakopoulos. Backstepping for nonsmooth systems. *Automatica*, 39(7):1259–1265, 2003.
- [Tsi89] J. Tsinias. Observer design for nonlinear systems. *Systems and Control Letters*, 13:135–142, 1989.

- [TTT01] R.H. Tütüncü, K.C. Toh, and M.J. Todd. SDPT3 – a MATLAB software package for semidefinite-quadratic-linear programming, version 3.0. Web page <http://www.math.nus.edu.sg/~mattohk/sdpt3.html>, 2001.
- [UB90] C.M. Uang and V.V. Bertero. Evaluation of seismic energy in structures. *Earthquake Engineering and Structural Dynamics*, 19:77–90, 1990.
- [Var04] A. Varga. Numerical awareness in control. *IEEE Control Systems Magazine*, 24(1):14–17, 2004.
- [Wen76] Y.K. Wen. Method of random vibration of hysteretic systems. *Journal of Engineering Mechanics Division, ASCE*, 102(2):249–263, 1976.
- [WS96] C. Wen and Y.C. Soh. A robust adaptive controller without a priori knowledge from modelling errors. In *Proceedings of the 35th Conference on Decision and Control*, pages 843–848, December 1996.
- [WY98] Y. Wu and X. Yu. Adaptive control of linear MIMO systems using backstepping approach. In *Proceedings of the American Control Conference*, pages 599–603, June 1998.
- [WZS99] C. Wen, Y. Zhang, and Y.C. Soh. Robustness of an adaptive backstepping controller without modification. *Systems and Control Letters*, 36:87–100, 1999.
- [YC03] J. Yu and J. Chang. A new adaptive backstepping control algorithm for motion control systems – an implicit and symbolic computation approach. *International Journal of Adaptive Control and Signal Processing*, 17:19–32, 2003.
- [YLV94] J.N. Yang, Z. Li, and S. Vongchavalitkul. Stochastic hybrid control of hysteretic structures. *Probabilistic Engineering Mechanics*, 9:125–133, 1994.
- [ZI98] Y. Zhang and P.A. Ioannou. Robustness and performance of a modified adaptive backstepping controller. *International Journal of Adaptive Control and Signal Processing*, 12:247–265, 1998.

-
- [ZI00] Y. Zhang and P.A. Ioannou. A new linear adaptive controller: design, analysis and performance. *IEEE Transactions on Automatic Control*, 45(5):883–897, 2000.
- [ZIC96] Y. Zhang, P.A. Ioannou, and C.C. Chien. Parameter convergence of a new class of adaptive controllers. *IEEE Transactions on Automatic Control*, 41(10):1489–1493, 1996.
- [ZWS00] Y. Zhang, C. Wen, and Y.C. Soh. Adaptive backstepping control design for systems with unknown high-frequency gain. *IEEE Transactions on Automatic Control*, 45(12):2350–2354, 2000.